

# **Secondary Structure Formation in Homologous Peptides**

Von der Fakultät für Biowissenschaften, Pharmazie und Psychologie

der Universität Leipzig

genehmigte

**D I S S E R T A T I O N**

zur Erlangung des akademischen Grades

DOCTOR RERUM NATURALIUM

(Dr. rer. nat.)

vorgelegt

von

Diplom-Biochemiker Carsten Baldauf  
geboren am 23. Dezember 1977  
in Karl-Marx-Stadt

Dekan: Professor Kurt Eger

Gutachter: Professor Hans-Jörg Hofmann, Universität Leipzig  
Professor Claudio Toniolo, Università di Padova  
Professor Samuel H. Gellman, University of Wisconsin

Tag der Verteidigung: 27. Mai 2005

...

Die vorliegende Arbeit wurde im Zeitraum von Mai 2002 bis Februar 2005 unter der Betreuung von Herrn Prof. Dr. Hans-Jörg Hofmann am Institut für Biochemie an der Fakultät für Biowissenschaften, Pharmazie und Psychologie der Universität Leipzig angefertigt.

Ich danke Herrn Professor Dr. Hans-Jörg Hofmann für die Möglichkeit unter seiner Betreuung an diesem interessanten Thema zu arbeiten. Ich konnte viel lernen, nicht nur über Biochemie.

Ich danke Herrn Dr. Robert Günther für seine andauernde Unterstützung und Diskussionsbereitschaft. Es genügte meist ein Räuspern um seine Aufmerksamkeit auf meine Probleme zu lenken.

Ich danke den Mitarbeitern der Universitätsrechenzentrums Leipzig, besonders Herrn Andreas Rost, für die technische Unterstützung.

Ich danke meinem guten Freund René Meier für die unkomplizierte Hilfe beim Umgang mit moderner Rechentechnik.

Ich bin froh meine Promotionszeit mit fähigen Kollegen und guten Freunden verbracht zu haben, Dank also an Franka Pluder, Manja Lang, Ralf David und Nico Nöbel. Guten Appetit!

Ich danke meinen Eltern und meinen Freunden.

Ich danke der Deutschen Forschungsgemeinschaft für die finanzielle Förderung im Rahmen des Projektes „Sekundärstrukturbildung in Peptiden mit nicht-proteinogenen Aminosäuren“ (HO 2346/1).

## Bibliographische Beschreibung

Carsten Baldauf

Secondary Structure Formation in Homologous Peptides

Universität Leipzig, Dissertation,

Februar 2005

123 S., 234 Lit., 30 Abb., 29 Tab.

### Referat:

Thema dieser Arbeit ist die Sekundärstrukturbildung in Peptiden mit nicht-natürlichen Aminosäuren. Die Methoden der theoretischen Chemie, speziell der Quantenchemie, dienen zur Beschreibung der konformativen Eigenschaften von Oligomeren der homologen  $\alpha$ -,  $\beta$ -,  $\gamma$ -, und  $\delta$ -Aminosäuren. Es wurden Konformationsanalysen dieser peptidischen Foldamere durchgeführt. Neben Faltblatt- und Turn-artigen Strukturen stand vor allem die Bildung von helikalen Strukturen im Mittelpunkt. Von speziellem Interesse ist dabei die Realisierung röhrenartiger Strukturen (Nanotubes) durch Helices klassischen Typs wie auch gemischten Typs, der sogenannten  $\beta$ - oder „mixed“-Helices. Die gewonnenen Erkenntnisse tragen zum rationalen Strukturdesign von Peptiden und Foldameren sowie zum Verständnis von Strukturbildung und Faltung in Peptiden und Proteinen bei. Außerdem eröffnen sich Wege zu völlig neuartigen Strukturen.

## Table of Contents

<b>1</b>	<b>Peptide Foldamers – An Introduction</b>	6
1.1	Introductory Remarks – Motivation	6
1.2	Basic Types of Secondary Structure in Peptides and Proteins	7
1.3	Design of Peptide Foldamers	14
1.4	Ab Initio MO Theory and Peptide Structures	21
1.5	Aim of this Work	25
<b>2</b>	<b>Helix Formation and Folding in g-Peptides and Their Vinylogues</b> <i>Helv. Chim. Acta</i> <b>2003</b> (86), 2573-2588.	33
<b>3</b>	<b>Control of Helix Formation in Vinylogous g-Peptides by (E)- and (Z)- Double Bonds – A Way to Ion Channels and Monomolecular Nanotubes</b> <i>J. Org. Chem.</i> <b>2005</b> (70), <i>in press.</i>	53
<b>4</b>	<b>d-Peptides and d-Amino Acids as Tools for Peptide Structure Design – A Theoretical Study</b> <i>J. Org. Chem.</i> <b>2004</b> (69), 6214-6220.	74
<b>5</b>	<b>Mixed Helices – A General Folding Pattern in Homologous Peptides?</b> <i>Angew. Chem. Int. Ed.</i> <b>2004</b> (43), 1594-1597; <i>Angew. Chem.</i> <b>2004</b> (116), 1621-1624.	91
<b>6</b>	<b>Side Chain Control of Folding of the Homologous a-, b- and g-Peptides into Mixed Helices (b-Helices)</b> <i>Biopolymers (Pept. Sci.)</i> <b>2005</b> , <i>in press.</i>	99
	<b>Appendix 1: Contents of the Compact Disc</b>	120
	<b>Appendix 2: Publications</b>	121

# 1 Peptide Foldamers – An Introduction

## 1.1 Introductory Remarks - Motivation

Peptides and proteins play a key-role in many biological processes. They are of fundamental importance for the manifestation of life. The specific functions of native peptides and proteins are based on a definite three-dimensional structure. This 3D-structure is determined by intrinsic factors arising from the special sequence of amino acid residues and their steric and electronic properties and by external factors like the medium.<sup>1,2</sup> For an understanding of the peptide and protein functions knowledge about their structure is necessary. In most cases, such information is still obtained by experimental methods as for instance X-ray and NMR techniques. Due to the rapid development of the speed and storage capacities of modern computational facilities, the methods of theoretical chemistry become more and more important for the description of larger molecules and their properties. In particular, the applicability range of the methods of ab initio MO theory can be extended to larger biomolecules at approximation levels with continuously increasing reliability. Thus, theoretical methods become valuable partners of the various experimental methods in structure research. This concerns the systematic search of the conformational space of compounds, the estimation of the energetic relations between structure alternatives and the explanation of the stability or instability of special structures. Moreover, it is possible to treat fictive and hypothetical structures. Thus, the predictive power of theoretical methods might be a useful tool for the stimulation and planning of experimental research in various fields of chemistry.

In this work, it was tried to follow these ideas. It is intended to demonstrate the progress of quantum chemistry in the field of peptide and protein structure research. However, subject of this work are not the native peptides themselves, but oligopeptides composed of special non-proteinogenic amino acids. The original background of such studies, which will be discussed in more detail in the following paragraphs and chapters, is the search for possibilities to mimic native peptide structures by synthetic peptide analogues where one, several or even all proteinogenic amino acids in the sequence are replaced by unnatural amino acids. Bearing in mind the above-mentioned relationship between the definite three-dimensional structure of native peptides and their functions, any structural modification has to keep the groups which are essential for function in the correct spatial orientations. An important step in the folding of peptides and proteins into their definite three-dimensional structures is the formation of typical elements of secondary structure. It is obvious, that modified peptides have to be able to realize

the basic types of secondary structure elements in  $\alpha$ -peptides for mimicking their structures. Therefore, the focus of this work is on the investigation of the possibilities of secondary structure formation in oligomers of unnatural amino acids. Apart from the aspect of mimicking native peptides, another reason for such studies might be tempting. Even if peptide analogues are not able to adopt the typical structure elements of the native peptides, they could possibly realize completely novel definite structures with properties making them attractive for other purposes. Thus, systematic studies on the consequences of structural modifications of peptide and protein sequences via insertion of non-canonical amino acids for the secondary and tertiary structure formation provide useful tools for a general structure design.<sup>3-12</sup> On the one hand, such peptides represent a new quality in the efforts to ‘improve’ nature, on the other hand they bridge the gap to material and nano sciences.<sup>13-18</sup>

## 1.2 Basic Types of Secondary Structure in Peptides and Proteins

Since the focus of this work is on the secondary structure formation in oligopeptides of unnatural amino acids, which is referred to that in native peptides, a short overview on the most important secondary structure elements in  $\alpha$ -peptides could be useful. Native peptides and proteins are built up from 22 proteinogenic amino acids. From a chemical point of view, these proteinogenic amino acids are  $\alpha$ -amino acids. With exception of glycine, all other amino acids bear a special side chain in L-configuration at the  $C_{\alpha}$ -atom. By condensation between the amino group of one amino acid and the carboxy group of a second one, a so-called peptide bond is formed leading to a dipeptide. This process may be continued and provides oligopeptides, polypeptides and finally proteins. The conformation of a polypeptide chain is primarily determined by the values for the backbone torsion angles  $\omega$ ,  $\phi$  and  $\psi$  (cf. scheme in Figure 1a). It is common to denote definite structures characterized by typical values of these backbone torsion angles as secondary structure elements. The angle  $\omega$  describes the rotation around the peptide bond ( $\angle C_{\alpha}CNC_{\alpha}$ ). Due to the partial double bond character of this bond, the rotation reveals two energy minima, at  $0^{\circ}$  corresponding to a *cis*-peptide bond and at  $180^{\circ}$  corresponding to a *trans*-peptide bond. The *trans*-peptide bond is mostly preferred in peptides and proteins because of steric advantages. Only for peptide bonds with the amino acid proline, the *cis*-orientation is distinctly higher populated. Due to the considerable rotational barrier, the peptide bonds are kept fixed in their planar arrangements. Thus, the conformational space available for a peptide is essentially determined by the backbone torsion angles  $\phi$  and  $\psi$  of the amino acid constituents.

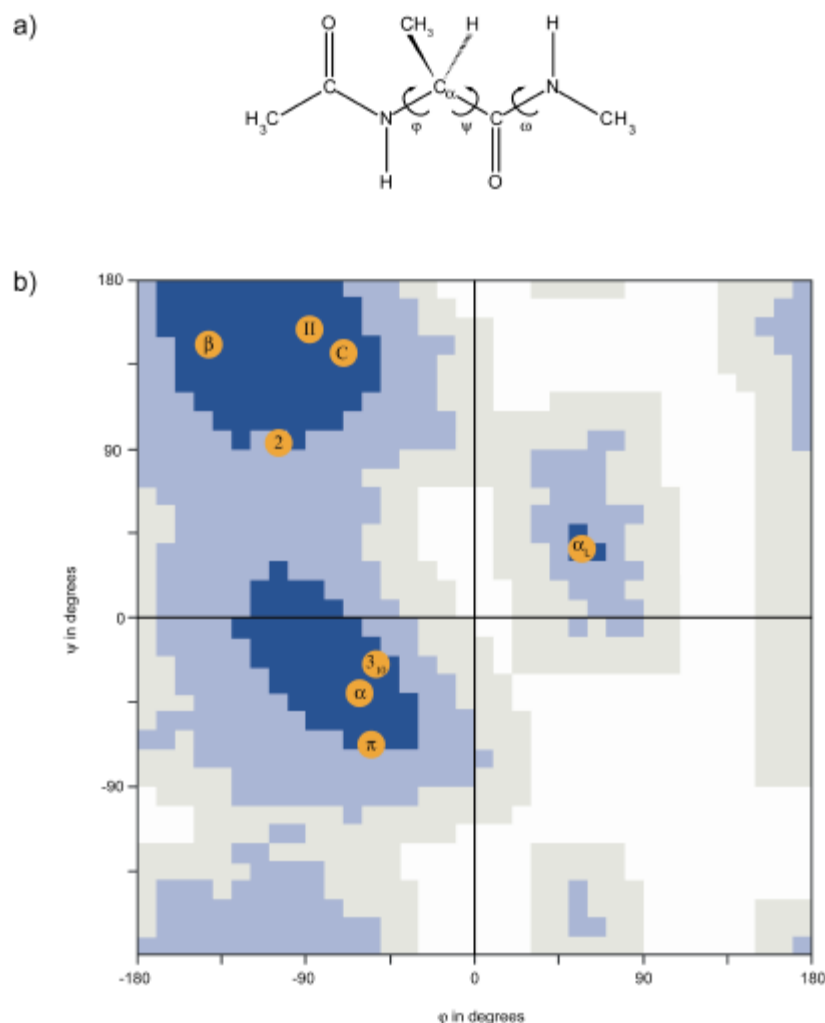


**Fig. 1.** a) Blocked alanine residue with the backbone torsion angles  $\omega$ ,  $\phi$  and  $\psi$ . b) Ramachandran ( $\phi$ ,  $\psi$ )-plot of the available conformational space of amino acid constituents in a peptide sequence derived from the torsion angle data for 463 protein crystal-structures (accessible regions blue, forbidden regions white).<sup>22</sup> Special conformations are indicated:  $\beta$ -strands ( $\beta$ ), left-handed poly-glycine and poly-L-proline helix (II), collagen (C), 2.2<sub>7</sub>-bend (2), right-handed 3<sub>10</sub>-helix (3<sub>10</sub>), right-handed  $\alpha$ -helix ( $\alpha$ ), right-handed  $\pi$ -helix ( $\pi$ ), left-handed  $\alpha$ -helix ( $\alpha_L$ ).

The angle  $\phi$  describes the torsion around the  $\text{N}-\text{C}_\alpha$  bond ( $\angle\text{CNC}_\alpha\text{C}$ ), while  $\psi$  describes the rotation around the  $\text{C}_\alpha-\text{C}$  bond ( $\angle\text{NC}_\alpha\text{CN}$ ).<sup>19-21</sup>

A first idea of the ( $\phi$ ,  $\psi$ ) conformational space which is available for a single amino acid constituent in a sequence provides the Ramachandran plot. The original basis of this diagram is a mere geometric inspection of the sterically accessible conformations via van der Waals contacts. Figure 1b shows such a plot, which is confirmed by the torsion angle data experimentally obtained for thousands of amino acid constituents of peptides and proteins by X-ray-analyses.<sup>22</sup> Two regions in this plot are of special importance, since they correspond to periodic secondary structures. In periodic secondary structures, the corresponding backbone angles of all amino acid constituents have the same values. In the third quadrant of the plot, the region of



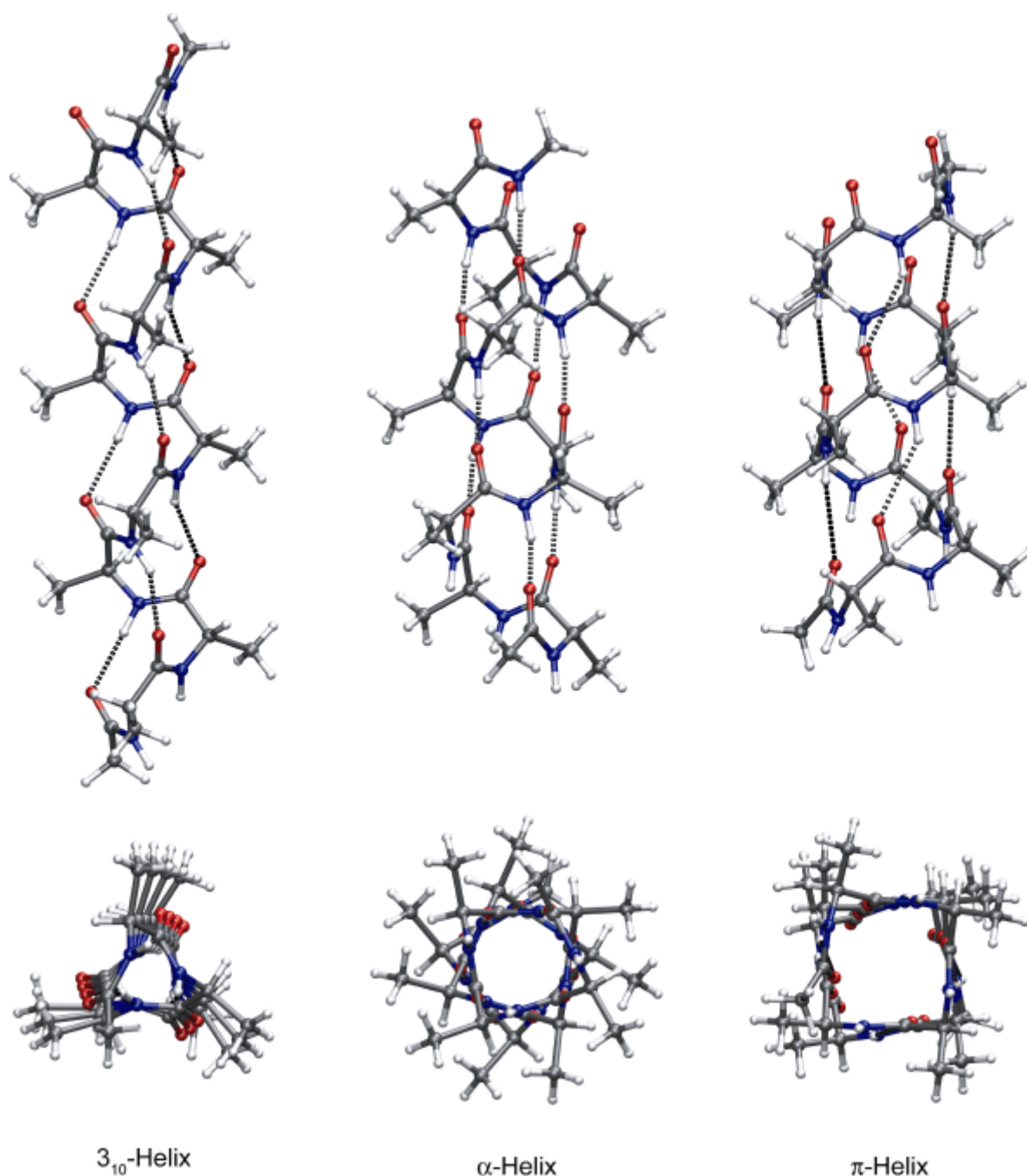


**Fig. 2.** Basic helices in  $\alpha$ -peptides (first line: side view, second line: top view).

peptide helices, e. g. the  $\alpha$ -,  $3_{10}$ -, and  $\pi$ -helices, is indicated. These helices can be distinguished by their hydrogen bonding patterns. In the  $\alpha$ -helices, hydrogen bonds are formed between the NH-group of the amino acids ( $i+4$ ) and the CO-group of residues  $i$  in backward direction of the sequence. The idealized torsion angle values in all amino acids of this helix are about  $\varphi = -60^\circ$  and  $\psi = -40^\circ$ .<sup>23</sup> In this case, a right-handed helix is obtained. Inversion of the signs of the values for  $\varphi$  and  $\psi$  leads to the left-handed helix, which is, however, energetically disfavored by destabilizing side chain contacts. The hydrogen bonds of the  $\alpha$ -helix show a rather perfect parallelism to the helix axis. Looking at the structure along the helix axis, the staggered

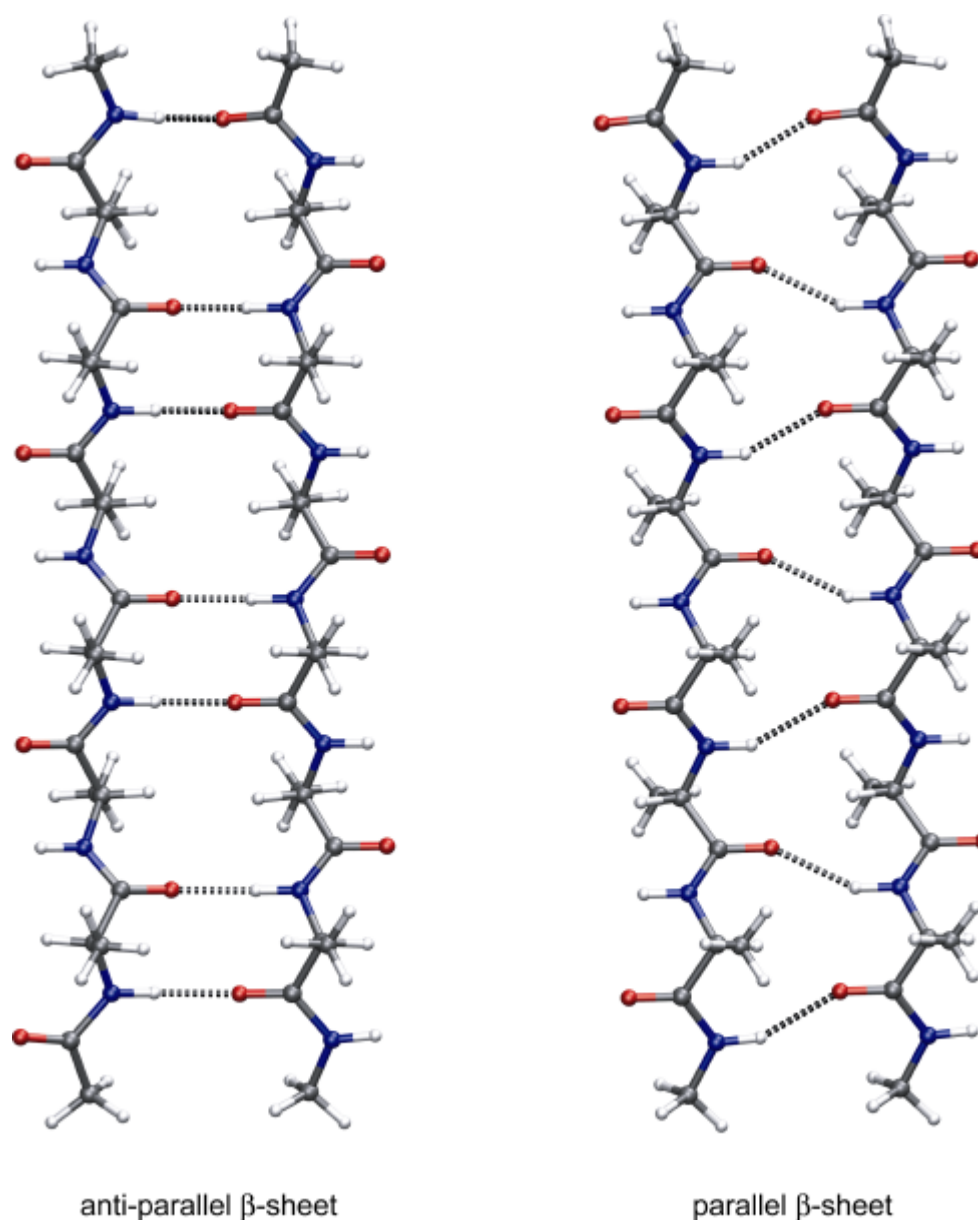


**Fig. 3.** Schematic representation of anti-parallel and parallel  $\beta$ -sheet structures.

arrangements of the side chains can be seen which minimize their contacts (cf. Figure 2). Each hydrogen bond closes a turn or pseudocycle of 13 atoms. In comparison to the  $\alpha$ -helix, the  $3_{10}$ -helix is a scarce secondary structure element in proteins, which appears mostly at the C-terminal ends of  $\alpha$ -helices. The  $i \leftarrow (i+3)$  amino acid interactions lead to ten-membered hydrogen-bonded pseudocycles. The  $3_{10}$ -helix is more tightly wound with a triangular shape in the top view (cf. Figure 2). The  $C_{\alpha}$ -atoms are approximately arranged in one line and the side chain packing is less ideal than in the  $\alpha$ -helix. Besides, the hydrogen bond directions deviate considerably from the parallelism to the helix axis. The idealized torsion angle values for this helix type are about  $\varphi = -50^{\circ}$  and  $\psi = -30^{\circ}$ .<sup>24,25</sup> The top view of the third helical structure, the  $\pi$ -helix, shows a square-like shape (cf. Figure 2). The amino acid interactions  $i \leftarrow (i+5)$  provide 16-membered pseudocycles. The idealized backbone torsion angle values are about  $\varphi = -60^{\circ}$  and  $\psi = -70^{\circ}$ . To

realize this helix, the bond angle  $\tau$  ( $\angle\text{NC}_\alpha\text{C}$ ) has to be extended to about  $115^\circ$  from the ideal tetrahedron angle of  $109.5^\circ$ .<sup>25</sup> The existence of this helix type is still under debate. Whereas all helices in  $\alpha$ -peptides discussed so far are forming hydrogen bonds in backward direction along the sequence, Son *et al.* suggested a  $\lambda$ -helix with hydrogen bonds pointing in the forward direction along the sequence on the basis of molecular mechanics and dynamics studies. Hydrogen bonds in this helix between the peptidic NH of residue  $i$  and the peptidic CO of residue  $(i+5)$  lead to 17-membered pseudocycles.<sup>26</sup> Until now, this helix type was not confirmed by experiments.

Another type of a periodic secondary structure is indicated in the second quadrant of the Ramachandran plot. This structure with approximate backbone torsion angles  $\phi = -120^\circ$  and  $\psi = 140^\circ$  is called  $\beta$ -strand. The alignment of at least two  $\beta$ -strands in parallel or anti-parallel orientation provides  $\beta$ -sheet structures (cf. Figure 3), which are stabilized by hydrogen bonds formed in the plane between the two strands. The anti-parallel  $\beta$ -sheet has a twofold symmetry axis perpendicular to the direction of the strands and the direction of the hydrogen bonds. In the parallel  $\beta$ -sheets, the hydrogen bonds are not exactly perpendicular to the strand direction as in the anti-parallel sheet structures. The side chains of the residues of one strand point alternately up and down related to the plane of the sheet, but the side chains of equivalent residues of two adjacent strands point in the same direction.<sup>23,25</sup>

The periodic character and the overall shape of the described strands and helices enables the formation of 'structure proteins' like keratin, myosin, and silk proteins from insects. 'Functional proteins' like enzymes or receptors have a globular shape to realize their specific interactions with endogenous substrates and ligands. For the formation of globular structures, it is necessary to reverse the direction of the peptide chain.<sup>23,25</sup> This is realized by turn and loop elements. Contrary to strands and helices, turns are non-periodic structures, i.e. the amino acid residues in turns and

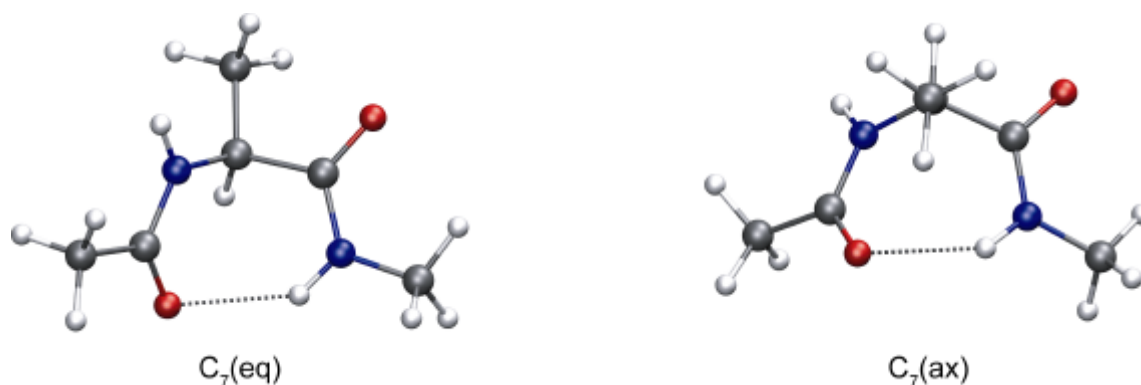


**Fig. 4.** Models of the two  $\gamma$ -turn conformers  $C_7(\text{eq})$  and  $C_7(\text{ax})$  in a blocked alanine residue.

loops have different values for  $\phi$  and  $\psi$ , respectively. The smallest peptide units that are able to reverse the peptide chain are  $\gamma$ - and  $\beta$ -turns. A  $\gamma$ -turn consists of three amino acids (cf. Figure 4). Its conformation is determined by the torsion angles of the central amino acid. The first and third amino acid are connected by a hydrogen bond. Thus, a seven-membered hydrogen-bonded pseudocycle results. The inverse  $\gamma$ -turn  $C_7(\text{eq})$  (Figure 4) has torsion angle values  $\phi$  of about  $-80^\circ$  and  $\psi$  of about  $70^\circ$ . The notation 'eq' characterizes the equatorial orientation of the side chain at the  $C_\alpha$  atom referred to the  $C_7$ -ring plane. In the  $\gamma$ -turn  $C_7(\text{ax})$  the signs of the backbone torsion angles are inverted. This turn is distinctly less stable than its equatorial counterpart and does not occur in proteins. Much more important than  $\gamma$ -turns are  $\beta$ -turns, which are formed by four consecutive amino acids (Figure 5). According to Venkatachalam, there are eight alternatives of  $\beta$ -turns.<sup>23,25,27,28</sup> Most  $\beta$ -turns are stabilized by an interaction between the NH group of residue  $(i+3)$  and the peptidic CO of residue  $i$  leading to a ten-membered hydrogen-bonded pseudocycle. Not all the formally thinkable  $\beta$ -turns can be found in proteins. Most important are the  $\beta\text{I}$  ('common'-turn) and the  $\beta\text{II}$  turns ('glycine'-turn). For each of the basic turns, also their approximate mirror images are able to reverse the sequence direction. These inverse turns are indicated by an additional prime at the basic symbol, e.g.  $\beta\text{I}'$  and  $\beta\text{II}'$  turns. The  $\beta\text{III}$  and  $\beta\text{III}'$  turns represent a single turn of a right- or left-handed  $3_{10}$ -helix, respectively. The  $\beta\text{VI}$  turns occur with the amino acid proline in the third position and consider the possibility of *cis*-peptide bonds. The idealized and calculated torsion angles for the  $\beta$ -turns explicitly described here are given in Table 1. Besides the  $\gamma$ - and  $\beta$ -turns, several other possibilities to reverse the sequence direction are known realized via still more consecutive amino acid residues. These turns and loops are not only of importance for the realization of compact globular proteins, but play also a role in

**Table 1.** Idealized<sup>27</sup> and Calculated<sup>28</sup> (HF/6-31G\*) Backbone Torsion Angles<sup>a</sup> for the  $\beta\text{I}$ ,  $\beta\text{II}$ ,  $\beta\text{III}$ , and  $\beta\text{VIa}$ -Turns in  $\alpha$ -Peptides

Turn <sup>b</sup>	$\phi_{i+1}$	$\psi_{i+1}$	$\phi_{i+2}$	$\psi_{i+2}$
$\beta\text{I}$	-60/-73	-30/-19	-90/-100	0/8
$\beta\text{II}$	-60/-60	120/134	80/67	0/20
$\beta\text{III}$	-60/-	-30/-	-60/-	-30/-
$\beta\text{VIa}$	-60/-60	120/146	-90/-61	0/-3

<sup>a</sup> Angles in degrees; <sup>b</sup> first values idealized, second values calculated for a blocked alanine dipeptide (No minimum conformations were found for  $\beta\text{III}$  at the HF/6-31G\* level of ab initio MO theory.); for  $\beta\text{VIa}$ : Ac-L-Ala-L-Pro-NHMe).

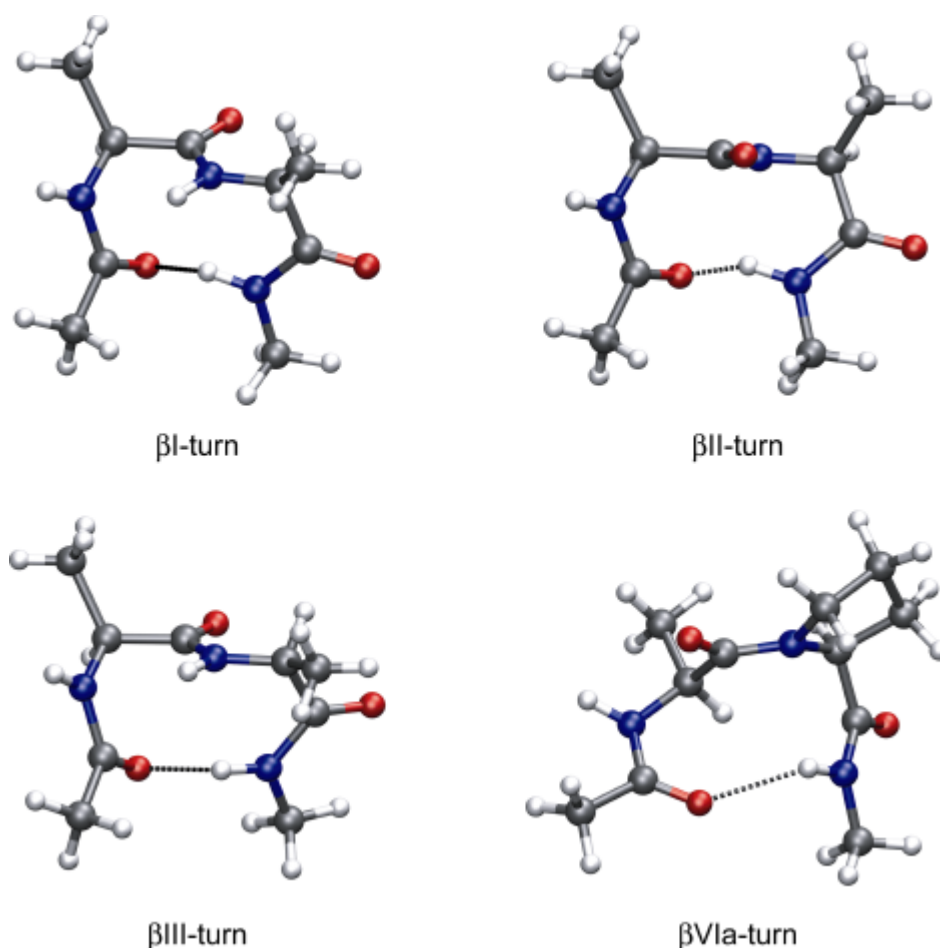


**Fig. 5.** Four important  $\beta$ -turn possibilities in  $\alpha$ -peptides.

molecular recognition. A general overview on the possibilities of hydrogen bonding in  $\alpha$ -peptides with contemplations on new folding patterns was given by Toniolo.<sup>29</sup>

Another secondary structure type deserves mentioning here since it is generalized in the later parts of this work. The above-described periodic secondary structures are composed of L-amino acids. In some bacteria, e.g. *Bacillus brevis*, helical structures are formed by peptides consisting alternately of D- and L- $\alpha$ -amino acids. The sequence of the (mostly hydrophobic) amino acids forms a right-handed helix.<sup>27,30</sup> But this helix is characterized and stabilized by intramolecular hydrogen bonds alternately changing their directions. This leads to alternating hydrogen-bonded pseudocycles of different size. The inner helix diameter is large enough to let some ions or water pass (cf. Figure 6a). The interior is polar due to the carbonyl oxygen atoms and can substitute the stabilizing solvation shell of ions. The hydrophobic side chains can interact outside with the lipids of the membrane. A well-known representative of this unusual helix type with alternating periodicity is Gramicidin A (Figure 6a), where 20- and 22-membered hydrogen-bonded pseudocycles alternate.<sup>31-34</sup> Figure 6b shows the similarities between the hydrogen bonding patterns of this helix type and a  $\beta$ -sheet structure. Therefore, such helices with alternating hydrogen bonding patterns are sometimes denoted as  $\beta$ -helices.

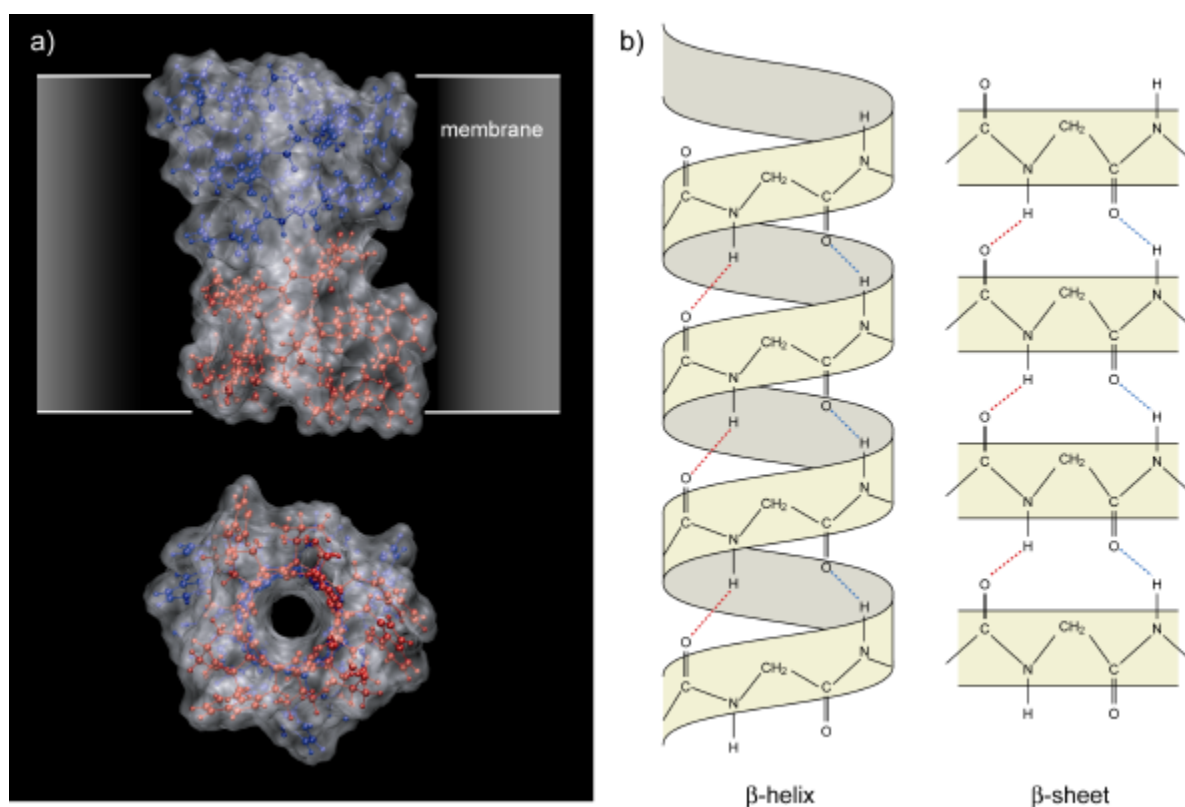
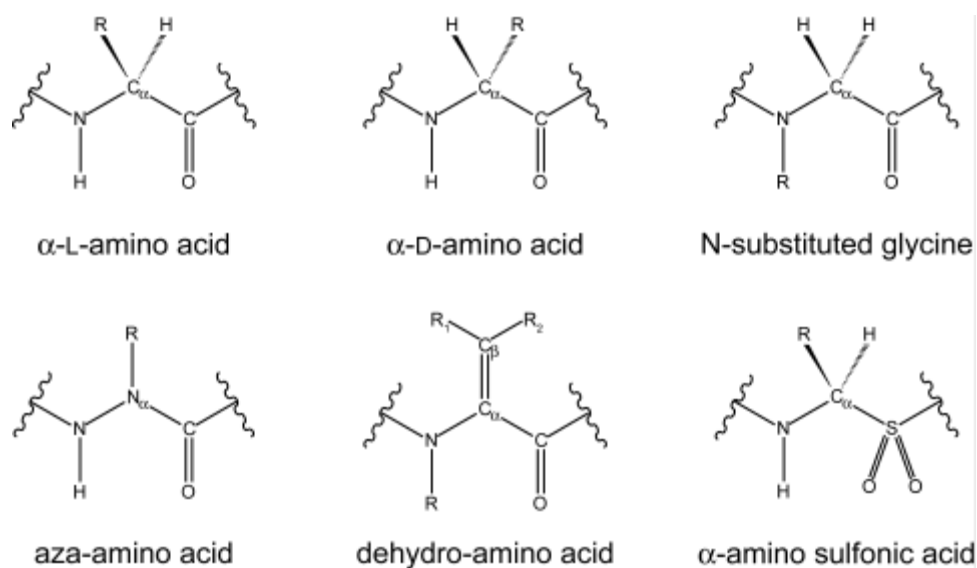


**Fig. 6.** a) Model of a transmembrane channel formed by two gramicidin A chains (ref. 32; pdb entry 1MAG). b) Schematic comparison of a single-stranded  $\beta$ -helix and a parallel  $\beta$ -sheet, based on ref. 29.

### 1.3 Design of Peptide Foldamers

The use of native peptides for pharmacological purposes has some serious limitations. Most important are the low resistance against proteases, the bad transport properties due to the polar structure and the sometimes insufficient selectivity against receptor subtypes. It was frequently found, that the proteolytic stability is increased via the replacement of proteinogenic amino acids in peptide sequences by unnatural amino acids.<sup>3-7,10</sup> This opens a wide field for peptide modification. There are several possibilities to derive new building blocks from the proteinogenic amino acids:

- changes of the amino acid side chain,
- shifting the side chain from the  $C_{\alpha}$ -atom to the amino nitrogen atom of the amino group,
- replacement of the  $C_{\alpha}$ -atom by other atoms,
- modifications of the peptide bond, and
- extension of the backbone.



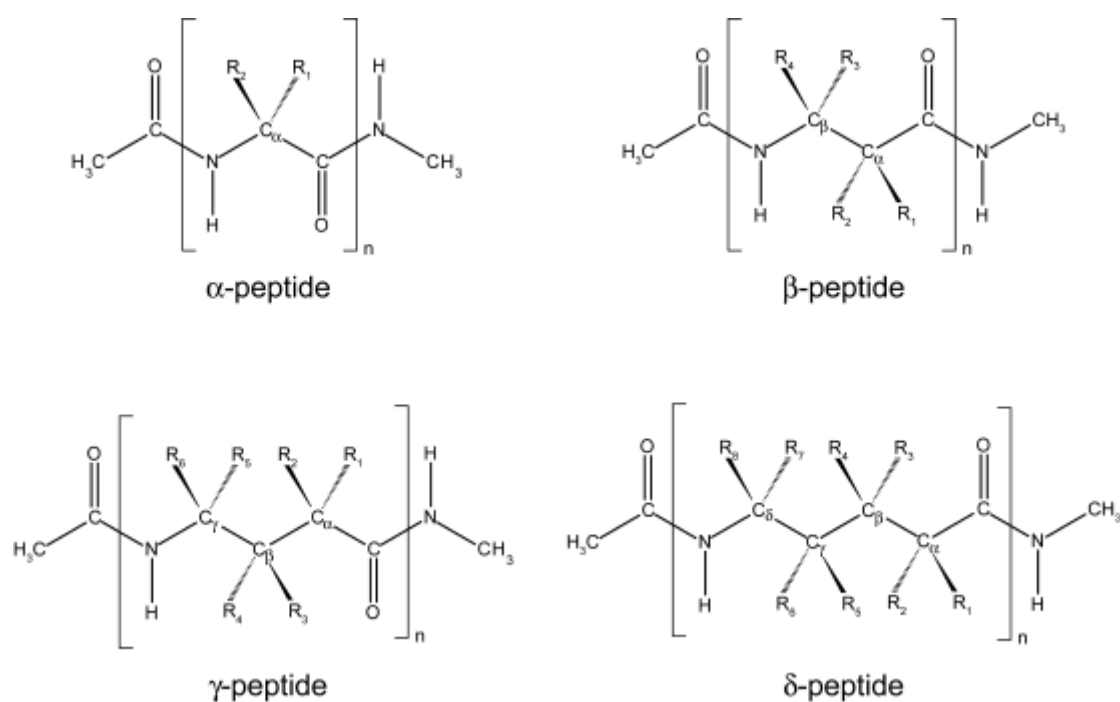
**Fig. 7.** Selected examples of amino acid modification.

Figure 7 shows only a few representative examples. A very simple possibility is the substitution of a D-amino acid for its native L-counterparts. Shifting the amino acid side chain from the  $C_{\alpha}$ -atom to the amino nitrogen atom yields N-substituted glycines. Oligomers of these N-substituted glycines are called peptoids.<sup>35-40</sup> Another example results from the replacement of the  $C_{\alpha}$ -atom by a nitrogen atom, which can still bear the side chain. This leads to azaamino acids.<sup>41-43</sup> Dehydro-amino acids are obtained connecting the backbone  $C_{\alpha}$  and the side chain  $C_{\beta}$  atoms via a double bond.<sup>29,44</sup> Examples for a replacement of the peptide bond are the insertions of either sulfonamide or phosphonamide moieties.<sup>45</sup> Besides the aforementioned strategies, the extension of the amino acid backbone by homologation is of great importance. Thus, the homologous  $\beta$ -,  $\gamma$ -, and  $\delta$ -amino acids can be derived from the  $\alpha$ -amino acids (cf. Figure 8). At a first sight,  $\delta$ -amino acid constituents seem to be especially interesting, since they correspond approximately to an  $\alpha$ -dipeptide unit. In this case, the central peptide bond of a dipeptide is replaced by a C-C single bond, which allows the introduction of additional substituents.<sup>46-48</sup>

For a long period it was generally accepted, that oligomers of  $\beta$ -,  $\gamma$ - and  $\delta$ -amino acids are not able to adopt defined secondary structures in contrast to the well-defined secondary structures of  $\alpha$ -peptides, although this was never really examined. It was simply assumed that the homologation leads to an increased flexibility of the amino acid and oligomer backbones. During the last ten years, this view had to be completely changed. In particular, the investigations on  $\beta$ -peptides showed an enormous potential for secondary structure formation.<sup>18,49,50</sup> Even biological effects of  $\beta$ -peptides were found.<sup>51,52</sup> Although less intensively investigated, secondary structure formation occurs also in  $\gamma$ -peptides and even secondary structures of  $\delta$ -peptides

attracted the attention of the scientific community (cf. Figure 8). In the meantime, all these activities can be seen as part of a general concept of secondary structure formation in oligomers composed of *any* chemical monomers, the foldamer concept. The term foldamer was originally introduced by Gellman for any large molecule with a strong tendency to adopt a specific compact conformation.<sup>14</sup> A later definition denotes oligomers that fold into conformationally ordered states in solution as foldamers.<sup>16</sup> Since a strict definition cannot be given, the authors continue with some complementary features:

- The compact structures of foldamers should be stabilized by a collection of noncovalent interactions between nonadjacent monomer units.
- Foldamers have usually regular repeating structure elements in their backbones.
- Foldamers are of oligomeric and not of polymeric size.
- Folding into their definite structure is a dynamic process, meaning that the molecule can unfold to adopt a set of random conformations and refold. Hence, molecules without conformational flexibility are not regarded as foldamers.
- When folded, these molecules possess a unique set of atomic coordinates, or at the very least, a few sets of different coordinates. Since these molecules adopt a compact (folded) conformation in solution, the solvent may have an important influence on the folded state.<sup>16,53</sup>



**Fig. 8.** Sketch of oligomers of the homologous  $\alpha$ -,  $\beta$ -,  $\gamma$ -, and  $\delta$ -amino acids.



Stimulated by the research on  $\beta$ -peptide foldamers, the activities in foldamer research increased considerably in the last decade, which is documented in numerous comprehensive reviews.<sup>11,13,15-18,49,50,54-66</sup>

This work is confined to peptide or peptidomimetic foldamers with the focus on the homologous  $\beta$ -,  $\gamma$ -, and  $\delta$ -peptides. The occurrence of numerous different secondary structures in these classes of compounds makes visible that the extended backbone with the additional single bonds does not increase the backbone flexibility so much to prevent secondary structure formation, but rather increases the diversity of secondary structures in comparison to  $\alpha$ -peptides.<sup>67-71</sup> According to the experimental data and calculations on blocked  $\beta$ -amino acid monomers, secondary structures with hydrogen bonds formed between neighboring peptide bonds compete with others forming hydrogen bonds between more distant peptide linkages. This

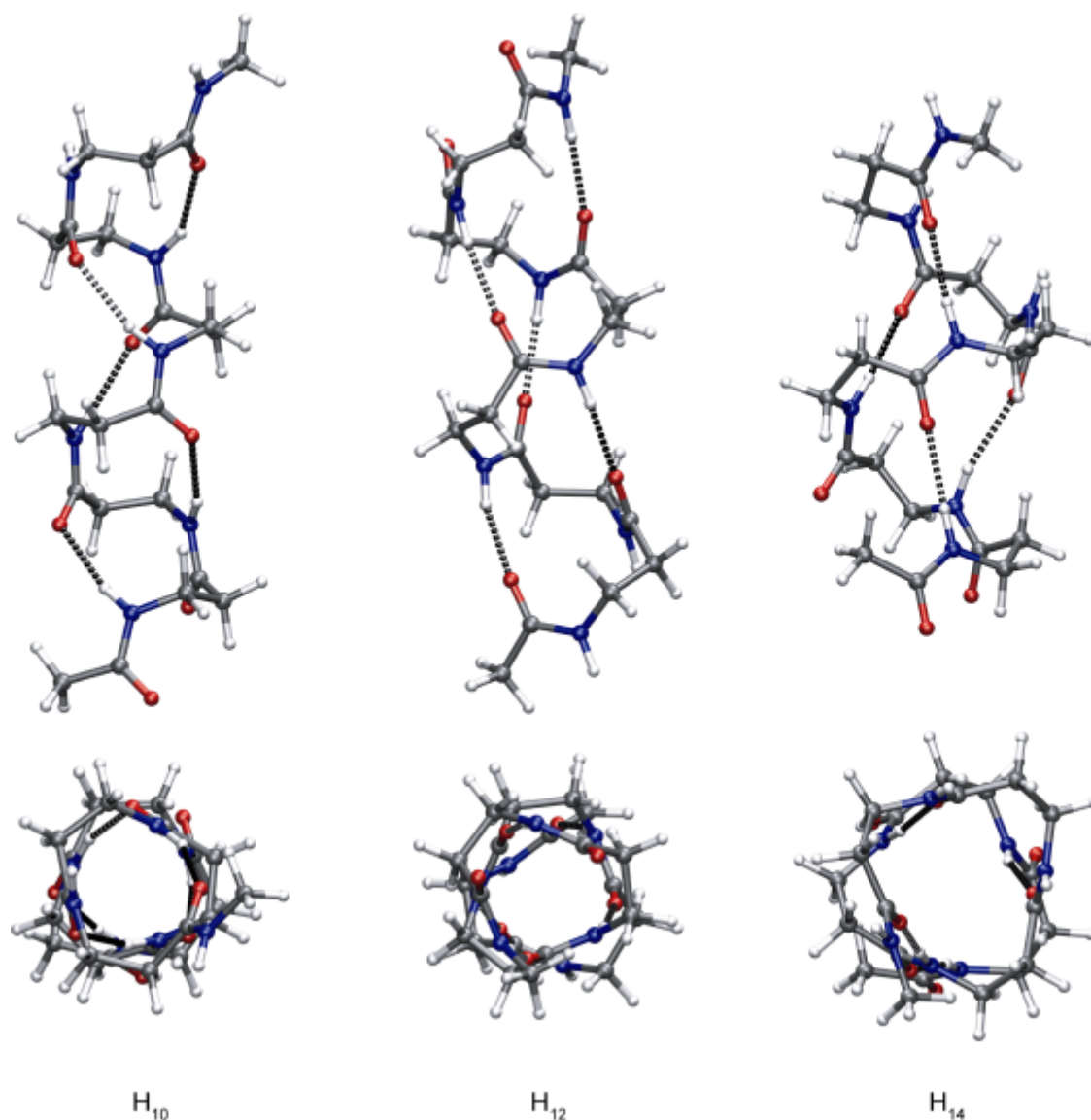


**Fig. 9.** Helical  $\beta$ -peptide conformers  $H_{10}$ ,  $H_{12}$ , and  $H_{14}$ . First row: side view, second row: top view.

can also be observed in oligomers of  $\gamma$ -amino acids ( $\gamma$ -peptides) with a tendency to favor secondary structures forming the hydrogen bonds between neighboring peptide bonds with increasing length of the backbone.<sup>69,72,73</sup> Like in  $\alpha$ -peptides, various types of helices can be found in  $\beta$ -peptides. The  $H_{14}$ -helix is stabilized by interactions of the amide proton of residue  $i$  and the carbonyl function of residue  $(i+2)$  thus forming a 14-membered pseudocycle. In this case, the hydrogen bond is formed in the forward direction of the sequence, which is in contrast to the helices of  $\alpha$ -peptides (cf. Figure 9). From that reason, also the dipole of the  $H_{14}$ -helix has the opposite direction in comparison to that of an  $\alpha$ -helix. The diameter of the  $H_{14}$ -helix of the  $\beta$ -peptides is with 4.7 Å slightly larger than that of the  $\alpha$ -helix (4.3 Å). The  $H_{14}$ -structure can be selectively synthesized by the linkage of *trans*-2-aminocyclohexanecarboxylic acid (ACHC) constituents<sup>74-76</sup> or with acyclic  $\beta$ -(*S*)-substituted  $\beta$ -amino acids.<sup>77-79</sup> Another helical secondary structure is the  $H_{12}$ -helix (cf. Figure 9), which was found by Gellman's group.<sup>80,81</sup> This secondary structure was observed in oligomers of *trans*-aminocyclopentane carboxylic acid (ACPC). The hydrogen bonding pattern exhibits  $i \leftarrow (i+3)$  amino acid interactions leading to 12-membered

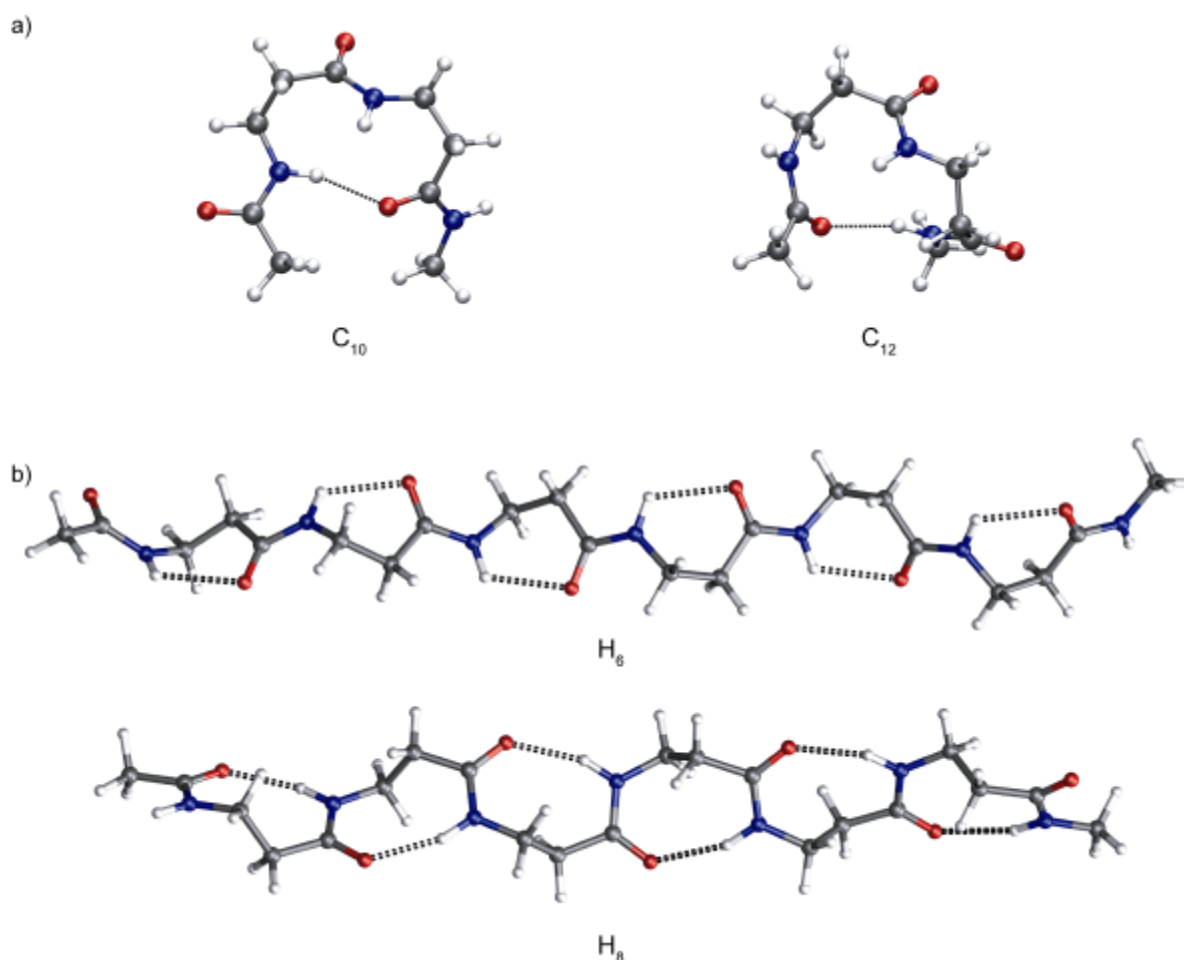


**Fig. 10.**  $\beta$ -Peptides are able to mimic the secondary structures of the  $\alpha$ -peptides: a) turn-like conformers  $C_{10}$  and  $C_{12}$ ; b) strand-like structures  $H_6$  and  $H_8$ .

hydrogen-bonded pseudocycles. The helix dipole and the hydrogen bonding pattern are comparable with those of the  $3_{10}$ -helix of the  $\alpha$ -peptides. The synthesis of  $\beta$ -peptide oligomers from *cis*-substituted oxetane rings leads to helical structures with ten-membered rings.<sup>82-84</sup> Figure 9 shows also a model of this helical type. Oligomers of  $\beta$ -amino acids with different substituents at the  $\alpha$ - and  $\beta$ -positions form extended structures (cf. Figure 10b).<sup>85,86</sup> To complete the possibilities of  $\beta$ -peptide structure design, it should be mentioned that even the formation of turns is possible. Figure 10a shows two examples for turn structures. In contrast to the  $\beta$ -turns of the  $\alpha$ -peptides, the ten-membered pseudocycle of  $C_{10}$  is closed by an hydrogen bond in the forward direction along the sequence, whereas the  $C_{12}$  turn shows formally the same  $i \leftarrow (i+3)$  hydrogen bonding pattern as a  $\beta$ -turn. However, due to the elongated backbone of the  $\beta$ -amino acid building blocks, a twelve-membered pseudocycle is formed now. The above-mentioned  $\beta$ -helix with alternating periodicity of the  $\alpha$ -peptides finds also a counterpart in the  $\beta$ -peptide class, which was described by Seebach and co-workers as a “mixed helix” (Figure 11).<sup>87</sup> The special features and peculiarities of these structures are subject of the Chapters 5 and 6.

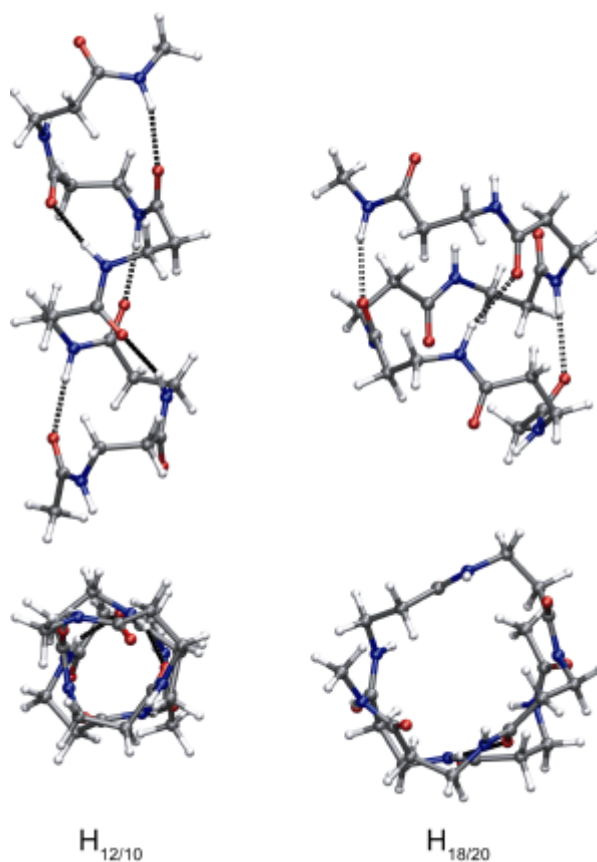


**Fig. 11.** Two different mixed helices of the  $\beta$ -peptides. The hydrogen bonds are formed alternately in the backward ( $i \leftarrow (i+3)$  or  $i \leftarrow (i+5)$ ) and forward ( $i \rightarrow (i+1)$  or  $i \rightarrow (i+3)$ ) direction along the sequence.

Of course, all the structure modifications discussed above for  $\alpha$ -amino acids, are also possible for the homologous amino acids. Thus, the substitution of the  $C_{\beta}$ -atom of a  $\beta$ -amino acid by oxygen or nitrogen leads to two other interesting amino acids in peptide foldamer research, the  $\alpha$ -aminoxy acids and  $\alpha$ -hydrazino acids (Figure 12). These amino acids are constituents of aminoxy and hydrazino peptide analogues and foldamers. In a tripeptide composed of valine and alanine which are flanking an  $\alpha$ -aminoxy residue, a  $\gamma$ -turn-like geometry is obtained.<sup>88,89</sup> Longer oligomers consisting only of  $\alpha$ -aminoxy acids form helices with 1.8 residues per turn.<sup>90-92</sup> In both cases, eight-membered pseudocycles are formed between the peptidic NH of residue  $(i+3)$  and the peptidic CO of amino acid  $i$ . For hydrazino peptides experimental information on secondary structure elements is still missing, although their synthesis is possible.<sup>93-95</sup> There are some hints on periodic structures with eight-membered hydrogen-bonded pseudocycles. On the basis of ab initio MO theory, a rather complete overview on the secondary structure possibilities in hydrazino peptides was given. Thus, a helical structure stabilized by hydrogen bonds between the amino acids  $i$  and  $(i+2)$  forming 14-membered pseudocycles is suggested to be most stable.<sup>96</sup>

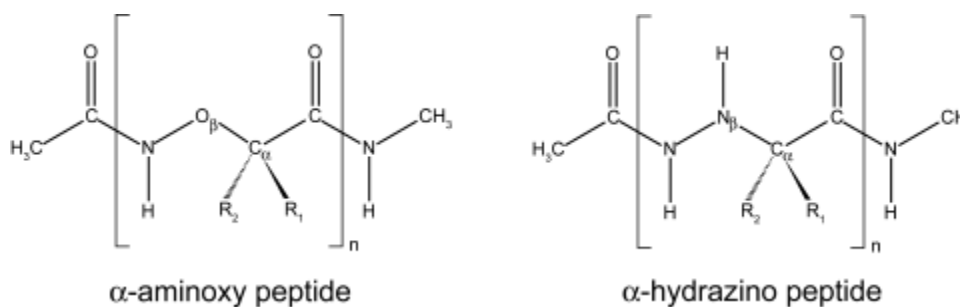


**Fig. 12.** Structure of aminoxy and hydrazino peptides.

The aforementioned modification of the peptide bond with a sulfonamide moiety is practicable for the  $\beta$ -peptides too.<sup>97,98</sup> In contrast to the relatively unstable  $\alpha$ -sulfonamido peptides, rather stable compounds are accessible in  $\beta$ -sulfonamido peptides. Unfortunately, there are no convincing experimental hints on the formation of secondary structures until now.<sup>99</sup>

The information given on the secondary structures of  $\beta$ -peptides illustrates the enormous potential in this class of compounds. Thus, it can be expected that secondary structure formation should also occur in the oligomers of  $\gamma$ - and  $\delta$ -amino acids. Since these compounds are subject of the following chapters, the details are given there.

## 1.4 Ab Initio MO Theory and Peptide Structures

Theoretical chemistry offers a wide variety of methods for the treatment of molecular structures. Molecular mechanics and quantum chemical approaches are of special importance. The methods of molecular mechanics are based on empirical force fields which are derived from rather simple ideas of classical physics on the potentials of bond length, bond angle and torsion angle variations additionally considering the electrostatic and van der Waals-London interactions between the atoms of a molecule.<sup>100</sup> Although molecular mechanics is often the only realistic possibility to get structure information on large proteins, it suffers from serious drawbacks. Therefore, these methods were not employed in this work. More reliable are quantum chemical methods, which are based on two fundamentally different concepts, the molecular orbital (MO) theory and the valence bond (VB) theory. In most applications and also in this work, MO theory is preferred. The methods of MO theory can be divided into two groups, ab initio<sup>101-104</sup> and semiempirical MO methods.<sup>105</sup> Although attractive for the treatment of biomolecules because of the less computational efforts to be realized, semiempirical MO theory was not employed in this work since it fails considerably to describe peptide structures.<sup>106</sup> Thus, all calculations performed in this work are based on ab initio MO theory.

In ab initio calculations, the time-independent Schrödinger equation is solved for a given molecule.<sup>101-104</sup> The solutions are the wave functions and the energies for all possible states. On the basis of these data, the various chemical and physical properties can be calculated. Since an exact solution of the Schrödinger equation is impossible for the most molecular systems, some simplifications are necessary. Most important are:

- the Born-Oppenheimer approximation, which considers the positions of the nuclei fixed due their larger masses in comparison to that of the electrons. Thus, the wave function can be split into an electronic and a nuclear wave function. The latter can be neglected for most chemical purposes.
- the model of independent particles, which describes the movement of each electron in an average field of all others. Thus, it is possible to split the total electronic wave function into electronic one-electron wave functions (Hartree-Fock (HF) ansatz). However for the calculation of this average field knowledge of the wave function is required, which is only obtained after having the Schrödinger equation solved. Therefore, there is need of a “first estimation” of the wave function to be able to calculate an approximated average field. Such a wave function can for instance be obtained by the solution of the Schrödinger equation for the system neglecting the

electron interaction completely. In this case, the Schrödinger equation can always be solved. Now, it is postulated that the solution of the Schrödinger equation employing this field provides an improved wave function, from which an improved average field results. This procedure can be continued in an iterative procedure until the self-consistency of the field (self-consistent-field method, HF-SCF).

- The molecular wave functions (molecular orbitals, MOs) are approximated by a linear combination of atomic orbitals (LCAO-MO-approximation).

Methods solving the Schrödinger equation according to this procedure are called ab initio methods of the HF-SCF-LCAO-MO type. Apart from the aforementioned basic approximations, only the size of the LCAO-MO ansatz (basis set) has influence on the results. Among the various suggestions for basis sets, the basis set schemes developed by Pople and co-workers are widely accepted.<sup>104</sup>

First ab initio MO studies on peptide structures employing these basis sets were carried out by Schäfer and coworkers in the early eighties.<sup>107-110</sup> The STO-3G or 4-31G basis sets used in these studies provided a first insight into the preferred conformational states of the glycine and alanine diamides HCO-Gly-NH<sub>2</sub> and HCO-Ala-NH<sub>2</sub>, respectively. A milestone of the quantum chemical work on peptide structures was the computation of a complete energetic Ramachandran plot with all minimum and transition state conformations for the blocked alanine and glycine derivatives at the 3-21G and 6-31G\* levels of ab initio MO theory by Pople's group in 1991.<sup>111</sup> The results of this study stimulated the work of numerous other groups in this field.<sup>112-116</sup> An energetic Ramachandran plot for a blocked alanine constituent (MeCO-Ala-NHMe) calculated in our group at the same approximation level (HF/6-31G\*) is shown in Figure 13.<sup>117</sup> The comparison with the empirical plot in Figure 1b reveals the similarities. The forbidden regions (white in Figure 1b) are areas of high energy in this plot. Also the accessible regions (blue) have their counterparts in the energetic plot and correspond to the areas of minimal energy. Some, but not all of the secondary structures of  $\alpha$ -peptides correspond to minimum conformations of an amino acid constituent in the energetic Ramachandran plot. Thus, the right-handed helical structures in the third quadrant are completely missing.

In the meantime, numerous systematic investigations on the influence of the size of basis sets on peptide conformation indicate that the 6-31G\* split-valence basis, which considers polarization functions at all non-hydrogen atoms, provides rather satisfactory results. Enlargement of the basis set does not really improve the quality of the data. Therefore, this basis set was used throughout this work. Calculations at the Hartree-Fock level consider the exchange, but not the Coulomb correlation of the electrons. Fortunately, correlation effects do not play a

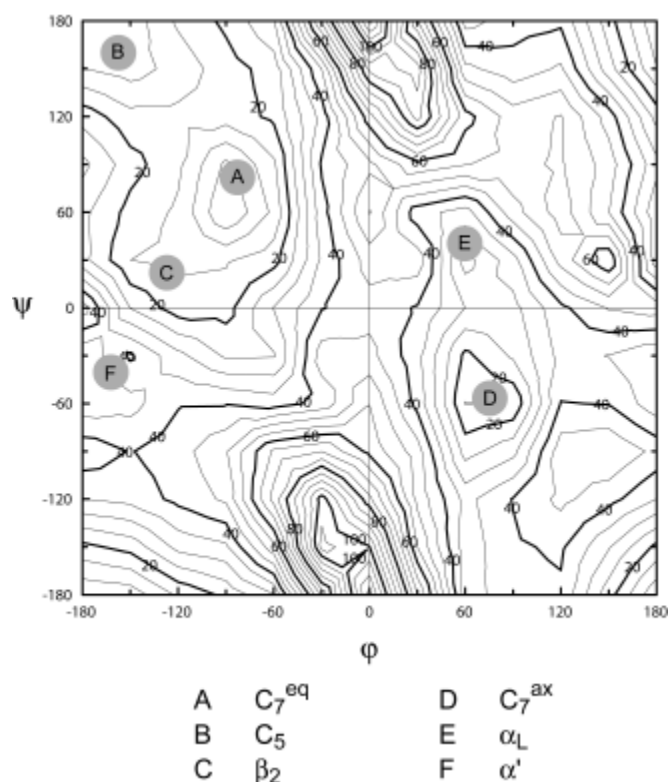


**Fig. 13.** Energetic Ramachandran plot calculated at the HF/6-31G\* level of ab initio MO theory. The basic minima for secondary structures are indicated in the plot.

significant role in conformation problems, which is also confirmed for peptide structures.<sup>118</sup> Nevertheless, the HF calculations in this work are mostly complemented by the application of the density functional theory (DFT)<sup>119,120</sup> selecting the B3LYP functional<sup>121,122</sup> to estimate the correlation effects. The optimum structures at all approximation levels were obtained by complete geometry optimization. In many cases the character of the conformers, which are minimum energy conformations, was confirmed by the calculation of the matrix of force constants. Knowledge on the force constants allows also the calculation of thermodynamic properties like free enthalpies, enthalpies and entropies.

It can be expected that the structure of peptides is influenced by solvents. Conventional ab initio MO theory describes the properties of the molecules only in vacuo. The description of solvent effects is a rather cumbersome matter. There are various approaches to solve this problem. They can be divided into models, which consider the solvent implicitly<sup>123-125</sup> or explicitly.<sup>126-128</sup> The explicit treatment of solvent molecules (supermolecule approximation) within ab initio MO theory is not realistic for the systems in this work. The implicit methods which describe the solvents as an unstructured dielectric continuum are better practicable, although all specific interactions get lost. Thus, the results of such calculations provide more the general trends of solvent influence. Their quantitative aspects should not be overestimated.

In this work two continuum approaches were employed:

- a quantum-mechanical Onsager-Self-Consistent-Reaction-Field (SCRF) model, which places the solute inside a spherical cavity. The electrostatic properties of the solute are projected to the cavity surface and interact with the solvent reaction field. The necessary radii of the sphere can be obtained from the molecular volumes or the Connolly molecular surface area.
- a Polarizable Continuum Model (PCM), which was introduced by Tomasi and co-workers, which calculates the molecular free energy of a solute in a solvent considering the exact shape of the solute.<sup>123,125</sup>

The electrostatic energies calculated in both models can be complemented by the cavitation energy and the van der Waals-London interactions (dispersion energy) between solute and solvent.<sup>123</sup>

The problems of continuum models could partially be overcome by so-called QM/MM models, which combine a quantum chemical (QM) description of the solute with a more or less great part of the nearest solvation shells with a molecular mechanical (MM) treatment of the remaining solvent molecules.<sup>126,127,129-132</sup> Despite all efforts in this important field, there is no really successful method of this type until now. The quantum chemical part is mostly realized via semi-empirical methods which have anyway considerable problems to describe the isolated peptide structures correctly. Besides, it is obviously a very delicate problem to describe the contact region between the pure quantum chemical and molecular mechanic parts of the system correctly.



## 1.5 Aim of this Work

It is intended in this work to describe various aspects of secondary structure formation in  $\alpha$ -,  $\beta$ -,  $\gamma$ -, and  $\delta$ -peptides by systematic conformational analyses employing the methods of ab initio MO theory. The studies should provide an overview on the secondary structure possibilities in homologous peptides and contribute to a better understanding of the origin of the various structure alternatives. It is of special interest to search for possibilities of a selective influencing of folding to derive rules which could be applied in a rational structure design. Based on the results, experimental work on peptide foldamers might be stimulated to create novel structure types. In detail, the focus is on the following aspects:

- (i) the possibilities of helix formation in  $\gamma$ -peptides (Chapter 2),<sup>73</sup>
- (ii) the direction of secondary structure formation in  $\gamma$ -peptides via insertion of (*E*)- or (*Z*)-double bonds (vinylogous  $\gamma$ -peptides in Chapters 2 and 3),<sup>73,133</sup>
- (iii) the extension of the foldamer concept to  $\delta$ -peptides and the search for secondary structure elements like helices, strands and turns (Chapter 4),<sup>48</sup>
- (iv) the extension of the ‘mixed’- or  $\beta$ -helix concept to the homologous  $\gamma$ - and  $\delta$ -peptides (Chapter 5),<sup>134</sup> and
- (v) the investigation of substituent effects in the homologous  $\alpha$ -,  $\beta$ - and  $\gamma$ -peptides on the formation of ‘mixed’- or  $\beta$ -helices and other helical structures (Chapter 6).<sup>135</sup>

## References

- (1) Anfinsen, C. B. *Science* **1973**, *181*, 223.
- (2) Anfinsen, C. B.; Scheraga, H. A. *Adv. Prot. Chem.* **1975**, *29*, 205.
- (3) Hruby, V. J. *Life Sci.* **1982**, *31*, 189.
- (4) Toniolo, C. *Int. J. Peptide Protein Res.* **1990**, *35*, 287.
- (5) Olson, G. L.; Bolin, D. R.; Bonner, M. P.; Bös, M.; Cook, C. M.; Fry, D. C.; Graves, B. J.; Hatada, M.; Hill, D. E.; Kahn, M.; Madison, V. S.; Rusiecki, V. K.; Sarabu, R.; Sepinwall, J.; Vincent, G. P.; Voss, M. E. *J. Med. Chem.* **1993**, *36*, 3039.
- (6) Giannis, A.; Kolter, T. *Angew. Chem. Int. Edit.* **1993**, *32*, 1244; *Angew. Chem.* **1993**, *105*, 1303.
- (7) Hruby, V. J.; Li, G.; Haskell-Luevano, C.; Shenderovich, M. *Biopolymers* **1997**, *43*, 219.
- (8) Martin, S. F.; Dorsey, G. O.; Gane, T.; Hillier, M. C.; Kessler, H.; Baur, M.; Mathä, B.; Erickson, J. W.; Bhat, T. N.; Munshi, S.; Gulnik, S. V.; Topol, I. A. *J. Med. Chem.* **1998**, *41*, 1581.
- (9) Martin, S. F.; Dwyer, M. P.; Hartmann, B.; Knight, K. S. *J. Org. Chem.* **2000**, *65*, 1305.
- (10) Hruby, V. J.; Balse, P. M. *Curr. Med. Chem.* **2000**, *7*, 945.
- (11) Perez, J. J.; Corcho, F.; Llorens, O. *Curr. Med. Chem.* **2002**, *9*, 2209.
- (12) David, R.; Richter, M. P. O.; Beck-Sickinger, A. G. *Eur. J. Biochem.* **2004**, *271*, 663.
- (13) Seebach, D.; Matthews, J. L. *J. Chem. Soc., Chem. Commun.* **1997**, *21*, 2015.
- (14) Gellman, S. H. *Acc. Chem. Res.* **1998**, *31*, 173.
- (15) Barron, A. E.; Zuckermann, R. N. *Curr. Opin. Chem. Biol.* **1999**, *3*, 681.
- (16) Hill, D. J.; Mio, M. J.; Prince, R. B.; Hughes, T. S.; Moore, J. S. *Chem. Rev.* **2001**, *101*, 3893.
- (17) Cheng, R. P.; Gellman, S. H.; DeGrado, W. F. *Chem. Rev.* **2001**, *101*, 3219.
- (18) Seebach, D.; Beck, A. K.; Bierbaum, D. J. *Chem. & Biodiv.* **2004**, *1*, 1111.
- (19) Voet, D.; Voet, J. G. *Biochemie*, VCH: Weinheim, New York, Basel, Cambridge, Tokyo, 1994.
- (20) Stryer, L. *Biochemie*, Spektrum, Akad. Verl.: Heidelberg, Berlin, Oxford, 1995.
- (21) Jakubke, H.-D. *Peptide*, Spektrum, Akad. Verl.: Heidelberg, Berlin, Oxford, 1996.

- (22) Morris, A. L.; MacArthur, M. W.; Hutchinson, E. G.; Thornton, J. M. *Proteins* **1992**, *12*, 345.
- (23) Richardson, J. S.; Richardson, D. S. In *Prediction of Protein Structure and the Principles of Protein Conformation*; Fasman, G. D., Ed.; Plenum Press: New York, London, 1989, p 1.
- (24) Toniolo, C.; Benedetti, E. *Trends Biochem. Sci.* **1991**, *16*, 350.
- (25) Ebert, G. *Biopolymere*; Teubner: Stuttgart, 1993.
- (26) Son, H. S.; Hong, B. H.; Lee, C. W.; Yun, S.; Kim, K. S. *J. Am. Chem. Soc.* **2001**, *123*, 514.
- (27) Venkatachalam, C. M. *Biopolymers* **1968**, *6*, 1425.
- (28) Möhle, K.; Gußmann, M.; Hofmann, H.-J. *J. Comput. Chem.* **1997**, *18*, 1414.
- (29) Toniolo, C. *CRC Crit. Rev. Biochem.* **1980**, *9*, 1.
- (30) De Santis, P.; Morosetti, S.; Rizzo, R. *Macromolecules* **1974**, *7*, 52.
- (31) Urry, D. W.; Goodall, M. C.; Glickson, J. D.; Mayers, D. F. *Proc. Natl. Acad. Sci. U. S. A.* **1971**, *68*, 1907.
- (32) Ramachandran, G. N.; Chandrasekaran, R. *Indian J. Biochem. Biophys.* **1972**, *9*, 1.
- (33) Ketchum, R. R.; Roux, B.; Cross, T. A. *Structure* **1997**, *5*, 1655.
- (34) Kovacs, F.; Quine, J.; Cross, T. A. *Proc. Natl. Acad. Sci. U. S. A.* **1999**, *96*, 7910.
- (35) Patch, J. A.; Kirshenbaum, K.; Seuryneck, S. L.; Zuckermann, R. N.; Barron, A. E. In *Pseudo-Peptides in Drug Discovery*; Nielsen, P. E., Ed.; WILEY-VCH: Weinheim, 2004, p 1.
- (36) Simon, R. J.; Kania, R. S.; Zuckermann, R. N.; Huebner, V. D.; Jewell, D. A.; Banville, S.; Ng, S.; Wang, L.; Rosenberg, S.; Marlowe, C. K.; Spellmeyer, D. C.; Tan, R. Y.; Frankel, A. D.; Santi, D. V.; Cohen, F. E.; Bartlett, P. A. *Proc. Natl. Acad. Sci. U. S. A.* **1992**, *89*, 9367.
- (37) Möhle, K.; Hofmann, H.-J. *J. Mol. Model.* **1996**, *2*, 307.
- (38) Moehle, K.; Hofmann, H.-J. *Biopolymers* **1996**, *38*, 781.
- (39) Armand, P.; Kirshenbaum, K.; Falicov, A.; Dunbrack, R. L. J.; Dill, K. A.; Zuckermann, R. N.; Cohen, F. E. *Fold. Des.* **1997**, *2*, 369.
- (40) Kirshenbaum, K.; Barron, A. E.; Goldsmith, R. A.; Armand, P.; Bradley, E. K.; Truong, K. T.; Dill, K. A.; Cohen, F. E.; Zuckermann, R. N. *Proc. Natl. Acad. Sci. U. S. A.* **1998**, *95*, 4303.

- (41) Gante, J. *Synthesis* **1989**, 6, 405.
- (42) Gante, J.; Krug, M.; Lauterbach, G.; Weitzel, R.; Hiller, W. *J. Peptide Sci.* **1995**, 1, 201.
- (43) Thormann, M.; Hofmann, H.-J. *J. Mol. Struct. (Theochem)* **1998**, 469, 63.
- (44) Rose, G. D.; Gierasch, L. M.; Smith, J. A. *Adv. Prot. Chem.* **1985**, 37, 1.
- (45) Radkiewicz, J. L.; McAllister, M. A.; Goldstein, E.; Houk, K. N. *J. Org. Chem.* **1998**, 63, 1419.
- (46) Banerjee, A.; Pramanik, A.; Bhattacharjya, S.; Balaram, P. *Biopolymers* **1996**, 39, 769.
- (47) Karle, I. L.; Pramanik, A.; Banerjee, A.; Bhattacharjya, S.; Balaram, P. *J. Am. Chem. Soc.* **1997**, 119, 9087.
- (48) Baldauf, C.; Günther, R.; Hofmann, H.-J. *J. Org. Chem.* **2004**, 69, 6214.
- (49) DeGrado, W. F.; Schneider, J. P.; Hamuro, Y. *J. Pept. Res.* **1999**, 54, 206.
- (50) Seebach, D.; Kimmerlin, T.; Sebesta, R.; Campo, M. A.; Beck, A. K. *Tetrahedron* **2004**, 60, 7455.
- (51) Hamuro, Y.; Schneider, J. P.; DeGrado, W. F. *J. Am. Chem. Soc.* **1999**, 121, 12200.
- (52) Gademann, K.; Ernst, M.; Hoyer, D.; Seebach, D. *Angew. Chem. Int. Edit.* **1999**, 38, 1223; *Angew. Chem.* **1999**, 111, 1302.
- (53) <http://www.foldamers.org>.
- (54) Banerjee, A.; Balaram, P. *Curr. Sci.* **1997**, 73, 1067.
- (55) Kirshenbaum, K.; Zuckermann, R. N.; Dill, K. A. *Curr. Opin. Struct. Biol.* **1999**, 9, 530.
- (56) Palomo, C.; Aizpurua, J. M.; Ganboa, I.; Oiarbide, M. *Amino Acids* **1999**, 16, 321.
- (57) Stigers, K. D.; Soth, M. J.; Nowick, J. S. *Curr. Opin. Chem. Biol.* **1999**, 3, 714.
- (58) Andrews, M. J. I.; Tabor, A. B. *Tetrahedron* **1999**, 55, 11711.
- (59) McReynolds, K. D.; Gervay-Hague, J. *Tetrahedron: Asymm.* **2000**, 11, 337.
- (60) North, M. *J. Pept. Sci.* **2000**, 6, 301.
- (61) Cubberley, M. S.; Iverson, B. L. *Curr. Opin. Chem. Biol.* **2001**, 5, 650.
- (62) Martinek, T. A.; Fülöp, F. *Eur. J. Biochem.* **2003**, 270, 3657.
- (63) Ghosh, I.; Chmielewski, J. *Curr. Opin. Chem. Biol.* **2004**, 8, 640.
- (64) Cheng, R. P. *Curr. Opin. Struct. Biol.* **2004**, 14, 512.

- (65) Sanford, A. R.; Yamato, K.; Yang, X. W.; Yuan, L. H.; Han, Y. H.; Gong, B. *Eur. J. Biochem.* **2004**, *271*, 1416.
- (66) Huc, I. *Eur. J. Org. Chem.* **2004**, 17.
- (67) Wu, Y.-D.; Wang, D.-P. *J. Am. Chem. Soc.* **1998**, *120*, 13485.
- (68) Wu, Y.-D.; Wang, D.-P. *J. Am. Chem. Soc.* **1999**, *121*, 9352.
- (69) Möhle, K.; Günther, R.; Thormann, M.; Sewald, N.; Hofmann, H.-J. *Biopolymers* **1999**, *50*, 167.
- (70) Günther, R.; Hofmann, H.-J.; Kuczera, K. *J. Phys. Chem. B* **2001**, *105*, 5559.
- (71) Günther, R.; Hofmann, H.-J. *Helv. Chim. Acta* **2002**, *85*, 2149.
- (72) Dado, G. P.; Gellman, S. H. *J. Am. Chem. Soc.* **1994**, *116*, 1054.
- (73) Baldauf, C.; Günther, R.; Hofmann, H.-J. *Helv. Chim. Acta* **2003**, *86*, 2573.
- (74) Appella, D. H.; Christianson, L. A.; Karle, I. L.; Powell, D. R.; Gellman, S. H. *J. Am. Chem. Soc.* **1996**, *118*, 13071.
- (75) Appella, D. H.; Christianson, L. A.; Karle, I. L.; Powell, D. R.; Gellman, S. H. *J. Am. Chem. Soc.* **1999**, *121*, 6206.
- (76) Barchi, J.; Huang, X.; Appella, D.; Christianson, L.; Durell, S.; Gellman, S. *J. Am. Chem. Soc.* **2000**, *122*, 2711.
- (77) Seebach, D.; Overhand, M.; Kühnle, F. N. M.; Martinoni, B.; Oberer, L.; Hommel, U.; Widmer, H. *Helv. Chim. Acta* **1996**, *79*, 913.
- (78) Seebach, D.; Ciceri, P. E.; Overhand, M.; Jaun, B.; Rigo, D.; Oberer, L.; Hommel, U.; Amstutz, R.; Widmer, H. *Helv. Chim. Acta* **1996**, *79*, 2043.
- (79) Hintermann, T.; Seebach, D. *Synlett* **1997**, 437.
- (80) Appella, D. H.; Christianson, L. A.; Klein, D. A.; Powell, D. R.; Huang, X.; Barchi, J., Jr.; Gellman, S. H. *Nature (London)* **1997**, *387*, 381.
- (81) Appella, D. H.; Christianson, L. A.; Klein, D. A.; Richards, M. R.; Powell, D. R.; Gellman, S. H. *J. Am. Chem. Soc.* **1999**, *121*, 7574.
- (82) Watterson, M. p.; Pickering, L.; Smith, M. D.; Hudson, S. J.; Marsh, P. R.; Mordaunt, J. E.; Watkin, D. J.; Newman, C. E.; Fleet, G. W. J. *Tetrahedron: Asymm.* **1999**, *10*, 1855.
- (83) Claridge, T. D. W.; Long, D. D.; Hungerford, N. L.; Aplin, R. T.; Smith, M. D.; Marquess, D. G.; Fleet, G. W. J. *Tetrahedron Lett.* **1999**, *40*, 2199.

- (84) Claridge, T. D. W.; Goodman, J. M.; Moreno, A.; Angus, D.; Barker, S. F.; Taillefumier, C.; Watterson, M. P.; Fleet, G. W. J. *Tetrahedron Lett.* **2001**, *42*, 4251.
- (85) Krauthäuser, S.; Christianson, L. A.; Powell, D. R.; Gellman, S. H. *J. Am. Chem. Soc.* **1997**, *119*, 11719.
- (86) Seebach, D.; Abele, S.; Gademann, K.; Jaun, B. *Angew. Chem. Int. Edit.* **1999**, *38*, 1595; *Angew. Chem.* **1999**, *111*, 1700.
- (87) Seebach, D.; Gademann, K.; Schreiber, J. V.; Matthews, J. L.; Hintermann, T.; Jaun, B. *Helv. Chim. Acta* **1997**, *80*, 2033.
- (88) Yang, D.; Ng, F.-F.; Li, Z.-J. *J. Am. Chem. Soc.* **1996**, *118*, 9794.
- (89) Yang, D.; Qu, J.; Li, W.; Wang, D. P.; Ren, Y.; Wu, Y. D. *J. Am. Chem. Soc.* **2003**, *125*, 14452.
- (90) Yang, D.; Qu, J.; Li, B.; Ng, F.-F.; Wang, X.-C.; Cheung, K.-K.; Wang, D.-P.; Wu, Y.-D. *J. Am. Chem. Soc.* **1999**, *121*, 589.
- (91) Wu, Y.; Wang, D.; Chan, K.; Yang, D. *J. Am. Chem. Soc.* **1999**, *121*, 11189.
- (92) Peter, C.; Daura, X.; van Gunsteren, W. F. *J. Am. Chem. Soc.* **2000**, *122*, 7461.
- (93) Guy, L.; Vidal, J.; Collet, A. *J. Med. Chem.* **1998**, *41*, 4833.
- (94) Cheguillaume, A.; Lehardy, F.; Bouget, K.; Baudy-Floc'h, M.; Le Grel, P. *J. Org. Chem.* **1999**, *64*, 2924.
- (95) Cheguillaume, A.; Salaun, A.; Sinbandhit, S.; Potel, M.; Gall, P.; Baudy-Floc'h, M.; Le Grel, P. *J. Org. Chem.* **2001**, *66*, 4923.
- (96) Günther, R.; Hofmann, H.-J. *J. Am. Chem. Soc.* **2001**, *123*, 247.
- (97) Moree, W. J.; Vandermarel, G. A.; Liskamp, R. J. *J. Org. Chem.* **1995**, *60*, 5157.
- (98) Monnee, M. C. F.; Marijne, M. F.; Brouwer, A. J.; Liskamp, R. M. J. *Tetrahedron Lett.* **2000**, *41*, 7991.
- (99) de Jong, R.; Rijkers, D. T. S.; Liskamp, R. M. J. *Helv. Chim. Acta* **2002**, *85*, 4230.
- (100) Allen, M. P. In *NIC Series - Computational Soft Matter: From Synthetic Polymers to Proteins*; Attig, N., Binder, K., Grubmüller, H., Kremer, K., Eds.; NIC-Directors: Jülich, 2004; Vol. 23, p 1.
- (101) Birner, P.; Hofmann, H.-J.; Weiss, C. *MO-theoretische Methoden in der organischen Chemie*; Akademie-Verlag: Berlin, 1979.

- (102) Scholz, M.; Köhler, H.-J. *Quantenchemie*, VEB Deutscher Verlag der Wissenschaften: Berlin, 1981; Vol. 3.
- (103) Schmidtke, H.-H. *Quantenchemie*, 2 ed.; VCH Verlagsgesellschaft mbH: Weinheim-New York-Basel-Cambridge-Tokyo, 1994.
- (104) Hehre, W. J.; Radom, L.; Schleyer, P. v. R.; Pople, J. A. *Ab initio Molecular Orbital Theory*, John Wiley & Sons: New York, 1986.
- (105) Pople, J. A.; Beveridge, D. L. *Approximate Molecular Orbital Theory*, McGraw Hill: New York, 1970.
- (106) Möhle, K.; Hofmann, H.-J.; Thiel, W. *J. Comput. Chem.* **2001**, *22*, 509.
- (107) Sellers, H. L.; Schäfer, L. *Chem. Phys. Lett.* **1979**, *63*, 609.
- (108) Schäfer, L.; Vanalsenoy, C.; Scarsdale, J. N.; Klimkowski, V. J.; Ewbank, J. D. *J. Comput. Chem.* **1981**, *2*, 410.
- (109) Vanalsenoy, C.; Scarsdale, J. N.; Schäfer, L. *J. Mol. Struct. (Theochem)* **1982**, *7*, 297.
- (110) Siam, K.; Klimkowski, V. J.; Ewbank, J. D.; Vanalsenoy, C.; Schäfer, L. *J. Mol. Struct. (Theochem)* **1984**, *19*, 171.
- (111) Head-Gordon, T.; Head-Gordon, M.; Frisch, M. J.; Brooks III., C. L.; Pople, J. A. *J. Am. Chem. Soc.* **1991**, *113*, 5989.
- (112) Ramek, M.; Cheng, V. K. W.; Frey, R. F.; Newton, S. Q.; Schäfer, L. *J. Mol. Struct. (Theochem)* **1991**, *81*, 1.
- (113) Frey, R. F.; Coffin, J.; Newton, S. Q.; Ramek, M.; Cheng, V. K. W.; Momany, F. A.; Schäfer, L. *J. Am. Chem. Soc.* **1992**, *114*, 5369.
- (114) Böhm, H.-J.; Brode, S. *J. Am. Chem. Soc.* **1991**, *113*, 7129.
- (115) Gould, I. R.; Kollmann, P. A. *J. Phys. Chem.* **1992**, *96*, 9255.
- (116) Rommel-Möhle, K.; Hofmann, H.-J. *J. Mol. Struct. (Theochem)* **1993**, *285*, 211.
- (117) Baldauf, C.; Günther, R.; Hofmann, H.-J. *J. Mol. Struct. (Theochem)* **2004**, *675*, 19.
- (118) Möhle, K.; Hofmann, H.-J. *J. Mol. Model.* **1998**, *4*, 53.
- (119) Parr, R. G.; Yang, W. *Density-Functional Theory of Atoms and Molecules*, Oxford University Press: Oxford, 1989.
- (120) Kohn, W.; Sham, L. J. *Phys. Rev. A* **1965**, *140*, 1133.

- (121) Becke, A. D. *J. Chem. Phys.* **1988**, *88*, 1053.
- (122) Becke, A. D. *Phys. Rev. A* **1988**, *38*, 3098.
- (123) Tomasi, J.; Persico, M. *Chem. Rev.* **1994**, *94*, 2027.
- (124) Vreven, T.; Mennucci, B.; da Silva, C. O.; Morokuma, K.; Tomasi, J. *J. Chem. Phys.* **2001**, *115*, 62.
- (125) Tomasi, J.; Cammi, R.; Mennucci, B.; Cappelli, C.; Corni, S. *Phys. Chem. Chem. Phys.* **2002**, *4*, 5697.
- (126) Gao, J. L.; Xia, X. F. *Science* **1992**, *258*, 631.
- (127) Gao, J. L. *J. Phys. Chem.* **1992**, *96*, 6432.
- (128) Levy, R. M.; Gallicchio, E. *Annu. Rev. Phys. Chem.* **1998**, *49*, 531.
- (129) Gao, J. L. *J. Phys. Chem.* **1992**, *96*, 537.
- (130) Bakowies, D.; Thiel, W. *J. Phys. Chem.* **1996**, *100*, 10580.
- (131) Gogonea, V.; Suarez, D.; van der Vaart, A.; Merz, K. W. *Curr. Opin. Struct. Biol.* **2001**, *11*, 217.
- (132) Schlegel, H. B. *J. Comput. Chem.* **2003**, *24*, 1514.
- (133) Baldauf, C.; Günther, R.; Hofmann, H.-J. *J. Org. Chem.* **2005**, *70*, in press.
- (134) Baldauf, C.; Günther, R.; Hofmann, H.-J. *Angew. Chem. Int. Edit.* **2004**, *43*, 1594; *Angew. Chem.* **2004**, *116*, 1621.
- (135) Baldauf, C.; Günther, R.; Hofmann, H.-J. *Biopolymers* **2005**, in press.

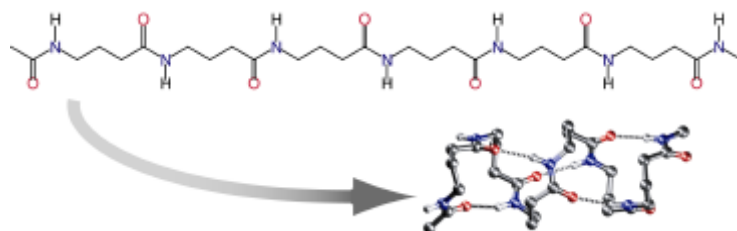


## 2 Helix Formation and Folding in $g$ -Peptides and Their Vinylogues

by Carsten Baldauf, Robert Günther, and Hans-Jörg Hofmann

published in HELVETICA CHIMICA ACTA

Vol. 86 (2003) pages 2573-2588



**Abstract.** A complete overview of all possible periodic structures with characteristic H-bonding patterns is provided for oligomers composed of  $g$ -amino acids ( $g$ -peptides) and their vinylogues by a systematic conformational search on hexamer model compounds employing *ab initio* MO theory at various levels of approximation (HF/6-31G\*, DFT/B3LYP/6-31G\*, SCRF/HF/6-31G\*, PCM//HF/6-31G\*). A wide variety of structure alternatives with definite backbone conformations and H-bonds formed in forward and backward directions along the sequence was found in this class of foldamers. All formally conceivable H-bonded pseudocycles between 7- and 24-membered rings are predicted in the periodic hexamer structures, which are mostly helices. The backbone elongation in comparison to  $a$ - and  $b$ -peptides allows several possibilities to realize identical H-bonding patterns. In good agreement with experimental data, helical structures with 14- and 9-membered pseudocycles are most stable. It is shown that the introduction of an (*E*)-double bond into the backbone of the  $g$ -amino acid constituents, which leads to vinylogous  $g$ -amino acids, supports the folding into helices with larger H-bonded pseudocycles in the resulting vinylogous  $g$ -peptides. Due to the considerable potential of secondary structure formation,  $\gamma$ -peptides and their vinylogues might be useful tools in peptide and protein design and even in material sciences.

## Introduction

The imitation and the improvement of structural features of peptides and proteins are great challenges for chemists and biochemists. The application of native peptides for pharmacological and pharmaceutical purposes often suffers from their insufficient resistance to proteases and their unfavorable transport properties. Besides, better selectivity for different receptor subtypes is desired [1,2]. It is an old idea to solve these problems by substitution of non-proteinogenic amino acids for one or several natural amino acids in the sequence. In the last years, the consistent extension of this idea led to the search for oligomers that are composed only of non-proteinogenic amino acids [3-11]. Since protein and peptide structures are essentially determined by characteristic secondary-structure elements such as helices, sheets, and turns, the modified compounds still have to reflect the steric and electronic properties of their native counterparts to keep or even to improve the biological activity. Consequently, such oligomers should be able to form definite backbone conformations.

All these efforts to develop efficient peptidomimetics could be considered as part of a general search for oligomers built from 'any' chemical monomer unit that folds into definite conformational states. The term foldamer was suggested for such structures [4]. It is obvious that this concept goes far beyond the structural imitation of peptides or the other two major backbones of biopolymers, ribonucleic acids and polysaccharides, even if peptidomimetics remain a topic of outstanding interest [4-11]. Due to the wide variety of chemical monomer units, foldamers with specific properties could be expected, which might be interesting in other fields as, for instance, in material sciences.

Very interesting and surprising results were obtained for oligomers composed of **b**-amino acids (**b**-peptides). In comparison to **a**-amino acids, each **b**-amino acid constituent contributes an additional CH<sub>2</sub> group to the backbone. Contrary to original assumptions of higher conformational flexibility in the backbone that could prevent the formation of ordered structures, several elements of secondary structure have been found [4,9-11]. Most impressive were diverse helix types with H-bonded pseudocycles of different sizes. One of these helices, a 2.5<sub>1</sub> helix with 12-membered pseudocycles (C<sub>12</sub>) [12-14], corresponds to the familiar **a**-helix in the **a**-peptides by the backward direction of the H-bonds between the peptidic NH group of amino acid *i* and the peptidic CO group of amino acid (*i* - 3) along the sequence (1←4 interaction). But, different from native peptides and proteins, there are also **b**-peptide helices forming the H-bonds in the forward direction, such as a 3<sub>1</sub> helix with H-bonds arranged in 14-membered pseudocycles (C<sub>14</sub>)

between the NH group of amino acid  $i$  and the CO group of amino acid  $(i+2)$  ( $1\rightarrow 3$  interaction) [14-16]. Even periodically alternating helices, sometimes called 'mixed' helices, were found, where two different pseudocycles, *e.g.*, 10- and 12-membered, are alternating with their H-bonds in the forward and backward directions along the sequence [17-19]. Apart from the various helix types, **b**-peptides are also able to realize sheet- and turn-like structures [20-24]. Thus, it is not surprising that foldamer characteristics could be predicted and experimentally confirmed in **b**-peptide derivatives such as hydrazino [25,26] and aminoxy peptides [27-30]. Moreover, it can be expected that further homologation of the monomer unit leading to **g**-amino acids makes well-defined backbone conformations in the corresponding **g**-peptides also possible.

Formal possibilities of H-bonding in **g**-peptides are illustrated in *Fig. 1,a*. Obviously, competition between periodic structure alternatives with nearest-neighbor ( $C_7$  and  $C_9$  pseudocycles) and non-nearest-neighbor H-bonds with larger H-bonded pseudocycles ( $C_{12}$ ,  $C_{14}$ , and higher) could be expected. Some of these structures were confirmed in experimental studies. Thus, early investigations on polymers of **g**-linked D-glutamic acid, which is the main constituent of the capsule of *Bacillus anthracis*, indicated helical structures with 17- or 19-membered H-bonded pseudocycles [31]. Recently, it has been reported that unsubstituted **g**-amino acids adopt  $C_9$ -conformations [32]. Other studies show that substituents at the **g**-peptide backbone favor the formation of helices with 14-membered pseudocycles [33-39].

$C_7$  pseudocycles are defined by an interaction between the peptidic NH and CO groups within the same monomer constituent ( $1\rightarrow 1$  interaction), whereas the  $C_9$  pseudocycles are formed between the two amino acids adjacent to a monomer unit ( $1\leftarrow 3$  interaction). Oligomeric structures of **a**- and **b**-peptides with closer H-bonded pseudocycles tend more to the formation of sheet- or ribbon-like structures, whereas helices are more probable in structures with larger pseudocycles. In **g**-peptides, structures with nearest-neighbor H-bonds could possibly be more favored relative to their non-nearest-neighbor H-bonded counterparts than in **a**- and **b**-peptides. The backbone elongation improves the possibilities for an effective orientation of the H-bond donor and acceptor parts in the closer pseudocycles [32]. An interesting idea to avoid the formation of smaller pseudocycles and to favor *a priori* helices with larger pseudocycles could be the introduction of an (*E*)-double bond between the C(**a**) and C(**b**) atoms of the **g**-amino acid constituents, which rigidifies the backbone and restricts the conformational possibilities [40]. The scheme of the possible H-bonding patterns in the corresponding vinylogous **g**-peptides (*Fig. 1,b*) shows that the formation of the smaller H-bonded pseudocycles becomes impossible by this type of modification. Vinylogous **g**-amino acids are synthetically accessible [41,42]. Their introduction

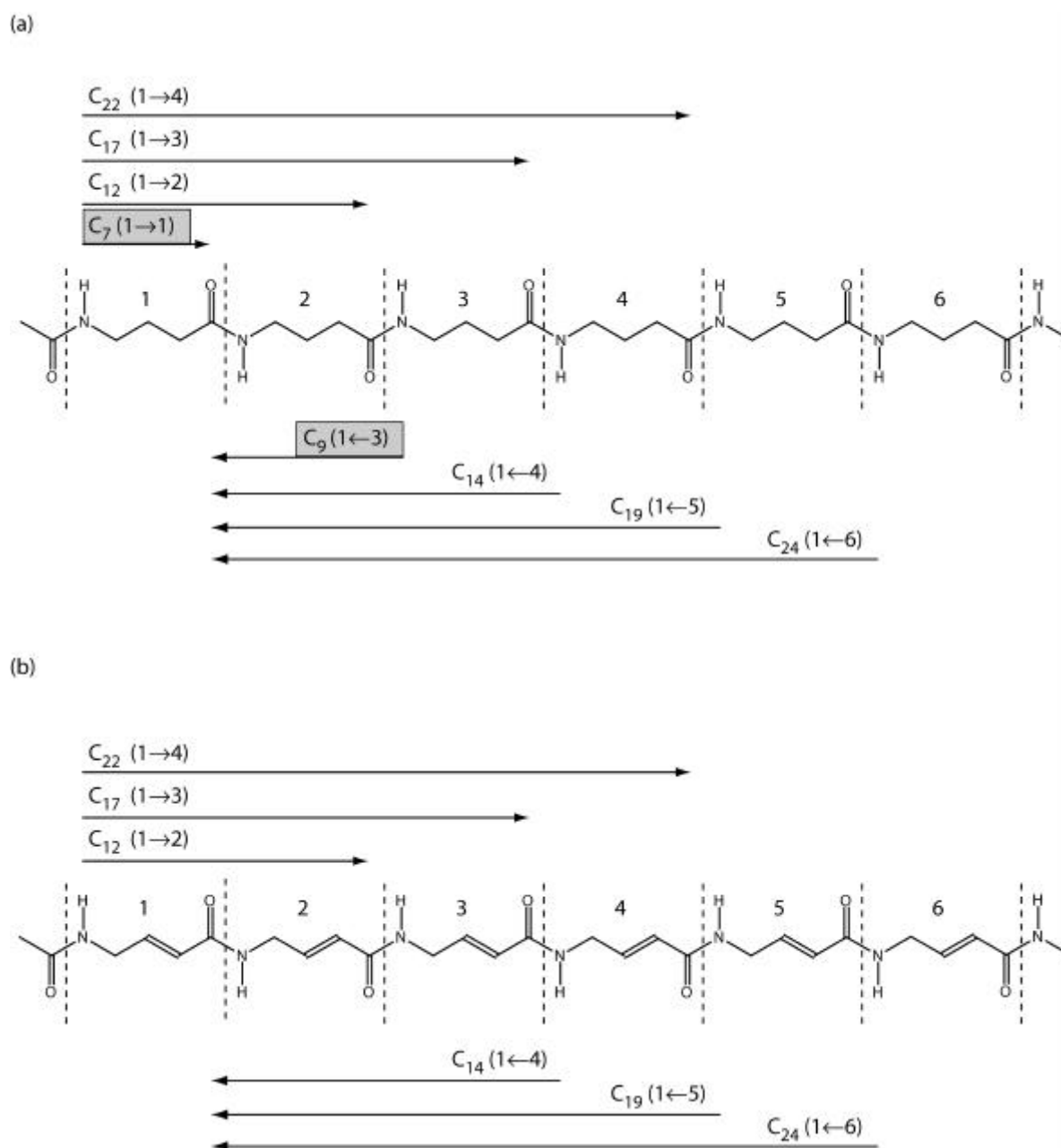


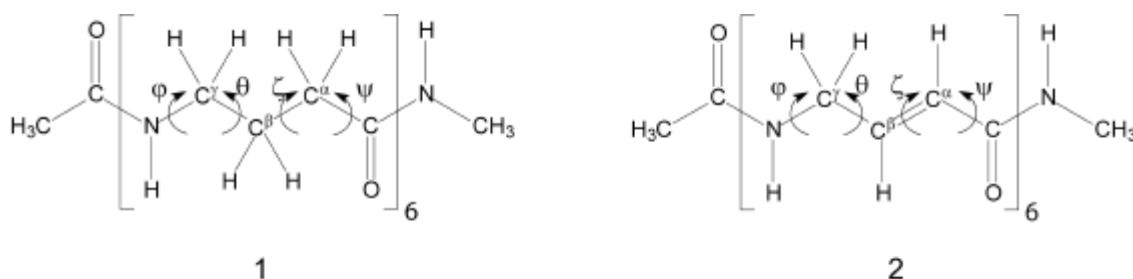
**Fig. 1.** Possible H-bonding patterns in  $g$ -peptides (a) and their vinylogues (b). Nearest neighbor H-bonded pseudocycles  $C_7$  and  $C_9$  are highlighted.

into  $\alpha$ -peptide sequences as monomer constituents was successfully performed and some oligomers were also synthesized [43,44], but structural data for the oligomers have not been available until now.

In the last years, numerous quantum chemical conformational analyses of non-proteinogenic amino acids and their oligomers were reported [26,28,45-59]. The *ab initio* MO methods employed proved to be reliable tools to obtain a rather complete overview on the possibilities of secondary-structure formation in these classes of compounds. In this study, we want to extend our investigations to  $g$ -peptides and their vinylogues and focus especially on ordered periodic structures with characteristic H-bonding patterns.

## Methods

Numerous studies show that the major types of secondary structure elements in *a*- and *b*-peptides and their derivatives can be deduced from the conformer pool of the blocked monomer constituents, even when H-bonding is still impossible in the monomer unit [26,28,45-68]. Nonetheless, it cannot be excluded that higher ordered structures exist, but become only possible in longer sequences by cooperativity effects. Therefore, such a monomer approach has to be complemented by conformational searches on oligomer structures, as it was shown in some molecular-dynamics studies on various peptidomimetics [30,69-74]. Here, we employ another strategy to find all periodic structures with specific H-bond patterns. Periodic conformations of the blocked  $\gamma$ -peptide hexamer **1** were generated by a systematic variation of the backbone torsion angles *j*, *q*, *z*, and *y* in each monomer constituent between  $-150^\circ$  and  $180^\circ$  in steps of  $30^\circ$ . The torsion angles *w* of the peptide bonds were set to values of  $-165^\circ$ ,  $180^\circ$ , and  $165^\circ$ , respectively. From the resulting pool of *ca.* 36,000 conformations, we selected those fitting into possible periodic H-bonding patterns up to 24-membered H-bonded pseudocycles according to general geometry criteria of H-bonds. These structures were starting points for geometry optimizations at the HF/6-31G\* level of *ab initio* MO theory [75].



All conformers that retained the periodic H-bonding patterns were reoptimized at the B3LYP/6-31G\* approximation level of density functional theory (DFT) to estimate the influence of electron correlation energy [76,77]. The same procedure was employed for the corresponding vinylogous *g*-peptide hexamer **2** with exception that the torsion angles *z* were assigned the same values as the angles *w* because of the approximately planar arrangement at the (*E*)-double bond. Thus, the pool of starting conformations is reduced to *ca.* 9,000 conformations in this case.

Since some solvation influence could be expected on peptide structures, an estimation of medium effects was performed employing the *Onsager* self-consistent-reaction-field (SCRF) model and the polarizable-continuum model (PCM), respectively [78-80]. The geometries of the HF/6-31G\* minima were the starting points in both cases. Whereas the starting structures in the SCRF/HF/6-31G\* calculations were subject to complete geometry optimization, the PCM energies arise from single-point calculations (PCM//HF/6-31G\*). The PCM energies were not

available for all conformers, probably because of by inconsistencies of the formalism resulting from delicate surface-area problems in some cases. To simulate an aqueous environment, the dielectric constant was set to  $\epsilon = 78.4$ . The radii of the solute molecules necessary within the SCRF model were estimated from the *Conolly* surface areas of the gas-phase monomers. Even if both models neglect specific solute-solvent interactions, the results might be considered as a first estimation of the general trend of solvation influence.

All quantum chemical calculations were performed employing the GAUSSIAN98 [81] and GAMESS-US [82] program packages.

## Results and Discussion

The *Tables 1* and *2* provide information on the backbone torsion angles  $\mathbf{j}$ ,  $\mathbf{q}$ ,  $\mathbf{z}$ , and  $\mathbf{y}$  of all periodic minimum conformations of the blocked  $\mathbf{g}$ -peptide hexamer **1** with H-bonding patterns in the forward and backward direction obtained at the HF/6-31G\* level of *ab initio* MO theory. The corresponding data at further levels of approximation (B3LYP/6-31G\*, SCRF/HF/6-31G\*) are part of the *Supplementary Material*. In the following paragraphs, the symbol  $H_x$  denotes the general helix type with the index  $x$  giving the size of the H-bonded pseudocycles  $C_x$ . The bold face notation  $\mathbf{H}_x$  ( $\mathbf{vH}_x$  in the case of vinylogous  $\gamma$ -peptides) stands for an actual conformer of this type. Regarding the torsion angle values in all conformers in detail,  $\mathbf{j}$  corresponds to *anti-clinal* (*ac*) [83] and *syn-clinal* (*sc*), and, in a few cases, also to *anti-periplanar* (*ap*) orientations. The two central torsion angles  $\mathbf{q}$  and  $\mathbf{z}$  correspond only to *sc* and *ap* arrangements. The torsion angle  $\mathbf{y}$  exhibits values for all three mentioned conformation types (*ac*, *ap*, *sc*).

Referring to the scheme of H-bond possibilities in *Fig. 1,a*, it is striking that all pseudocycles between  $C_7$  and  $C_{24}$  can be realized in ordered periodic structures. *Fig. 2* shows the most stable hexamer structure for each pseudocycle type. In the majority of cases, several alternatives exist for the same pseudocycle, which is demonstrated for the  $H_7$ ,  $H_{12}$ , and  $H_{14}$  helices in *Fig. 3*. This is not surprising for the structures with the nearest-neighbor H-bonded pseudocycles  $C_7$  and  $C_9$ . If there are several minimum-energy conformations with these pseudocycle types in the monomer constituents, the same or different of them may be arranged in periodic and aperiodic oligomers. This is already known from the  $\mathbf{b}$ -peptides, where several oligomeric structures with nearest neighbor H-bonded pseudocycles could be localized [23,24,53,69] whereas the larger pseudocycles are only present in singular periodic oligomers [12-16]. Obviously, the homologation in the monomer constituents opens up the possibility for conformational alternatives in the larger pseudocycles, too. In numerous cases, structure alternatives with

**Table 1.** Backbone Torsion Angles of Conformers of the Blocked **g**-Peptide Hexamer **1** with H-Bonds Formed in the Forward Direction Obtained at the HF/6-31G\* Level of *ab initio* MO Theory <sup>a</sup>

Conf.	<i>j</i>	<i>q</i>	<i>z</i>	<i>y</i>	Conf.	<i>j</i>	<i>q</i>	<i>z</i>	<i>y</i>
<b>H<sub>7</sub><sup>I</sup></b>	178.2	-64.1	91.4	158.4	<b>H<sub>17</sub><sup>I</sup></b>	77.4	70.9	-76.8	152.2
	179.5	-65.1	91.0	155.9		81.7	67.5	-79.8	145.5
	-179.7	-65.2	91.0	154.6		84.7	64.3	-167.0	-175.9
	-179.9	-65.3	90.8	155.0		75.8	65.8	-80.6	149.2
	-179.8	-65.4	90.7	155.5		78.5	60.4	-171.2	-168.6
	177.9	-65.4	88.8	163.2		75.4	66.4	-72.9	137.4
<b>H<sub>7</sub><sup>II</sup></b>	-89.1	-48.8	-50.9	-101.6	<b>H<sub>17</sub><sup>II</sup></b>	120.1	-56.2	73.0	58.9
	-93.6	-48.6	-50.4	-103.6		-168.3	178.6	63.2	60.0
	-94.4	-48.4	-50.1	-103.6		155.0	-69.9	75.5	58.0
	-94.6	-48.3	-50.1	-103.9		170.7	-169.5	74.3	90.7
	-94.7	-48.3	-50.2	-104.3		140.0	-71.8	73.5	63.5
	-92.9	-48.7	-50.4	-102.1		119.1	-179.6	69.1	-168.4
<b>H<sub>12</sub><sup>I</sup></b>	78.9	68.5	-77.1	147.0	<b>H<sub>22</sub><sup>I</sup></b>	146.5	177.3	179.7	98.7
	85.7	70.2	-76.8	144.8		85.3	177.0	178.6	89.8
	87.0	70.1	-76.9	145.6		78.6	178.9	180.0	90.6
	86.3	69.9	-77.1	147.5		82.9	178.9	-177.1	97.7
	85.9	69.3	-78.6	151.4		79.4	177.5	173.8	96.2
	84.1	66.3	-73.9	135.3		78.8	-176.2	173.8	157.0
<b>H<sub>12</sub><sup>II</sup></b>	123.1	-59.9	76.3	58.9	<b>H<sub>22</sub><sup>II</sup></b>	91.8	66.4	-176.6	-157.5
	155.4	-67.2	77.3	63.2		81.6	65.1	-170.8	-174.3
	156.6	-69.2	75.5	67.4		77.3	64.4	-165.1	-168.3
	154.2	-69.0	75.9	68.4		78.7	63.8	-169.2	-166.3
	151.9	-68.0	77.2	67.1		75.1	62.7	-167.6	-163.2
	150.6	-66.1	76.3	63.8		74.8	65.1	-167.8	-107.3

<sup>a</sup> Torsion angles in degrees.

identical H-bonding patterns exhibit the values for the torsion angles *j*, *q*, *z*, and *y* in reversed order, *e.g.*, **H<sub>12</sub><sup>I</sup>/H<sub>12</sub><sup>II</sup>**, **H<sub>14</sub><sup>II</sup>/H<sub>14</sub><sup>III</sup>**, and others (Tables 1 and 2). A comparison of the torsion angles of some representatives with the same H-bond orientations shows strong interrelationships, *e.g.*, **H<sub>9</sub><sup>I</sup>/H<sub>14</sub><sup>I</sup>/H<sub>19</sub><sup>I</sup>**, **H<sub>14</sub><sup>II</sup>/H<sub>19</sub><sup>II</sup>**, and **H<sub>14</sub><sup>III</sup>/H<sub>19</sub><sup>III</sup>**, respectively. This is similar to the situation in **a**-peptides concerning the relation between the **a**- and  $3_{10}$ -helices there. Thus, the possibility of interconversion between such structures has to be considered, in particular in the case of small energy differences. A special comment is deserved for the two helices with the 17-membered pseudocycles **H<sub>17</sub><sup>I</sup>** and **H<sub>17</sub><sup>II</sup>**. The values of the two central torsion angles *q* and *z* are not the same in all monomer constituents as it is demanded for periodic structures, but are alternating. Interestingly, these alternating values correspond to those in the periodic H<sub>12</sub> and H<sub>22</sub> hexamers with the smaller and larger pseudocycles, respectively, which have the same direction of H-bond

**Table 2.** Backbone Torsion Angles of Conformers of the Blocked  $g$ -Peptide Hexamer **1** with H-Bonds Formed in Backward Direction Obtained at the HF/6-31G\* Level of *ab initio* MO Theory <sup>a</sup>

Conf.	<i>j</i>	<i>q</i>	<i>z</i>	<i>y</i>	Conf.	<i>j</i>	<i>q</i>	<i>z</i>	<i>y</i>
<b>H<sub>9</sub><sup>I</sup></b>	98.7	-69.5	-75.5	99.3	<b>H<sub>19</sub><sup>I</sup></b>	118.4	-65.5	-71.1	179.1
	97.4	-69.7	-75.2	97.0		168.1	-64.6	-69.1	164.0
	97.4	-69.6	-75.1	97.0		148.1	-64.7	-68.7	160.1
	97.5	-69.6	-75.2	97.0		172.3	-67.5	-70.2	159.9
	97.5	-69.8	-75.3	97.1		154.1	-63.5	-69.8	160.1
	98.4	-70.5	-74.5	100.1		170.2	-64.7	-71.4	161.8
<b>H<sub>9</sub><sup>II</sup></b>	75.1	-161.2	72.9	4.5	<b>H<sub>19</sub><sup>II</sup></b>	72.7	64.2	-170.9	148.4
	75.0	-161.3	73.5	3.1		70.9	61.8	-165.3	148.9
	74.8	-161.1	73.4	3.3		73.1	64.9	-169.2	150.6
	74.9	-161.2	73.5	3.1		75.5	63.8	171.8	139.3
	74.8	-161.6	73.2	3.9		78.1	62.8	-172.8	153.3
	74.9	-162.9	72.5	5.4		83.0	59.1	171.7	147.5
<b>H<sub>9</sub><sup>III</sup></b>	44.8	52.2	-157.9	65.3	<b>H<sub>19</sub><sup>III</sup></b>	123.1	179.5	64.2	87.8
	43.6	52.3	-156.2	64.1		139.1	-173.5	64.4	80.7
	43.9	52.1	-155.6	64.1		125.9	-174.7	63.1	78.1
	44.4	51.9	-155.4	63.8		146.3	-176.4	62.2	76.4
	44.5	51.9	-155.9	64.3		134.0	-172.0	62.6	70.8
	46.9	51.7	-156.6	70.6		151.5	-175.8	64.3	70.6
<b>H<sub>14</sub><sup>I</sup></b>	106.1	-62.6	-67.5	165.6	<b>H<sub>24</sub><sup>I</sup></b>	-133.3	-176.5	-65.8	-93.8
	136.5	-63.2	-68.2	138.3		-137.9	-174.8	-66.9	-103.0
	138.0	-60.1	-65.1	141.4		-154.8	176.4	-69.0	-103.5
	132.9	-61.0	-66.0	144.4		-105.2	-177.4	-64.9	-90.6
	135.3	-63.4	-66.7	143.0		-174.6	-178.8	-63.0	-68.5
	138.3	-61.0	-64.1	139.7		-166.4	178.9	-61.8	-66.4
<b>H<sub>14</sub><sup>II</sup></b>	-64.5	-60.1	154.9	-118.2	<b>H<sub>24</sub><sup>II</sup></b>	75.4	175.9	165.9	81.4
	-64.4	-59.3	156.1	-118.5		72.8	177.9	167.7	83.2
	-64.2	-59.1	153.3	-117.2		75.6	174.8	166.9	53.3
	-62.8	-58.6	155.1	-120.7		82.4	173.8	175.4	85.5
	-68.5	-61.2	159.9	-108.3		78.7	175.5	171.6	65.6
	-73.8	-58.9	175.1	-126.3		81.1	175.3	172.0	66.0
<b>H<sub>14</sub><sup>III</sup></b>	95.2	-169.4	64.9	81.8					
	98.9	-165.4	61.1	70.4					
	108.8	-163.7	62.2	68.7					
	104.6	-163.2	62.7	70.3					
	104.4	-164.5	59.8	67.0					
	122.3	-169.5	65.0	45.6					

<sup>a</sup> Torsion angles in degrees.

formation. Nonetheless, the C<sub>17</sub> pseudocycle is maintained. All attempts to localize a completely periodic H<sub>17</sub> structure failed. Obviously, the C<sub>17</sub> H-bond pattern cannot periodically be kept in  $g$ -



peptides. This could be a hint that the possibility to keep special H-bonding patterns with alternative backbone conformations in the monomer constituents increases with proceeding homologation. Thus, completely aperiodic or alternating structures for the same H-bonding

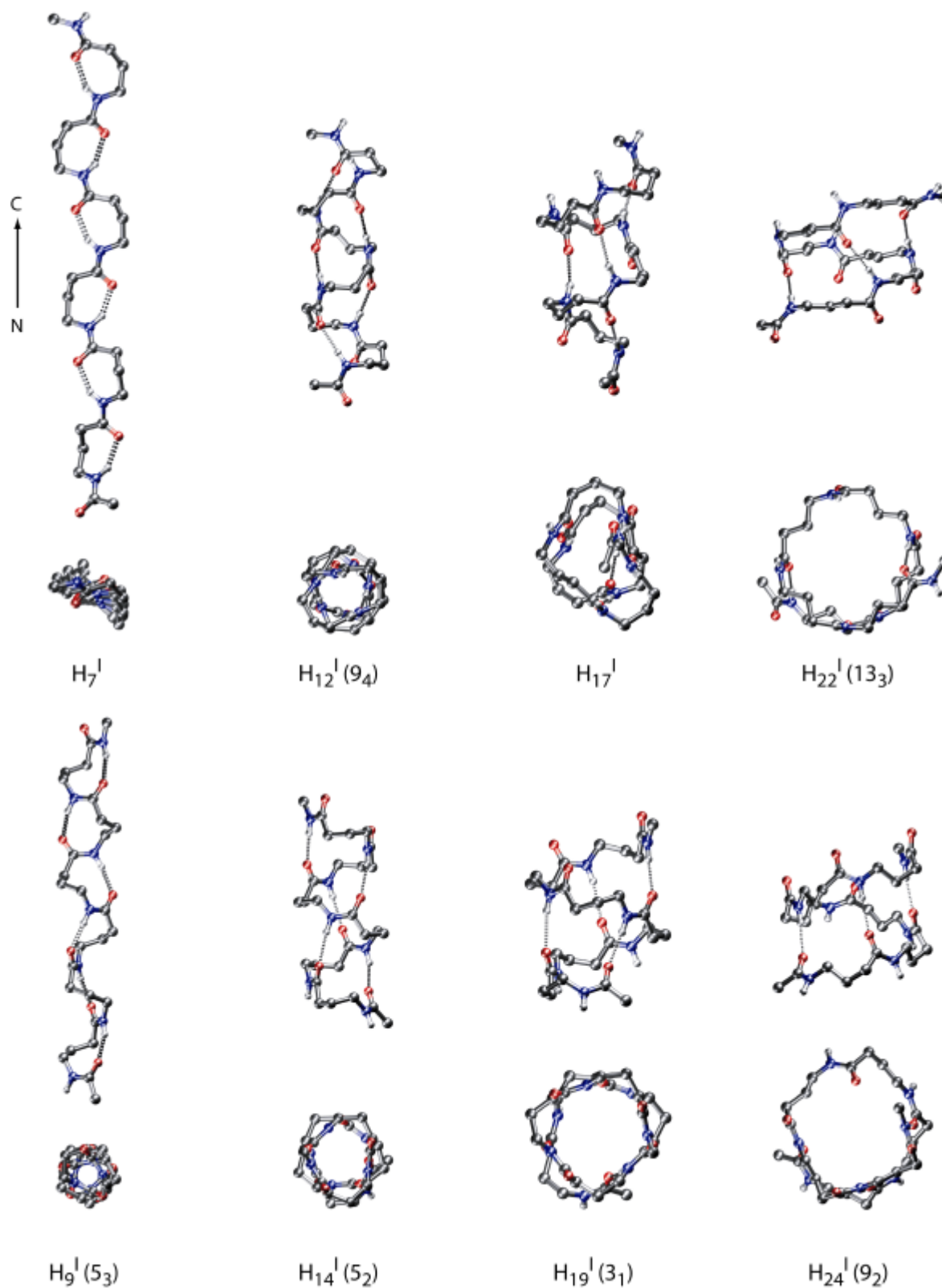


**Fig. 2.** Most-stable periodic structures of hexamer **1** for each type of H-bonded pseudocycle obtained at the HF/6-31G\* level of *ab initio* MO theory. (helix nomenclature in parentheses)

patterns become stronger competitive to periodic secondary structures.

According to the energy data in Table 3, the most stable hexamer is  $\mathbf{H}_{14}^I$  followed by  $\mathbf{H}_9^I$ , which is only by 5.8 kJ/mol less stable, and  $\mathbf{H}_{12}^I$  with 21.8 kJ/mol above  $\mathbf{H}_{14}^I$  at the HF/6-31G\* level of *ab initio* MO theory. The other alternatives are distinctly more unstable, but one has to keep in mind that only three pseudocycles can be formed in  $H_{22}$  and  $H_{24}$  helices in comparison to five H-bonds in  $H_{12}$  and  $H_{14}$  helices. The  $\mathbf{H}_{14}^I$  helix corresponds to the 2.6<sub>1</sub>-helix suggested by the groups of Seebach and co-workers [35-37] and Hanessian *et al.* [38,39]. It differs from the 3<sub>1</sub>-helix with 14-membered pseudocycles in the *b*-peptides above all by the opposite direction of H-bond formation, which is the same as in *a*-peptides. There is a rather perfect agreement between the calculated torsion angles and those from the crystal structure analysis of a substituted *g*-peptide tetramer [36,37]. Considering the small energy difference between  $\mathbf{H}_{14}^I$  and  $\mathbf{H}_9^I$  and remembering the strong geometric relatedness between these two conformers (Tables 2 and 3, Fig. 2), rapid interconversion of these helices may occur. It was already mentioned that the closer pseudocycles

**Table 3.** Relative Energies of the Conformers of the Blocked *g*-Peptide Hexamer **1** Obtained at Various Levels of *ab initio* MO Theory <sup>a</sup>

Conf.	<i>DE</i>			
	HF/6-31G*	B3LYP/6-31G*	SCRF/HF/6-31G* <sup>b)</sup>	PCM//HF/6-31G* <sup>b)</sup>
$\mathbf{H}_7^I$	34.6	31.4	42.1	n.a. <sup>c)</sup>
$\mathbf{H}_7^{II}$	48.4	57.3	107.0	n.a.
$\mathbf{H}_9^I$	5.8	<b>0.0</b> <sup>d)</sup>	33.8	13.3
$\mathbf{H}_9^{II}$	50.7	46.0	48.8	47.3
$\mathbf{H}_9^{III}$	125.1	129.6	158.7	126.2
$\mathbf{H}_{12}^I$	21.8	30.6	<b>0.0</b> <sup>e)</sup>	1.8
$\mathbf{H}_{12}^{II}$	66.0	75.0	26.4	44.5
$\mathbf{H}_{14}^I$	<b>0.0</b> <sup>f)</sup>	3.4	24.6	<b>0.0</b> <sup>g)</sup>
$\mathbf{H}_{14}^{II}$	73.5	81.4	84.6	n.a.
$\mathbf{H}_{14}^{III}$	83.6	82.9	91.0	n.a.
$\mathbf{H}_{17}^I$	34.1	73.0	44.9	22.3
$\mathbf{H}_{17}^{II}$	96.1	107.9	95.9	n.a.
$\mathbf{H}_{19}^I$	43.4	58.0	84.8	15.6
$\mathbf{H}_{19}^{II}$	60.8	78.2	83.1	n.a.
$\mathbf{H}_{19}^{III}$	81.8	85.9	88.0	n.a.
$\mathbf{H}_{22}^I$	78.2	101.2	125.2	n.a.
$\mathbf{H}_{22}^{II}$	82.0	103.5	124.6	n.a.
$\mathbf{H}_{24}^I$	99.5	110.8	140.9	n.a.
$\mathbf{H}_{24}^{II}$	101.8	97.1	133.5	n.a.

<sup>a)</sup> Relative energies in kJ/mol. <sup>b)</sup>  $e = 78.4$ . <sup>c)</sup> not available, *cf.* Text. <sup>d)</sup>  $E_T = -1968.409228$  a.u. <sup>e)</sup>  $E_T = -1956.409114$  a.u. <sup>f)</sup>  $E_T = -1956.361656$  a.u. <sup>g)</sup>  $E_T = -1956.413644$  a.u.

are the basis for sheet- or ribbon-like structures in *b*-peptides, whereas helix formation is observed only with larger pseudocycles. However, the backbone elongation in the *g*-amino acid constituents supports helix formation also with the closer pseudocycles  $C_7$  and  $C_9$ . In the case of the  $H_7$  conformers, the  $H_7^{II}$  helix is still less stable than the sheet-like conformer  $H_7^I$ , whereas the  $H_9^I$  helix is not only the most-stable structure of all  $H_9$  conformers, but belongs to the most-stable hexamer structures at all (Table 3, Figs. 2 and 3).

The stability order at the *Hartree-Fock* level is not essentially changed at the B3LYP/6-31G\* level of DFT (Table 3). The  $H_{14}^I$  and  $H_9^I$  hexamers remain closely together, but with a small preference of  $H_9^I$  by 3.4 kJ/mol now, which might be caused by overestimation of H-bonding

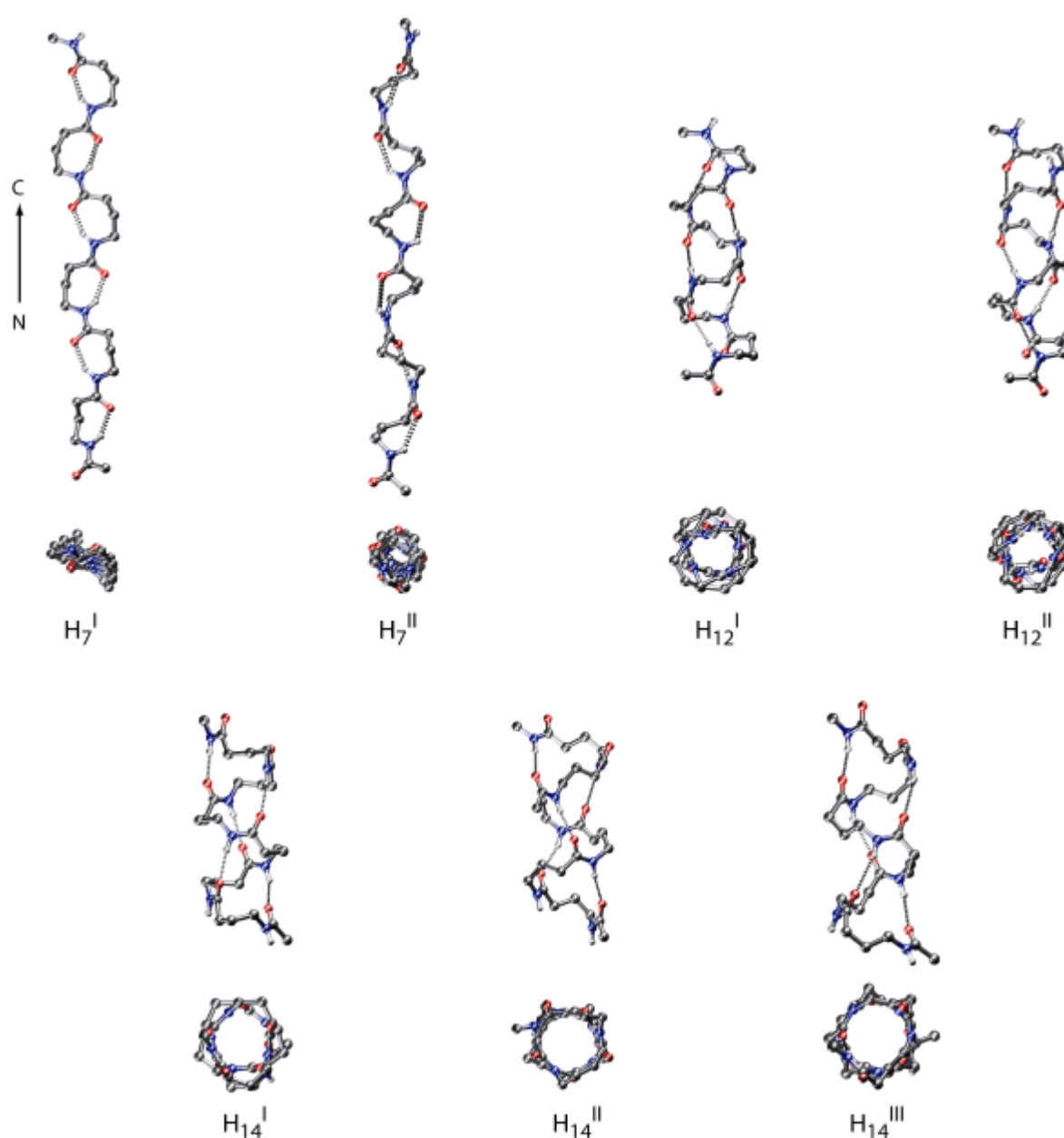


**Fig. 3.** All periodic conformers in the *g*-peptide hexamer **1** with 7-, 12-, and 14 membered H-bonded pseudocycles obtained at the HF/6-31G\* level of ab initio MO theory.

effects in DFT calculations. This would favor  $\mathbf{H}_9^{\text{I}}$  with one H-bond more than in  $\mathbf{H}_{14}^{\text{I}}$ . The  $\mathbf{H}_{12}^{\text{I}}$  helix is with 30.6 kJ/mol somewhat destabilized.

The estimation of the solvent influence on the conformer stability shows contradictory results (Table 3). Remarkable changes in the stability order are predicted by the *Onsager* SCRF model. Now, the  $\mathbf{H}_{12}^{\text{I}}$  hexamer is distinctly more stable than the competitive structures  $\mathbf{H}_{14}^{\text{I}}$  and  $\mathbf{H}_9^{\text{I}}$ . Even  $\mathbf{H}_{12}^{\text{II}}$  gets significant stabilization by the solvent continuum. This effect is unequivocally related to the distinctly higher dipole moment of  $\mathbf{H}_{12}^{\text{I}}$  ( $m = 30.5$  D) in comparison to  $\mathbf{H}_{14}^{\text{I}}$  ( $m = 24.8$  D) and  $\mathbf{H}_9^{\text{I}}$  ( $m = 25.4$  D). The global dipolar component is of considerable importance in the *Onsager* reaction-field model and may be overestimated in the estimation of the solvation energy in relation to local solvation effects. The SCRF model, which simulates the solute in a sphere when contacting the solvent continuum, may anyway be too simple for such linear structures like those investigated here. The PCM model, however, should be more advantageous in such cases since the electrostatic interactions between solute and solvent are calculated on the basis of the actual molecular surface area in contact with the solvent continuum, thus describing local electrostatic effects much better. The PCM model predicts  $\mathbf{H}_{14}^{\text{I}}$  again as the most stable helix followed by  $\mathbf{H}_{12}^{\text{I}}$  only 1.8 kJ/mol above and  $\mathbf{H}_9^{\text{I}}$  by 13.3 kJ/mol less stable. Obviously, these three forms are most probable to be found in structure determinations on  $\mathbf{g}$ -peptides.

In previous papers, it was shown that the typical secondary structure elements of  $\mathbf{b}$ -peptides could be derived from conformers of the monomer constituents, even when H-bonding is still impossible and becomes visible only in longer sequences [46,53,54]. It has to be proved whether such a monomer approach might be sufficient to derive the periodic structures also for the  $\mathbf{g}$ -peptides. For the  $C_7$  and  $C_9$  pseudocycles we find three conformers at the monomer level (*cf.* also [84]). In the case of the  $C_9$  pseudocycles, which are more stable than the  $C_7$  rings, these three monomeric conformers are in fact the basis for the hexamer structures in *Table 1*, whereas only two of the  $C_7$  conformers are present in the corresponding hexamers. The third conformer changes its oligomer geometry into one of the two other periodic structures. Performing geometry optimizations on blocked monomers with the corresponding torsion-angle values of the helices with the larger pseudocycles provides an indifferent picture. In some cases, e.g.,  $\mathbf{H}_{14}^{\text{I}}$ ,  $\mathbf{H}_{19}^{\text{I}}$ ,  $\mathbf{H}_{19}^{\text{III}}$ , and  $\mathbf{H}_{12}^{\text{II}}$ , we find a change into smaller pseudocycles ( $C_9$  and  $C_7$ ). In other cases, the geometry optimization provides conformers with considerably different geometry. Only the basic conformation of the  $\mathbf{H}_{12}^{\text{I}}$  helix is already present at the monomer level. Obviously, most of the higher secondary structures with characteristic H-bonding patterns in  $\mathbf{g}$ -peptides cannot immediately be derived from the conformer pool at the monomer level.

After the systematic conformational analysis on a  $\mathbf{g}$ -peptide hexamer, which provided a considerable number of conformers, it may be interesting to examine the consequences of the introduction of an (*E*)-double bond between the C(*a*) and C(*b*) atoms of the  $\mathbf{g}$ -amino acid constituents of the peptide backbone in the resulting vinylogous  $\mathbf{g}$ -peptides. In Table 4, the HF/6-31G\* geometry data of all conformers with periodic H-bonding patterns of the hexamer **2** are summarized. Geometry information obtained at other approximation levels is again part of the *Supplementary Material*. Table 5 presents the energy relations between the conformers. Our investigations show some differences in comparison to the situation in the  $\mathbf{g}$ -peptides. As expected, structures with nearest neighbor H-bonds like C<sub>7</sub> and C<sub>9</sub> cannot be formed due to the rigidity of the backbone after the introduction of the (*E*)-double bond. Even periodic structures with the larger C<sub>12</sub> pseudocycles are not yet possible. Beginning with the pseudocycle C<sub>14</sub> up to C<sub>24</sub>, all periodic hexamer structures are again available. They are visualized in Fig. 4. None of the vinylogous  $\mathbf{g}$ -peptide conformers in Table 4 can be derived from conformers at the monomer level. Starting geometry optimizations on blocked monomers with the torsion angle values of the

**Table 4.** Backbone Torsion Angles of Conformers of the Blocked Vinylogous  $\mathbf{g}$ -Peptide Hexamer **2** with H-Bonds Formed in Backward and Forward Direction Obtained at the HF/6-31G\* Level of *ab initio* MO Theory<sup>a</sup>

Conf.	<i>j</i>	<i>q</i>	<i>y</i>	Conf.	<i>j</i>	<i>q</i>	<i>y</i>
<b>vH<sub>14</sub></b>	71.4	18.2	164.2	<b>vH<sub>17</sub></b>	-166.6	-132.5	24.2
	65.1	15.4	163.7		84.7	-107.1	38.7
	65.6	16.9	160.5		93.6	-100.6	41.0
	66.0	16.8	161.4		83.5	-101.1	49.2
	67.6	15.1	155.1		84.2	-99.0	44.8
	81.6	-3.8	177.3		82.3	-93.9	45.6
<b>vH<sub>19</sub></b>	79.3	10.9	-175.8	<b>vH<sub>22</sub><sup>I</sup></b>	118.5	117.6	165.3
	70.1	33.1	-174.2		74.1	107.3	157.3
	80.0	16.6	-172.6		66.6	109.0	158.4
	83.4	16.1	-179.8		72.1	108.0	158.1
	87.8	14.3	-175.7		70.3	108.5	159.4
	114.5	-2.9	-176.0		73.3	130.5	-174.9
<b>vH<sub>24</sub></b>	77.2	-125.9	32.9	<b>vH<sub>22</sub><sup>II</sup></b>	103.6	-123.5	31.6
	76.3	-127.1	39.2		100.3	-116.7	35.8
	81.7	-116.2	-33.1		96.1	-110.4	37.3
	98.4	-117.3	30.5		90.4	-107.9	38.8
	94.2	-117.3	-18.8		85.9	-106.4	41.6
	103.4	-131.5	-20.6		87.5	-105.1	40.1

<sup>a</sup> Torsion angles in degrees.

**Table 5.** Relative Energies of Conformers of the Blocked Vinylogous  $\gamma$ -Peptide Hexamer **2** obtained at Various Levels of *ab initio* MO Theory <sup>a</sup>

Conf.	<i>DE</i>			
	HF/6-31G*	B3LYP/6-31G*	SCRF/HF/6-31G* <sup>b)</sup>	PCM//HF/6-31G* <sup>b)</sup>
<b>vH<sub>14</sub></b>	39.9	25.0	27.5	63.0
<b>vH<sub>17</sub></b>	67.2	57.2	44.3	82.5
<b>vH<sub>19</sub></b>	5.3	<b>0.0</b> <sup>c)</sup>	<b>0.0</b> <sup>d)</sup>	6.4
<b>vH<sub>22</sub><sup>I</sup></b>	<b>0.0</b> <sup>e)</sup>	10.8	14.8	<b>0.0</b> <sup>f)</sup>
<b>vH<sub>22</sub><sup>I</sup></b>	66.9	70.8	70.7	53.3
<b>vH<sub>24</sub></b>	74.7	77.4	55.1	53.3

<sup>a)</sup> Relative energies in kJ/mol. <sup>b)</sup>  $\epsilon = 78.4$ . <sup>c)</sup>  $E_T = -1960.996152$  a.u. <sup>d)</sup>  $E_T = -1949.245753$  a.u.

<sup>e)</sup>  $E_T = -1949.211533$  a.u. <sup>f)</sup>  $E_T = -1949.283589$  a.u.

conformers in *Table 4* leads to considerable structure changes. Contrary to the  $g$ -peptides, there is only one representative for each ring size with exception of  $C_{22}$ , which is realized in the two helices **vH<sub>22</sub><sup>I</sup>** and **vH<sub>22</sub><sup>II</sup>**. In any case, it can be seen that secondary-structure formation can *a priori* be directed to the formation of helices with larger pseudocycles by an appropriate type of rigidification of the peptide backbone. The backbone torsion angle values are more restricted in the vinylogous  $g$ -peptides in comparison to the  $g$ -peptides. Whereas  $j$  corresponds only to *sc* and  $q$  to *sp* and *ac* conformations, the torsion angle  $y$  assumes only values around  $0^\circ$  and  $180^\circ$ , respectively, due to conjugation effects.

In contrast to the  $g$ -peptides, the most stable conformers are **vH<sub>22</sub><sup>I</sup>** at the HF/6-31G\* level and **vH<sub>19</sub>** at the B3LYP/6-31G\* level (*Table 5*). Independent of the approximation levels, the energies of these two conformers are close together. This relationship is maintained when considering the solvent influence (*Table 5*). Despite the lesser number of H-bonds in the hexamer, the formation of the larger pseudocycles  $C_{19}$  and  $C_{22}$  is preferred over the formation of  $C_{14}$  pseudocycles in the vinylogous  $g$ -peptides, which predominate in the  $g$ -peptides. Besides, the relatively unstable **vH<sub>14</sub>** conformer found in the vinylogous  $g$ -peptide hexamer shows no strict correspondence to one of the three  $H_{14}$  conformers of the  $g$ -peptide hexamer.

A detailed look at the structure of the rather stable **vH<sub>22</sub><sup>I</sup>** helix of the vinylogous  $g$ -peptides (*Fig 4*), reveals a large inner diameter of *ca.* 3.5 Å. Thus, such structures could become important for the design of channels and tubes.

## Conclusions

Our systematic conformational search for periodic structures with characteristic H-bonding patterns in  $g$ -peptides provides a wide variety of structure alternatives. In comparison to

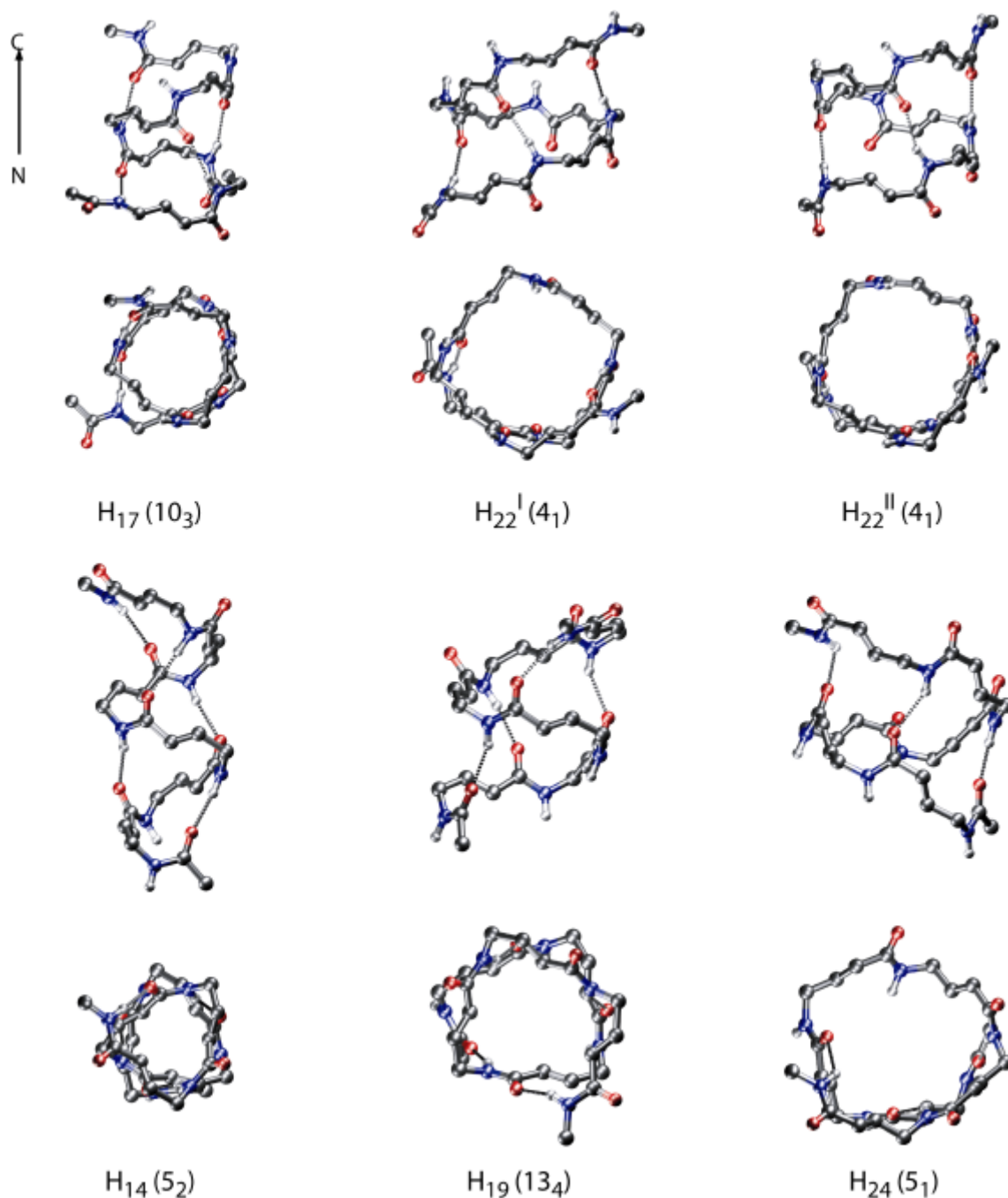


**Fig. 4.** All periodic conformers of the vinylogous  $g$ -peptide hexamer **2** obtained at the HF/6-31G\* level of *ab initio* MO theory (helix nomenclature in parentheses)

$b$ -peptides, the homologation of the peptide backbone increases the number of structures with definite backbone conformations and H-bonds formed in forward and backward directions along the sequence. All H-bonded pseudocycles with ring sizes between  $C_7$  and  $C_{24}$  are formally represented. In most cases there are several possibilities to realize identical H-bonding patterns. In good agreement with experimental data, periodic structures with 14- and 9-membered pseudocycles are most stable.

It can be shown that the introduction of an (*E*)-double bond into the backbone of the  $g$ -amino acid constituents supports the formation of helices with larger H-bonded pseudocycles

in the corresponding vinylogous  $\mathbf{g}$ -peptides, since closer rings cannot be formed any longer by this type of backbone modification. Special influence on the folding properties of  $\mathbf{g}$ -peptides and their vinylogues could also be expected from different substituent patterns at the backbone C-atoms.

Our study demonstrates the enormous potential of secondary structure formation in  $\mathbf{g}$ -peptides and their vinylogues, which is promising for peptide and protein design.

Support of this work by *Deutsche Forschungsgemeinschaft* (Projekt HO 2346/1 'Sekundärstrukturbildung in Peptiden mit nicht-proteinogenen Aminosäuren' and SFB 610 'Proteinzustände von zellbiologischer und medizinischer Relevanz') is gratefully acknowledged.

*Supplementary Material Available.* Tables of the backbone torsion angles in conformers of the  $\gamma$ -peptide hexamer **1** and its vinylogue **2** at the SCRF/HF/6-31G\* and DFT/B3LYP/6-31G\* levels are available on the compact disc attached at the end of this book.

## References

- [1] A. Giannis, T. Kolter, *Angew. Chem., Int. Ed.* **1993**, *32*, 1244.
- [2] H.-J. Böhm, G. Klebe, H. Kubinyi, 'Wirkstoffdesign', Spektrum Akademischer Verlag: Heidelberg-Berlin-Oxford, 1996.
- [3] D. J. Hill, M. J. Mio, R. B. Prince, T. S. Hughes, J. S. Moore, *Chem. Rev.* **2001**, *101*, 3893.
- [4] S. H. Gellman, *Acc. Chem. Res.* **1998**, *31*, 173.
- [5] K. D. Stigers, M. J. Soth, J. S. Nowick, *Curr. Opin. Chem. Biol.* **1999**, *3*, 714.
- [6] K. Kirshenbaum, R. N. Zuckermann, K. A. Dill, *Curr. Opin. Struct. Biol.* **1999**, *9*, 530.
- [7] A. E. Barron, R. N. Zuckermann, *Curr. Opin. Chem. Biol.* **1999**, *3*, 681.
- [8] M. S. Cubberley, B. L. Iverson, *Curr. Opin. Chem. Biol.* **2001**, *5*, 650.
- [9] D. Seebach, J. L. Matthews, *J. Chem. Soc., Chem. Commun.* **1997**, 2015.
- [10] W. F. DeGrado, J. P. Schneider, Y. Hamuro, *J. Peptide Res.* **1999**, *54*, 206.
- [11] R. P. Cheng, S. H. Gellman, W. F. DeGrado, *Chem. Rev.* **2001**, *101*, 3219.
- [12] D. H. Appella, L. A. Christianson, I. L. Karle, D. R. Powell, S. H. Gellman, *J. Am. Chem. Soc.* **1996**, *118*, 13071.
- [13] J. D. Winkler, E. L. Piatnitski, J. Mehlmann, J. Kaspárec, P. H. Axelsen, *Angew. Chem., Int. Ed.* **2001**, *40*, 743.



- [14] D. H. Appella, L. A. Christianson, D. A. Klein, D. R. Powell, X. Huang, J. Barchi, Jr., S. H. Gellman, *Nature (London)* **1997**, 387, 381.
- [15] D. Seebach, M. Overhand, F. N. M. Kühnle, B. Martinoni, L. Oberer, U. Hommel, H. Widmer, *Helv. Chim. Acta* **1996**, 79, 913.
- [16] J. M. Fernández-Santín, J. Aymamí, A. Rodríguez-Galán, S. Muñoz-Guerra, J. A. Subirana, *Nature (London)* **1984**, 311, 53.
- [17] D. Seebach, K. Gademann, J. V. Schreiber, J. L. Matthews, T. Hintermann, B. Jaun, *Helv. Chim. Acta* **1997**, 80, 2033.
- [18] D. Seebach, S. Abele, K. Gademann, G. Guichard, T. Hintermann, B. Jaun, J. L. Matthews, J. V. Schreiber, *Helv. Chim. Acta* **1998**, 81, 932.
- [19] M. Rueping, J. V. Schreiber, G. Lelais, B. Jaun, D. Seebach, *Helv. Chim. Acta* **2002**, 85, 2577.
- [20] S. Krauthäuser, L. A. Christianson, D. R. Powell, S. H. Gellman, *J. Am. Chem. Soc.* **1997**, 119, 11719.
- [21] Y. J. Chung, L. A. Christianson, H. E. Stanger, D. R. Powell, S. H. Gellman, *J. Am. Chem. Soc.* **1998**, 120, 10555.
- [22] D. Seebach, S. Abele, K. Gademann, B. Jaun, *Angew. Chem., Int. Ed.* **1999**, 39, 1595.
- [23] S. Abele, P. Seiler, D. Seebach, *Helv. Chim. Acta* **1999**, 82, 1559.
- [24] I. A. Motorina, C. Huel, E. Quiniou, J. Mispelter, E. Adjadj, D. S. Grierson, *J. Am. Chem. Soc.* **2001**, 123, 8.
- [25] A. Cheguillaume, A. Salaün, S. Sinbandhit, M. Potel, P. Gall, M. Baudy-Floc'h, P. Le Grel, *J. Org. Chem.* **2001**, 66, 4923.
- [26] R. Günther, H.-J. Hofmann, *J. Am. Chem. Soc.* **2001**, 123, 247.
- [27] D. Yang, F.-F. Ng, L. Zhan-Ji, *J. Am. Chem. Soc.* **1996**, 118, 9794.
- [28] Y. Wu, D. Wang, K. Chan, D. Yang, *J. Am. Chem. Soc.* **1999**, 121, 11189.
- [29] D. Yang, J. Qu, B. Li, F.-F. Ng, X.-C. Wang, K.-K. Cheung, D.-P. Wang, Y.-D. Wu, *J. Am. Chem. Soc.* **1999**, 121, 589.
- [30] C. Peter, X. Daura, W. van Gunsteren, *J. Am. Chem. Soc.* **2000**, 122, 7461.
- [31] H. N. Rydon, *J. Chem. Soc.* **1964**, 1328.
- [32] G. P. Dado, S. H. Gellman, *J. Am. Chem. Soc.* **1994**, 116, 1054.

- [33] M. Brenner, D. Seebach, *Helv. Chim. Acta* **2001**, *84*, 1181.
- [34] D. Seebach, A. K. Beck, M. Brenner, C. Gaul, A. Heckel, *Chimia* **2001**, *55*, 831.
- [35] T. Hintermann, K. Gademann, B. Jaun, D. Seebach, *Helv. Chim. Acta* **1998**, *81*, 983.
- [36] D. Seebach, M. Brenner, M. Rueping, B. Schweizer, B. Jaun, *Chem. Commun.* **2001**, 207.
- [37] D. Seebach, M. Brenner, M. Rueping, B. Jaun, *Chem.-Eur. J.* **2002**, *8*, 573.
- [38] S. Hanessian, X. Luo, R. Schaum, S. Michnick, *J. Am. Chem. Soc.* **1998**, *120*, 8569.
- [39] S. Hanessian, X. H. Luo, R. Schaum, *Tetrahedron Lett.* **1999**, *40*, 4925.
- [40] G. B. Liang, J. M. Desper, S. H. Gellman, *J. Am. Chem. Soc.* **1993**, *115*, 925.
- [41] P. Coutrot, C. Grison, S. Geneve, C. Didierjean, A. Aubry, A. Vicherat, M. Marraud, *Lett. Pept. Sci.* **1997**, *4*, 415.
- [42] M. Hagihara, N. J. Anthony, T. J. Stout, J. Clardy, S. L. Schreiber, *J. Am. Chem. Soc.* **1992**, *114*, 6568.
- [43] M. Hagihara, S. L. Schreiber, *J. Am. Chem. Soc.* **1992**, *114*, 6570.
- [44] C. Grison, S. Geneve, E. Halbin, P. Coutrot, *Tetrahedron* **2001**, *57*, 4903.
- [45] Y.-D. Wu, D.-P. Wang, *J. Chin. Chem. Soc.* **2000**, *47*, 129.
- [46] R. Günther, H.-J. Hofmann, *Helv. Chim. Acta* **2002**, *85*, 2149.
- [47] K. Möhle, H.-J. Hofmann, *J. Mol. Struct. (Theochem)* **1995**, *339*, 57.
- [48] K. Möhle, H.-J. Hofmann, *J. Mol. Model.* **1996**, *2*, 307.
- [49] K. Moehle, H.-J. Hofmann, *Biopolymers* **1996**, *38*, 781.
- [50] K. Möhle, H.-J. Hofmann, *J. Peptide Res.* **1998**, *51*, 19.
- [51] M. Thormann, H.-J. Hofmann, *J. Mol. Struct. (Theochem)* **1998**, *469*, 63.
- [52] M. Thormann, H.-J. Hofmann, *J. Mol. Struct. (Theochem)* **1998**, *431*, 79.
- [53] K. Möhle, R. Günther, M. Thormann, N. Sewald, H.-J. Hofmann, *Biopolymers* **1999**, *50*, 167.
- [54] Y.-D. Wu, D.-P. Wang, *J. Am. Chem. Soc.* **1998**, *120*, 13485.
- [55] P. A. Nielsen, P. O. Norrby, T. Liljefors, N. Rega, V. Barone, *J. Am. Chem. Soc.* **2000**, *122*, 3151.
- [56] J. J. Navas, C. Alemán, S. Muñoz-Guerra, *J. Org. Chem.* **1996**, *61*, 6849.

- [57] S. León, C. Alemán, S. Muñoz-Guerra, *Macromolecules* **1997**, *30*, 6662.
- [58] C. Alemán, J. Puiggali, *J. Mol. Struct. (Theochem)* **2001**, *541*, 179.
- [59] H. J. Lee, J. W. Song, Y. S. Choi, H. M. Park, K. B. Lee, *J. Am. Chem. Soc.* **2002**, *124*, 11881.
- [60] C. L. Brooks III, D. A. Case, *Chem. Rev.* **1993**, *93*, 2487.
- [61] T. Head-Gordon, M. Head-Gordon, M. J. Frisch, C. L. Brooks III., J. A. Pople, *J. Am. Chem. Soc.* **1991**, *113*, 5989.
- [62] R. F. Frey, J. Coffin, S. Q. Newton, M. Ramek, V. K. W. Cheng, F. A. Momany, L. Schäfer, *J. Am. Chem. Soc.* **1992**, *114*, 5369.
- [63] I. R. Gould, P. A. Kollmann, *J. Phys. Chem.* **1992**, *96*, 9255.
- [64] I. R. Gould, W. D. Cornell, I. H. Hiller, *J. Am. Chem. Soc.* **1994**, *116*, 9250.
- [65] C. Alemán, J. Casanovas, *J. Chem. Soc., Perkin Trans. 2* **1994**, 563.
- [66] G. Endredi, A. Perczel, O. Farkas, M. A. McAllister, G. I. Csonka, J. Ladik, I. G. Csizmadia, *J. Mol. Struct. (Theochem)* **1997**, *391*, 15.
- [67] K. Möhle, M. Gussmann, A. Rost, R. Cimiraglia, H.-J. Hofmann, *J. Phys. Chem. A* **1997**, *101*, 8571.
- [68] K. Rommel-Möhle, H.-J. Hofmann, *J. Mol. Struct. (Theochem)* **1993**, *285*, 211.
- [69] R. Günther, H.-J. Hofmann, K. Kuczera, *J. Phys. Chem. B* **2001**, *105*, 5559.
- [70] X. Daura, W. F. van Gunsteren, D. Rigo, B. Jaun, D. Seebach, *Chem. Eur. J.* **1997**, *3*, 1410.
- [71] X. Daura, K. Gademann, H. Schafer, B. Jaun, D. Seebach, W. F. van Gunsteren, *J. Am. Chem. Soc.* **2001**, *123*, 2393.
- [72] S. León, D. Zanuy, C. Alemán, S. Muñoz-Guerra, *Polymer* **1999**, *40*, 5647.
- [73] D. Zanuy, C. Alemán, S. Muñoz-Guerra, *Int. J. Biol. Macromol.* **1998**, *3*, 175.
- [74] D. Zanuy, C. Alemán, S. Muñoz-Guerra, *Macromol. Theory Simul.* **2000**, *9*, 543.
- [75] W. J. Hehre, L. Radom, P. v. R. Schleyer, J. A. Pople, 'Ab initio Molecular Orbital Theory', John Wiley & Sons: New York, 1986.
- [76] A. D. Becke, *J. Chem. Phys.* **1993**, *98*, 5648.
- [77] C. Lee, W. Yang, R. G. Parr, *Phys. Rev. B* **1988**, *37*, 785.
- [78] S. Miertus, E. Scrocco, J. Tomasi, *Chem. Phys.* **1981**, *55*, 117.

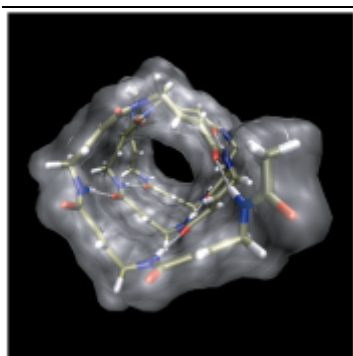
- [79] J. L. Pascual-Ahuir, E. Silla, J. Tomasi, R. Bonaccorsi, *J. Comput. Chem.* **1987**, *8*, 778.
- [80] J. Tomasi, M. Persico, *Chem. Rev.* **1994**, *94*, 2027.
- [81] M. J. Frisch, G. W. Trucks, H. B. Schlegel, G. E. Scuseria, M. A. Robb, J. R. Cheeseman, V. G. Zakrzewski, J. A. Montgomery, Jr., R. E. Stratmann, J. C. Burant, S. Dapprich, J. M. Millam, A. D. Daniels, K. N. Kudin, M. C. Strain, O. Farkas, J. Tomasi, V. Barone, M. Cossi, R. Cammi, B. Mennucci, C. Pomelli, C. Adamo, S. Clifford, J. Ochterski, G. A. Petersson, P. Y. Ayala, Q. Cui, K. Morokuma, P. Salvador, J. J. Dannenberg, D. K. Malick, A. D. Rabuck, K. Raghavachari, J. B. Foresman, J. Cioslowski, J. V. Ortiz, A. G. Baboul, B. B. Stefanov, G. Liu, A. Liashenko, P. Piskorz, I. Komáromi, R. Gomperts, R. L. Martin, D. J. Fox, T. Keith, M. A. Al-Laham, C. Y. Peng, A. Nanayakkara, M. Challacombe, P. M. W. Gill, B. Johnson, W. Chen, M. W. Wong, J. L. Andres, C. Gonzalez, M. Head-Gordon, E. S. Replogle, J. A. Pople, Gaussian 98; Revision A.11, Gaussian Inc., Pittsburgh PA, 1998.
- [82] M. W. Schmidt, K. K. Baldridge, J. A. Boatz, S. T. Elbert, M. S. Gordon, J. H. Jensen, S. Koseki, N. Matsunaga, K. A. Nguyen, S. J. Su, T. L. Windus, M. Dupuis, J. A. Montgomery, *J. Comput. Chem.* **1993**, *14*, 1347.
- [83] IUPAC, Commission on Macromolecular Nomenclature, *Pure Appl. Chem.* **1981**, *53*, 733.
- [84] D.-P. Wang, Ph. D. Thesis, Hong Kong University of Science and Technology, 1999.

### 3 Control of Helix Formation in Vinylogous $\gamma$ -Peptides by (E)- and (Z)-Double Bonds – A Way to Ion Channels and Monomolecular Nanotubes

by Carsten Baldauf, Robert Günther, and Hans-Jörg Hofmann

to be published in JOURNAL OF ORGANIC CHEMISTRY

Vol. 70 (2005) in press



**Abstract.** A complete overview on the alternative and competitive helices in vinylogous  $\gamma$ -peptides is given which was obtained on the basis of a systematic conformational analysis at various levels of ab initio MO theory (HF/6-31G\*, DFT/B3LYP/6-31G\*, PCM/HF/6-31G\*). Contrary to the parent  $\gamma$ -peptides, there is a strict control of helix formation by the configuration of the double bond between the C( $\alpha$ ) and C( $\beta$ ) atoms of the monomer constituents. (E)-double bonds favor helices with larger pseudocycles beginning with 14- up to 27-membered hydrogen-bonded rings, whereas the (Z)-configuration of the double bonds supports a distinct preference of helices with smaller 7- and 9-membered pseudocycles showing interactions between nearest-neighbor peptide bonds. The rather stable helices of the (E)-vinylogous peptides with 22-, 24-, and 27-membered hydrogen-bonded pseudocycles have inner diameters large enough to let molecules or ions pass. Thus, they could be interesting model compounds for the design of membrane channels and monomolecular nanotubes. Since (E)- and (Z)-vinylogous  $\gamma$ -amino acids and their oligomers are synthetically accessible, our study may stimulate structure research in this novel field of foldamers.

## Introduction

The design of oligomers which fold into definite secondary structures is a very actual and interesting field for synthetic chemists.<sup>1</sup> The monomers of these oligomers come from a wide variety of different structure classes. A particularly important group among them results from the homologation of the native  $\alpha$ -amino acids to  $\beta$ -,  $\gamma$ -, and  $\delta$ -amino acids, respectively. Obviously, studies on the oligomers of these amino acids aim at the mimicking of native peptide structures. They provide deeper insight into basic principles of folding and structure formation and contribute to a better understanding of the structure and function of biopolymers. Considering also more abiotic oligomers, we enter a realm of novel molecular scaffolds with functional properties, which could possibly be also of importance for material sciences and even information storage.

For oligomers with secondary structures formed by noncovalent interactions between nonadjacent monomers in solution the term foldamers was introduced.<sup>1a,b</sup> Foldamer research was essentially stimulated by the investigation of peptidic foldamers, in particular oligomers of  $\beta$ -amino acids ( $\beta$ -peptides).<sup>2</sup> Numerous ordered secondary structures, as for instance various helices, strands, and turns, were found. Thus, the most prominent secondary structure types of  $\beta$ -peptides are helices with 12- and 14-membered hydrogen-bonded pseudocycles ( $H_{12}$ ,  $H_{14}$ ), respectively.<sup>2c,d</sup> Definite secondary structures can also be expected in oligomers of  $\gamma$ - and  $\delta$ -amino acids. Thus, studies on  $\gamma$ -linked D-glutamic acids provided hints on helical structures with 17- or 19-membered rings,<sup>3a</sup> whereas unsubstituted  $\gamma$ -peptides adopt a poly- $C_9$ -conformation.<sup>3b</sup> Substituents at the  $\gamma$ -positions of the  $\gamma$ -peptide constituents enforce a helix with 14-membered pseudocycles.<sup>3c,d</sup> Secondary structure formation in  $\delta$ -peptides has a special note, since a  $\delta$ -amino acid constituent corresponds approximately to a dipeptide unit in the native  $\alpha$ -peptides. Thus, it can be supposed that  $\delta$ -peptides are able to mimic the secondary structure elements of the native peptides and proteins better than the other peptidic foldamers.<sup>4</sup>

Numerous theoretical studies employing ab initio MO theory and molecular dynamics techniques confirmed the experimental data and predicted further folding alternatives in sequences of homologous amino acids.<sup>5</sup> It was an interesting result that all important folding patterns in oligomers of  $\beta$ -peptides can be derived from the conformational properties of the blocked monomer units (monomer approach), even in the case of the helices  $H_{14}$  and  $H_{12}$  with hydrogen-bonded turns for which the structural requirements are not yet given in the monomers.<sup>5b,e</sup> Contrary to this, the experimentally indicated  $H_{14}$  helix of the  $\gamma$ -peptides with the

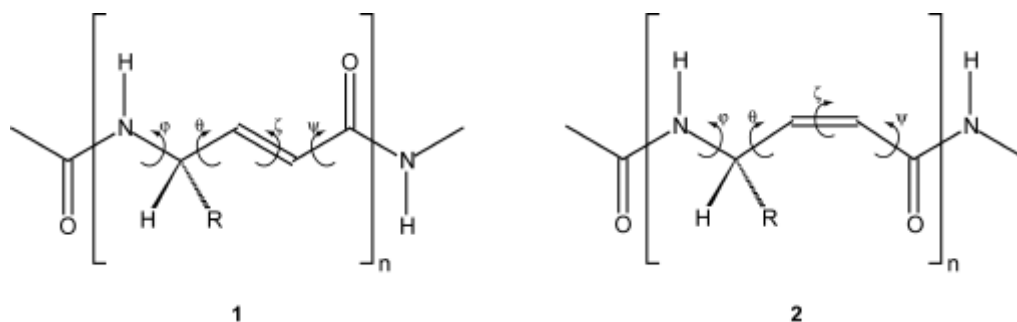
larger hydrogen-bonded cycles can only be obtained by conformational analyses on larger oligomers (oligomer approach).<sup>5i</sup> Studies on blocked monomers provide only secondary structures with interactions between neighboring peptide bonds, which are competitive to the aforementioned structures with the non-neighboring peptide bond interactions. Obviously, a critical sequence length is required for the formation of the latter ones.

It would be an advantage to find possibilities for a selective influencing of the secondary structure formation in peptides. This could be realized for instance by introduction of special side chains at the various backbone positions which can influence the secondary structure formation simply by their size or by specific interactions like hydrogen bonds, salt bridges or  $\pi$ -stacking, respectively. In fact, systematic theoretical studies on the substituent influence on  $\beta$ -peptide structures<sup>5h</sup> provide useful hints for the support of special secondary structure types. Introduction of steric restrictions into the backbone could be another possibility to control secondary structure formation. Experimental studies on  $\beta$ -peptides show impressively that the  $H_{12}$  helix is favored, when the  $C(\alpha)$  and  $C(\beta)$  backbone atoms are part of a cyclopentane ring,<sup>6a</sup> whereas the  $H_{14}$  helix is obtained when the  $C(\alpha)$  and  $C(\beta)$  atoms are part of a cyclohexane ring.<sup>6b</sup> In the same way, sugar amino acids of  $\gamma$ - and  $\delta$ -amino acid-type support selectively special secondary structure elements.<sup>4a-i</sup> Now, we want to turn the attention to the simple case of the introduction of (E)- and (Z)-double bonds into the peptide backbone. Whereas a double bond between the  $C(\alpha)$  and  $C(\beta)$  atoms of a  $\beta$ -amino acid constituent is less attractive for helix formation due to the resulting conjugated system,  $\gamma$ -amino acids having a double bond between the  $C(\alpha)$  and  $C(\beta)$  atoms (vinylogous  $\gamma$ -amino acids) might represent a good compromise between backbone rigidification and a sufficient conformational flexibility for secondary structure formation.<sup>5i</sup>

Several methods were suggested for the synthesis of both (E)- and (Z)-vinylogous  $\gamma$ -amino acids and their oligomers.<sup>7</sup> Despite their accessibility, structure information of vinylogous  $\gamma$ -peptides is not available until now. Therefore, we want to provide a complete overview on the possibilities of helix formation in vinylogous  $\gamma$ -peptides and its influencing by (E)- and (Z)-double bonds to stimulate synthetic work and structure research. Besides, we compare the monomer and the oligomer approach in order to see which secondary structures are already preformed in the blocked monomeric units and which are only available at a critical sequence length by taking profit from cooperative effects.

## Methodology

The monomer approach is based on a complete scan of the conformational space of the blocked unsubstituted (U) and  $\gamma$ -methylsubstituted (G) vinylogous  $\gamma$ -amino acid monomers **1** and **2** ( $n=1$ ) with (E)- and (Z)-double bonds, respectively. The considerable dimension of the conformation problem with the three backbone torsion angles  $\phi$ ,  $\theta$ , and  $\psi$  prevents the calculation of a grid with relatively small torsion angle intervals at higher levels of ab initio MO theory. Thus, we applied the following strategy. The torsion angle  $\psi$  was set at  $0^\circ$  and  $180^\circ$ ,



respectively. This is confirmed by conformational analyses on (E)- and (Z)-2-butenic acid N-methylamide at the HF/6-31G\* and DFT/B3LYP/6-31G\* levels of ab initio MO theory (Figure 1, cf. also refs. 8). All combinations of the values of  $-120^\circ$ ,  $-60^\circ$ ,  $0^\circ$ ,  $60^\circ$ ,  $120^\circ$  and  $180^\circ$  were assigned to the torsion angles  $\phi$  and  $\theta$ . The resulting structures were the starting points for complete geometry optimizations at the HF/6-31G\* level of ab initio MO theory. The optimized structures obtained were characterized as minimum conformations by the determination of the

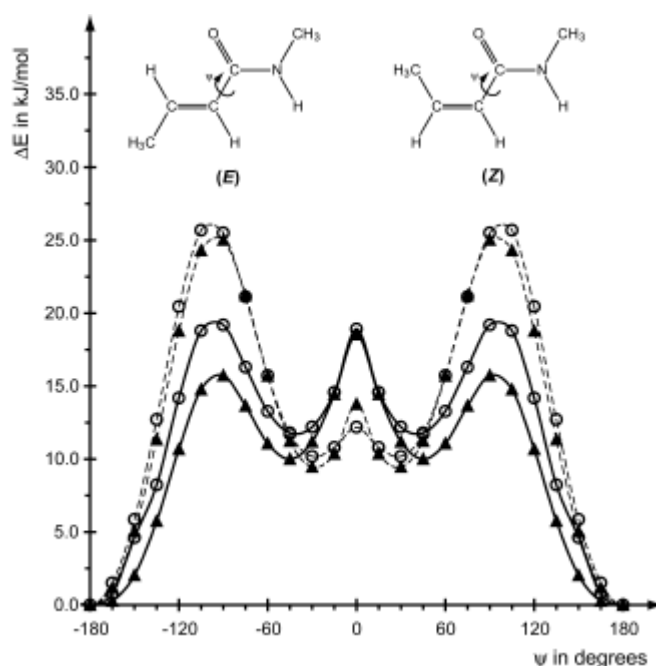


**FIGURE 1.** HF/6-31G\* ( $\blacktriangle$ ) and B3LYP/6-31G\* ( $\circ$ ) potential curves for (E)- (----) and (Z)- (—) 2-butenic acid N-methylamide.



vibration frequencies. Because of symmetry, there are always pairs of energetically equivalent conformers in the U series, where the torsion angles differ only by sign. This does not longer hold for the G derivatives, where only approximate backbone mirror image conformers can be expected. In all cases of G, where the pairs of the approximate backbone mirror images did not result from the grid search, the signs of the torsion angles of an obtained conformer were reversed and the corresponding conformation reoptimized to test for the possibility of the alternative backbone handedness. Such conformer alternatives were denoted by the same symbol, but adding a prime. For the minimum conformations the influence of correlation energy was estimated by optimization at the B3LYP/6-31G\* level of density functional theory (DFT). The solvent influence was described on the basis of a polarizable continuum model (PCM) by geometry optimization of the gas phase conformers at the PCM/HF/6-31G\* level of ab initio MO theory for the solvent water ( $\epsilon=78.4$ ).

The conformational analysis within the oligomer approach was performed at the level of the blocked hexamers **1** and **2** ( $n=6$ ) in two ways. At first, all periodic hexamers resulting from the conformers of the monomer approach were generated and optimized at the HF/6-31G\* level. Since there was a considerable lack of helical structures with non-neighboring peptide bond interactions in the case of the (E)- and (Z)-vinylogous peptides, we complemented this procedure by another strategy, which was already applied in our searches for the hydrogen-bonded helices of  $\gamma$ - and  $\delta$ -peptides and of mixed helices with an alternating hydrogen bonding pattern.<sup>5i,k,l</sup>

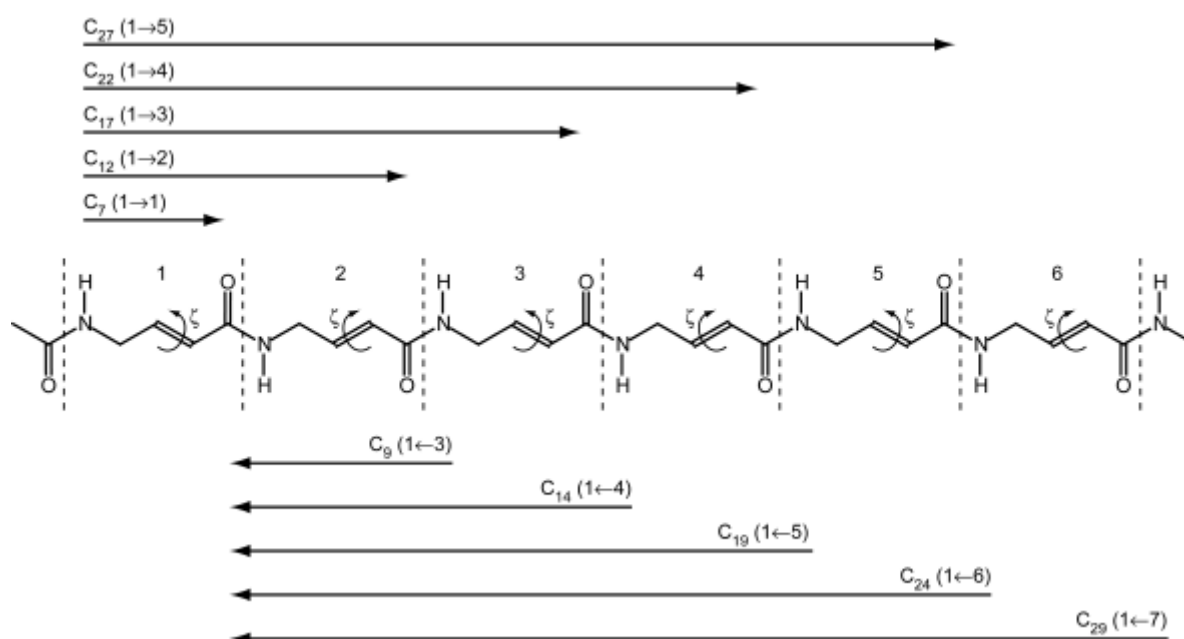


**FIGURE 2.** Possible hydrogen bonding patterns for helices of (E)- ( $\zeta=180^\circ$ ) and (Z)-vinylogous ( $\zeta=0^\circ$ )  $\gamma$ -peptides with the hydrogen bonds formed in forward and backward direction along the sequence.

Periodic structures of hexamers were systematically generated assigning all values from  $-150^\circ$  to  $180^\circ$  in steps of  $30^\circ$  to the backbone torsion angles  $\phi$ ,  $\theta$ , and  $\psi$ . The double bond torsion angles  $\zeta$  were set at  $-165^\circ$ ,  $180^\circ$ , and  $165^\circ$  for the (E)-hexamers and  $-15^\circ$ ,  $0^\circ$ , and  $15^\circ$  for the (Z)-hexamers, respectively, while values of  $-165^\circ$ ,  $180^\circ$ , and  $165^\circ$  were allowed for the  $\omega$  torsion angles. This procedure leads to 9,072 conformations. All structures out of these conformations, which fit into the possible periodic hydrogen bonding patterns in Figure 2 according to general geometry criteria for hydrogen bonds, were starting points for geometry optimizations at the HF/6-31G\* level of ab initio MO theory. The criteria for the acceptance of a conformation as a potential candidate for a helix with the periodic hydrogen-bonded pseudocycles of Figure 2, were the H...O distances between the hydrogen atoms of the peptidic NH bonds and the oxygen atoms of the corresponding peptidic CO bonds, which should be in the range of 1.8-2.4Å. Besides, the values of the angles  $\angle\text{NH}\cdots\text{O}$  and  $\angle\text{H}\cdots\text{OC}$  should be in between  $100$ - $180^\circ$ . In this way, 147 and 61 starting conformations for hydrogen-bonded helices resulted for the (E)- and (Z)-hexamers, respectively, additionally to the hexamers derived from the monomers. The optimized structures were characterized as minimum structures by the determination of the matrix of the force constants. On the basis of the vibration frequencies, the enthalpies, the thermal energy corrections, and the entropies of the various helices were calculated. For the minimum conformations, which still fulfill the helix properties of Figure 2, geometry optimizations at the B3LYP/6-31G\* level were complemented to estimate the influence of correlation effects. All helical HF/6-31G\* conformers were also subjected to PCM//HF/6-31G\* single-point calculations to examine the solvent influence. The quantum chemical calculations were performed employing the Gaussian98, Gaussian03, and the Gamess-US program packages.<sup>9</sup>

## Results and discussion

### *(E)-vinylogous g-peptides*

Table 1 contains the geometry data for the conformers of the blocked unsubstituted (U) and  $\gamma$ -methyl-substituted (G) model compounds **1** ( $n=1$ ) with an (E)-double bond obtained at the HF/6-31G\* level of ab initio MO theory. The corresponding geometry information at the DFT/B3LYP/6-31G\* and PCM/HF/6-31G\* levels is given as Supporting information. It is possible to collect the conformers in various families denoted by Arabic numerals with approximately the same values of  $\phi$  and  $\theta$ . The relative energies of the conformers are given in

**TABLE 1.** HF/6-31G\* Backbone Torsion Angles<sup>a</sup> for the Unsubstituted (U) and  $\gamma$ -Methyl-substituted (G) Conformers of **1** (n=1)

Conf.	$\phi$	$\theta$	$\zeta$	$\psi$	Conf.	$\phi$	$\theta$	$\zeta$	$\psi$
U1	-139.0	-125.8	-179.3	175.9	G3a	-136.6	11.9	179.4	-174.8
					G3b	-143.0	11.0	176.9	27.6
U2a	-84.7	113.7	-179.3	176.0					
U2b	-83.1	131.4	175.7	34.6	G4a	64.5	123.1	179.2	-176.4
U2c	-91.2	117.5	177.8	-29.3	G4b	60.2	117.3	176.5	23.4
					G4b'	-79.2	-122.7	-177.4	-24.0
U3a	-111.6	9.3	179.5	-174.2	G4c	61.5	123.1	-178.3	-24.7
U3b	-113.4	6.3	177.2	26.5	G4c'	-79.1	-125.3	177.0	28.1
U3c	-98.8	0.7	-176.7	-31.9					
					G5a	-152.6	122.2	178.9	-178.8
U4a	-80.9	-123.0	177.6	27.5	G5b	-160.1	115.1	-177.9	-31.6
U4b	-80.4	-120.8	-176.7	-23.9					
					G6a	-164.1	-27.7	-177.9	176.0
G1a	-147.4	-127.3	-179.8	176.2	G6b	-162.6	-27.0	178.3	30.2
G1b	-142.7	-123.3	176.8	30.8					
G1c	-140.7	-123.6	-176.7	-27.0	G7a	75.8	-5.2	179.9	171.9
					G7b	71.0	11.5	175.6	33.7
G2a	-83.8	110.6	-179.2	175.9	G7b'	-95.3	-3.7	-176.4	-32.1
G2a'	66.5	-129.6	-179.0	-172.6	G7c	75.2	6.5	-179.2	-24.2
G2b	-83.6	125.7	175.8	34.4					
G2b'	55.7	-152.9	-177.5	-34.6					
G2c	-91.3	113.9	-177.5	-29.4					
G2c'	64.6	-147.6	-179.5	24.8					

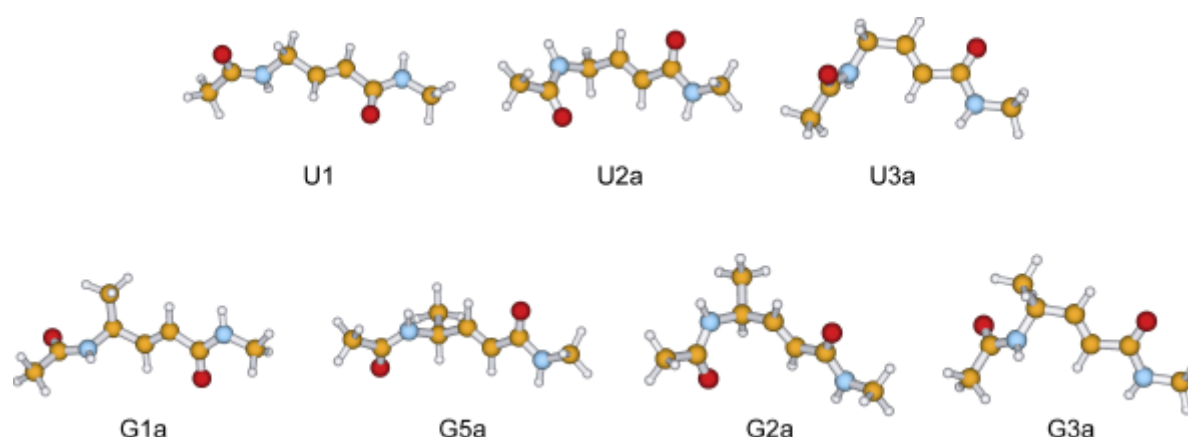
<sup>a</sup> Torsion angles in degrees.**FIGURE 3.** Sketch of the most stable conformers of **1** (n=1) at the HF/6-31G\* level of ab initio MO theory.

Table 2. There are only a few changes of the stability order at the various approximation levels. Some gas phase conformers disappear in the water continuum. The most stable conformers are visualized in Figure 3.

**TABLE 2.** Relative Energies<sup>a</sup> of the Unsubstituted (U) and  $\gamma$ -Methyl-substituted (G) Conformers of **1** (n=1) at the HF/6-31G\*, DFT/B3LYP/6-31G\* and PCM/HF/6-31G\*<sup>b</sup> Levels of ab Initio MO Theory

Conf.	$\Delta E(\text{HF})$	$\Delta E(\text{B3LYP})$	$\Delta E(\text{PCM})$
U1	<b>0.0</b> <sup>c</sup>	<b>0.0</b> <sup>d</sup>	<b>0.0</b> <sup>e</sup>
U2a	0.8	3.1	2.0
U2b	12.6	16.4	12.5
U2c	15.7	18.2	12.6
U3a	1.1	1.2	0.9
U3b	12.0	12.2	11.2
U3c	8.6	10.0	10.8
U4a	5.1	7.6	9.9
U4b	7.4	9.7	10.4
G1a	3.3	0.9	1.2
G1b	10.7	9.0	13.1
G1c	13.4	11.3	15.7
G2a	<b>0.0</b> <sup>f</sup>	<b>0.0</b> <sup>g</sup>	17.6
G2a'	14.7	14.0	→ G6a' <sup>i</sup>
G2b	12.5	13.5	2.6
G2b'	19.6	18.2	10.2
G2c	15.3	15.1	<b>0.0</b> <sup>h</sup>
G2c'	28.2	26.9	12.2
G3a	2.5	0.3	3.2
G3b	13.1	11.2	9.3
G4a	11.3	11.0	4.7
G4b	13.4	13.9	15.2
G4b'	12.7	→ G1c' <sup>i</sup>	12.9
G4c	13.1	13.6	15.0
G4c'	10.1	→ G1b' <sup>i</sup>	→ G2c' <sup>i</sup>
G5a	2.9	→ G2a' <sup>i</sup>	17.9
G5b	14.1	14.2	→ G2c' <sup>i</sup>
G6a	12.3	9.5	→ G3a' <sup>i</sup>
G6b	20.2	18.4	→ G3b' <sup>i</sup>
G7a	14.0	13.0	14.3
G7b	21.9	21.8	18.9
G7b'	10.0	9.2	→ G3b' <sup>i</sup>
G7c	27.8	26.8	→ G7b' <sup>i</sup>

<sup>a</sup> In kJ/mol. <sup>b</sup>  $\epsilon=78.4$ . <sup>c</sup>  $E_{\text{T}}=-530.704664$  a.u.<sup>d</sup>  $E_{\text{T}}=-533.932755$  a.u. <sup>e</sup>  $E_{\text{T}}=-530.717694$  a.u.<sup>f</sup>  $E_{\text{T}}=-569.741818$  a.u. <sup>g</sup>  $E_{\text{T}}=-573.248515$  a.u.<sup>h</sup>  $E_{\text{T}}=-569.750027$  a.u. <sup>i</sup> Optimization leads to the conformer after the arrow.

In the next step, periodic secondary structures were derived from the conformer pool of the unsubstituted monomer unit. Contrary to the blocked  $\beta$ - and  $\gamma$ -amino acids, there is no structure with a stabilizing hydrogen bond among the monomer conformers. Obviously, the (E)-double bond prevents the formation of hydrogen bonds between neighboring peptide bonds. Thus,

helices with larger hydrogen-bonded pseudocycles could only be expected in longer sequences of (E)-vinylogous amino acids. The oligomerization of all U conformers in Table 1 up to hexamers and their optimization provides helical minimum conformations in all cases (Table 3). However, only the hexamer derived from the conformer U2c represents a helix with 27-membered hydrogen-bonded pseudocycles ( $H_{27}^{II}$ ) according to the hydrogen bond patterns in Figure 2. Some of the helices without hydrogen bonds, such as those derived from the monomers U1, U2a, and U3a, are more stable than the helix with the 27-membered hydrogen-bonded cycles at the HF/6-31G\* level (Table 4). This tendency even increases regarding the data for the solvent water.

**TABLE 3.** HF/6-31G\* Backbone Torsion Angles<sup>a</sup> of all Periodic Hexamer Structures **1** (n=6) Derived from the Conformers U in Table 1

Conf.	$\varphi$	$\theta$	$\zeta$	$\psi$	Conf. <sup>b</sup>	$\varphi$	$\theta$	$\zeta$	$\psi$
(U1) <sub>6</sub>	-133.7	-125.7	-179.4	176.8	(U3b) <sub>6</sub>	-110.8	6.1	177.4	26.6
	-131.6	-125.5	-179.4	176.9		-100.0	5.0	177.8	26.0
	-130.2	-125.4	-179.4	177.0		-98.9	4.9	177.7	26.3
	-129.9	-125.4	-179.4	176.9		-98.6	4.9	177.7	26.2
	-131.2	-125.4	-179.5	176.7		-98.8	4.7	177.7	26.0
	-137.2	-125.5	-179.3	176.0		-99.7	4.1	177.4	25.5
(U2a) <sub>6</sub>	-84.6	113.3	-179.5	176.9	(U3c) <sub>6</sub>	-97.3	0.4	-176.5	-32.6
	-86.9	115.7	-179.9	176.5		-101.6	0.8	-176.7	-32.1
	-86.8	115.3	-179.8	176.3		-102.1	1.0	-176.7	-32.2
	-86.9	115.3	-179.8	176.3		-102.7	1.2	-176.7	-32.2
	-87.1	115.6	-179.9	176.4		-102.8	1.4	-176.7	-32.2
	-86.8	115.4	-179.6	175.1		-105.7	2.1	-176.8	-31.3
(U2b) <sub>6</sub>	-78.8	132.9	176.3	34.3	(U4a) <sub>6</sub>	-78.9	-123.9	177.9	26.5
	-77.6	127.5	176.9	34.0		-77.7	-124.0	178.1	25.9
	-77.9	126.9	177.0	33.9		-77.7	-124.0	178.1	25.9
	-78.3	126.8	176.9	34.0		-77.8	-124.0	178.1	25.9
	-78.8	127.7	176.6	34.4		-78.1	-123.7	178.0	26.1
	-80.5	127.9	176.2	34.1		-78.9	-123.8	178.0	26.5
(U2c) <sub>6</sub> ( $H_{27}^{II}$ )	-94.2	121.9	-179.0	-26.3	(U4b) <sub>6</sub>	-77.3	-122.9	-176.5	-23.4
	-104.3	123.7	-177.9	-29.7		-78.5	-124.4	-176.2	-26.9
	-78.8	142.2	175.6	38.9		-78.7	-124.6	-176.3	-26.8
	125.6	122.4	-175.5	-28.8		-78.8	-124.5	-176.3	-26.8
	-83.7	108.5	-174.8	-37.4		-79.5	-124.7	-176.1	-28.0
	-88.8	111.6	-176.7	-37.4		-82.4	-123.0	-176.6	-26.2
(U3a) <sub>6</sub>	-95.2	5.0	178.4	-173.5					
	-92.4	5.0	178.7	-174.4					
	-92.4	4.4	178.6	-174.5					
	-93.1	4.8	178.7	-174.4					
	-94.9	5.5	178.8	-174.2					
	-100.3	7.0	179.6	-175.4					

<sup>a</sup> Angles in degrees.

**TABLE 4.** Relative Energies<sup>a</sup> of Selected Periodic Hexamers **1** (n=6) at Various Approximation Levels of ab Initio MO Theory

Conf. <sup>b</sup>	$\Delta E(\text{HF})$	$\Delta E(\text{B3LYP})$	$\Delta E(\text{PCM})^c$
(U1) <sub>6</sub>	36.9	46.2	<b>0.0</b> <sup>d</sup>
(U2a) <sub>6</sub>	46.5	68.4	14.3
(U2b) <sub>6</sub>	107.6	133.4	73.9
(U2c) <sub>6</sub> (H <sub>27</sub> <sup>II</sup> )	64.3	75.7	89.8
(U3a) <sub>6</sub>	33.3	46.9	6.9
(U3b) <sub>6</sub>	110.3	116.2	62.9
(U3c) <sub>6</sub>	95.7	106.0	63.2
(U4a) <sub>6</sub>	68.7	92.5	55.4
(U4b) <sub>6</sub>	84.0	101.1	63.4
H <sub>19</sub>	5.3	<b>0.0</b> <sup>e</sup>	60.4
H <sub>22</sub> <sup>I</sup>	<b>0.0</b> <sup>f</sup>	10.8	43.4
H <sub>27</sub> <sup>I</sup>	17.2	33.7	31.1

<sup>a</sup> Energies in kJ/mol. <sup>b</sup> Monomers U from Table 3; Helices H<sub>x</sub> result from the oligomer approach in Table 5; H<sub>x</sub> denotes a helix with x-membered hydrogen-bonded pseudocycles. <sup>c</sup>  $\epsilon=78.4$ . <sup>d</sup> E<sub>T</sub>=-1949.239855 a.u. <sup>e</sup> E<sub>T</sub>=-1960.996152 a.u. <sup>f</sup> E<sub>T</sub>=-1949.211533 a.u.

It can be supposed that there are more helices in (E)-vinylogous peptides, which fulfill the hydrogen bonding patterns in Figure 2, than can be derived from the monomer pool. Indeed, the direct search for such helices in blocked hexamers of **1** (n=6) up to helices with 27-membered hydrogen-bonded pseudocycles provides helix alternatives with 14-, 17-, 19-, 22-, 24- and 27-membered pseudocycles according to Figure 2 (Table 5).<sup>5i</sup> The helices H<sub>17</sub>, H<sub>22</sub>, and H<sub>27</sub> form the hydrogen bonds in forward direction along the sequence, the helices H<sub>14</sub>, H<sub>19</sub>, and H<sub>24</sub> in backward direction. For the hydrogen bonding patterns in H<sub>22</sub> and H<sub>27</sub>, there are even two representatives denoted by upper-script Roman numbers in the order of decreasing stability. The H<sub>22</sub><sup>I</sup> and H<sub>19</sub> helices are the most stable helices among the hydrogen-bonded helix types (Table 4). They are also distinctly more stable than the helices without hydrogen bonds derived from the monomers U1, U2a, and U3a, respectively (Tables 3 and 4). This is particularly valid for apolar media, whereas the most stable helices without hydrogen bonds gain considerable stability in a polar environment because of their better interaction possibilities with the solvent due to the missing intramolecular peptide hydrogen bonds. The stability order of the helix hexamers within the two groups of helices with and without hydrogen bonds obtained on the basis of the energy data is essentially confirmed by the free enthalpy data resulting from the calculation of the vibration frequencies (see Table S5 of the Supporting information). However, it has to be mentioned, that the helices without hydrogen bonds get some stability at the free energy level in

**TABLE 5.** HF/6-31G\* Backbone Torsion Angles<sup>a</sup> for the Hydrogen-bonded Helical Structures of the Hexamer **1** (n=6) Found in the Oligomer Approach

Conf. <sup>b</sup>	$\phi$	$\theta$	$\zeta$	$\psi$	Conf. <sup>b</sup>	$\phi$	$\theta$	$\zeta$	$\psi$
H <sub>14</sub>	71.4	18.2	-166.2	164.2	H <sub>22</sub> <sup>II</sup>	103.6	-123.5	176.3	31.6
	65.1	15.4	-164.6	163.7		100.3	-116.7	173.7	35.8
	65.6	16.9	-164.6	160.5		96.1	-110.4	173.1	37.3
	66.0	16.8	-165.6	161.4		90.4	-107.9	172.5	38.8
	67.6	15.1	-165.1	155.1		85.9	-106.4	170.9	41.6
	81.6	-3.8	-179.4	177.3		87.5	-105.1	173.6	40.1
H <sub>17</sub>	-166.6	-132.5	176.6	24.2	H <sub>24</sub>	77.2	-125.9	175.8	32.9
	84.7	-107.1	166.6	38.7		76.3	-127.1	171.8	39.2
	93.6	-100.6	166.6	41.0		81.7	-116.2	177.1	-33.1
	83.5	-101.1	164.6	49.2		98.4	-117.3	172.7	30.5
	84.2	-99.0	163.7	44.8		94.2	-117.3	-177.2	-18.8
	82.3	-93.9	169.5	45.6		103.4	-131.5	-174.1	-20.6
H <sub>19</sub>	79.3	10.9	-173.3	-175.8	H <sub>27</sub> <sup>I</sup>	108.3	112.9	-179.5	165.7
	70.1	33.1	-172.9	-174.2		73.8	114.5	178.6	164.1
	80.0	16.6	-173.0	-172.6		73.3	110.5	179.6	160.1
	83.4	16.1	-172.3	-179.8		70.0	110.3	179.5	161.6
	87.8	14.3	-175.8	-175.7		71.4	118.5	178.4	169.0
	114.5	-2.9	180.0	-176.0		77.4	129.8	177.2	178.1
H <sub>22</sub> <sup>I</sup>	118.5	117.6	-178.4	165.3	H <sub>27</sub> <sup>II</sup>	-94.2	121.9	-179.0	-26.3
	74.1	107.3	-175.2	157.3		-104.3	123.7	-177.9	-29.7
	66.6	109.0	-174.0	158.4		-78.8	142.2	175.6	38.9
	72.1	108.0	-172.7	158.1		125.6	122.4	-175.5	-28.8
	70.3	108.5	-175.6	159.4		-83.7	108.5	-174.8	-37.4
	73.3	130.5	178.8	-174.9		-88.8	111.6	-176.7	-37.4

<sup>a</sup> Angles in degrees. <sup>b</sup> H<sub>x</sub> denotes a helix with x-membered hydrogen-bonded pseudocycles.

comparison to their hydrogen-bonded counterparts resulting from the entropy contributions. Due to the missing hydrogen bonds, the entropy values of these helices are distinctly higher than those of the hydrogen-bonded helices. Figure 4 visualizes the most stable helices of (E)-vinylogous  $\gamma$ -peptides.

### (Z)-vinylogous $\mathbf{g}$ -amino acids

The geometry data at the HF/6-31G\* level of ab initio MO theory for the various conformers of the unsubstituted (U) and  $\gamma$ -methyl-substituted (G) vinylogous  $\gamma$ -amino acid derivatives **2** (n=1) are given in Table 6. The data at the other approximation levels are again part of the Supporting information. Contrary to the monomers with (E)-double bonds, there are several conformers with 7- and 9-membered hydrogen-bonded pseudocycles (C<sub>7</sub>, C<sub>9</sub>). The most stable conformers U1, U2, G1, G2, and G3 are among them (Table 7). They are visualized in Figure 5. Some of the lesser stable conformers are stabilized by N $\cdots$ HN hydrogen bonds. Their C<sub>7</sub> pseudocycles are denoted by an asterisk. There are only a few inversions in the stability order of

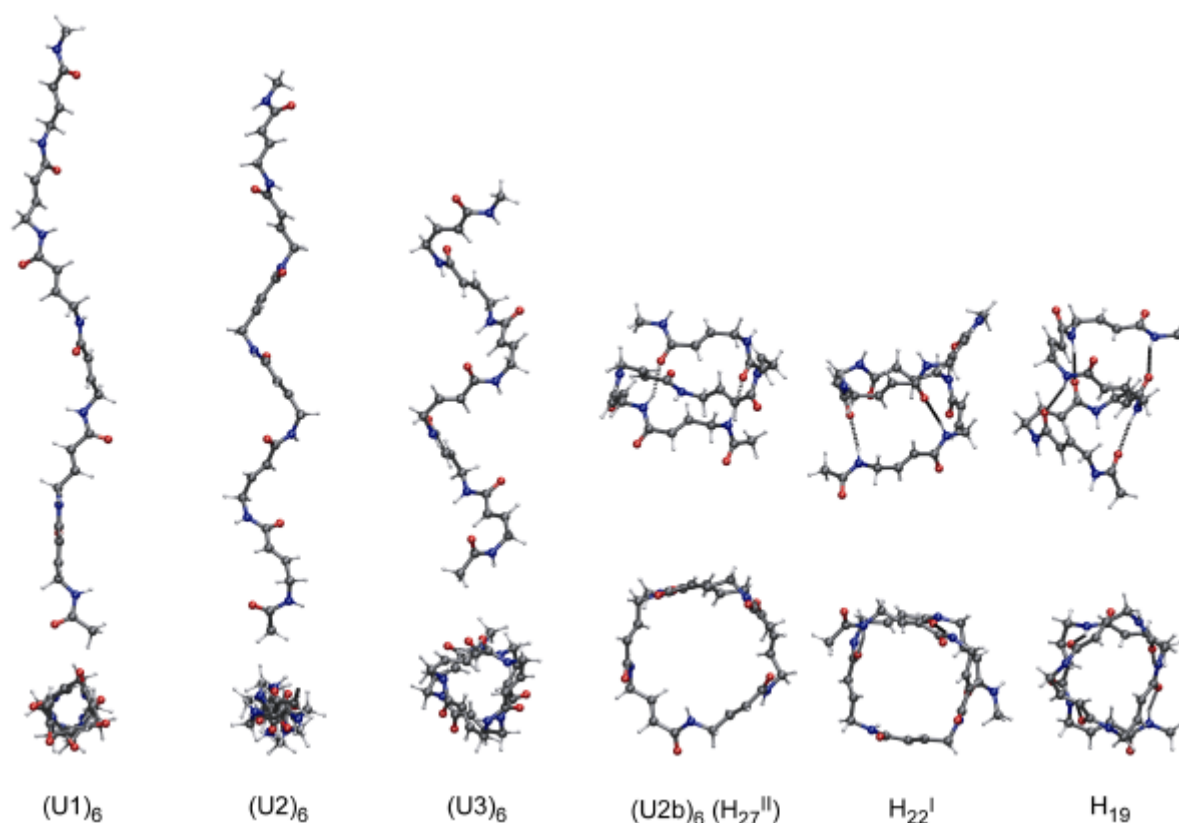


**FIGURE 4.** Most stable helices with and without hydrogen bonds of (E)-vinylogous  $\gamma$ -peptide hexamers **1**.

the most stable conformers at the other levels of ab initio MO theory. The hydrogen bonds of U1 and U4 are opened when considering the solvent within the polarizable continuum model. The situation for the helix formation in oligomers of (Z)-vinylogous  $\gamma$ -amino acids is rather different from that for the (E)-oligomers. The most stable helix conformers H<sub>7</sub> and H<sub>9</sub> are characterized by nearest-neighbor peptidic hydrogen bonds (Figure 6). They can immediately be derived from the monomer conformers U1 and U2 by oligomerization (Tables 6 and 8). Both helices are of comparable stability at the HF/6-31G\* level of ab initio MO theory and also in a polar environment, but H<sub>9</sub> is preferred at the DFT/B3LYP/6-31G\* level (Table 9). A rather unstable helix (U3)<sub>6</sub> without hydrogen bonds results from the extension of the monomer U3. The oligomerization of the other U conformers in Table 6 does not provide stable helices. It can be supposed that there are further helices in (Z)-vinylogous  $\gamma$ -peptides with larger hydrogen-bonded pseudocycles than in the helices H<sub>7</sub> and H<sub>9</sub>. Searching for such helices in hexamers in the same way as it was performed for the (E)-vinylogous  $\gamma$ -peptides provides in fact the helices H<sub>12</sub>, H<sub>14</sub>, and H<sub>17</sub>, but no helices with still larger pseudocycles (Table 8, Figure 6). However, these helices are distinctly less stable than the H<sub>7</sub> and H<sub>9</sub> conformers with the nearest-neighbor peptidic hydrogen bond interactions (Table 9).



**TABLE 6.** HF/6-31G\* Backbone Torsion Angles<sup>a</sup> for the Unsubstituted (U) and  $\gamma$ -Methyl-substituted (G) Conformers of **2** (n=1)

Conf.	$\phi$	$\theta$	$\zeta$	$\psi$	Type <sup>b</sup>	Conf.	$\phi$	$\theta$	$\zeta$	$\psi$	Type <sup>b</sup>
U1	80.9	74.8	-0.8	166.7	C <sub>7</sub>	G4	-75.5	150.3	-0.7	-161.5	
U2	80.5	-123.7	-0.1	45.7	C <sub>9</sub>	G5	64.0	139.4	-0.6	-172.5	
U3	84.9	126.2	0.2	50.4		G6	-163.5	80.8	-2.3	158.4	
U4	179.3	-91.6	-1.3	35.5	C <sub>7</sub> *	G7	-160.1	118.4	-1.8	52.1	
U5	-79.6	-122.6	1.7	54.7		G8	63.0	120.6	-0.2	52.4	
U6	78.5	34.7	1.2	60.1		G9	66.1	-119.7	3.2	70.5	C <sub>9</sub> <sup>ax</sup>
U7	106.2	-138.1	1.5	-41.7		G10	59.4	97.3	-3.0	-43.4	C <sub>7</sub> *
						G11	-86.8	-21.7	-1.4	-70.4	
G1	-79.8	122.8	0.1	-46.5	C <sub>9</sub> <sup>eq</sup>	G12	-74.7	-71.9	1.7	43.4	C <sub>7</sub> *
G2	-101.8	-47.5	-0.5	177.3	C <sub>7</sub> <sup>ax</sup>	G13	-158.6	-59.1	-2.2	17.4	C <sub>7</sub> *
G3	58.7	77.2	-1.4	168.0	C <sub>7</sub> <sup>eq</sup>						

<sup>a</sup> Torsion angles in degrees. <sup>b</sup> C<sub>x</sub> denotes a hydrogen-bonded pseudocycle with x atoms; eq, ax: pseudoequatorial or pseudoaxial orientation of the C( $\gamma$ ) substituents; An asterisk denotes NH...N hydrogen bonding.

**TABLE 7.** Relative Energies<sup>a</sup> of the Unsubstituted (U) and  $\gamma$ -Methyl-substituted (G) Conformers of **2** (n=1) at the HF/6-31G\*, DFT/B3LYP/6-31G\* and PCM/HF/6-31G\*<sup>b</sup> Levels of ab Initio MO Theory

Conf.	$\Delta E$ (HF)	$\Delta E$ (B3LYP)	$\Delta E$ (PCM)	Conf.	$\Delta E$ (HF)	$\Delta E$ (B3LYP)	$\Delta E$ (PCM)
U1	<b>0.0</b> <sup>c</sup>	0.5	<b>0.0</b> <sup>d</sup>	G4	9.4	14.9	<b>0.0</b> <sup>h</sup>
U2	3.5	<b>0.0</b> <sup>e</sup>	3.8	G5	10.1	14.6	4.1
U3	20.6	21.1	9.7	G6	17.8	→ G2 <sup>i</sup>	→ G4 <sup>i</sup>
U4	25.6	27.4	11.4	G7	25.9	30.3	17.6
U5	26.4	27.4	11.1	G8	26.9	32.1	21.5
U6	30.0	31.1	15.8	G9	27.3	26.8	24.4
U7	31.7	31.4	12.2	G10	27.8	31.3	21.0
G1	<b>0.0</b> <sup>f</sup>	<b>0.0</b> <sup>g</sup>	5.4	G11	28.7	34.2	17.9
G2	4.0	3.4	10.6	G12	38.4	38.2	36.3
G3	5.6	9.3	9.5	G13	41.0	37.5	41.5

<sup>a</sup> Angles in degrees. <sup>b</sup>  $\epsilon=78.4$  <sup>c</sup> E<sub>T</sub>=-530.705690 a.u. <sup>d</sup> E<sub>T</sub>=-530.730560 a.u.

<sup>e</sup> E<sub>T</sub>=-533.934239 a.u.

<sup>f</sup> E<sub>T</sub>=-569.741573 a.u.

<sup>g</sup> E<sub>T</sub>=-573.251058 a.u.

<sup>h</sup> E<sub>T</sub>=-569.745089 a.u. <sup>i</sup> Optimization leads to the conformer after the arrow.

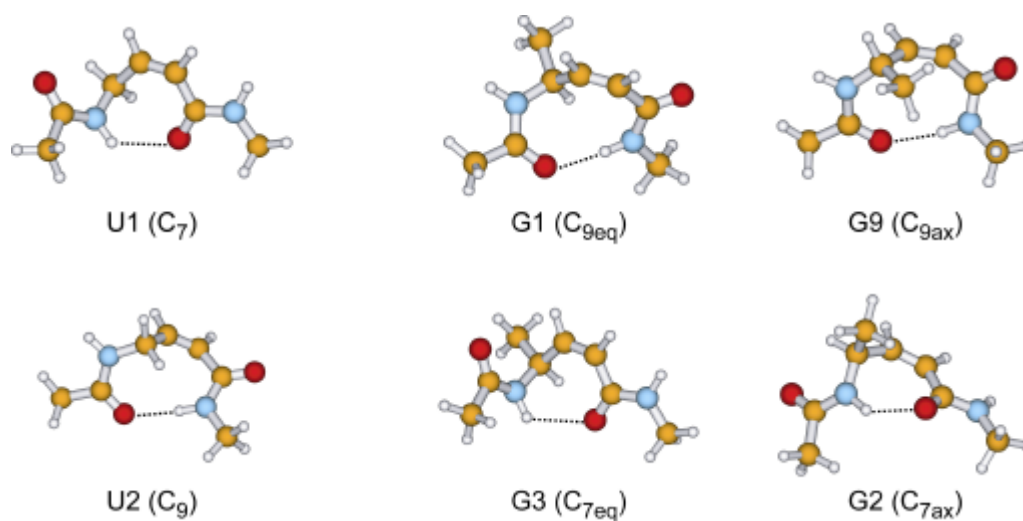


**FIGURE 5.** Sketch of the most stable conformers of **2** ( $n=1$ ) at the HF/6-31G\* level.

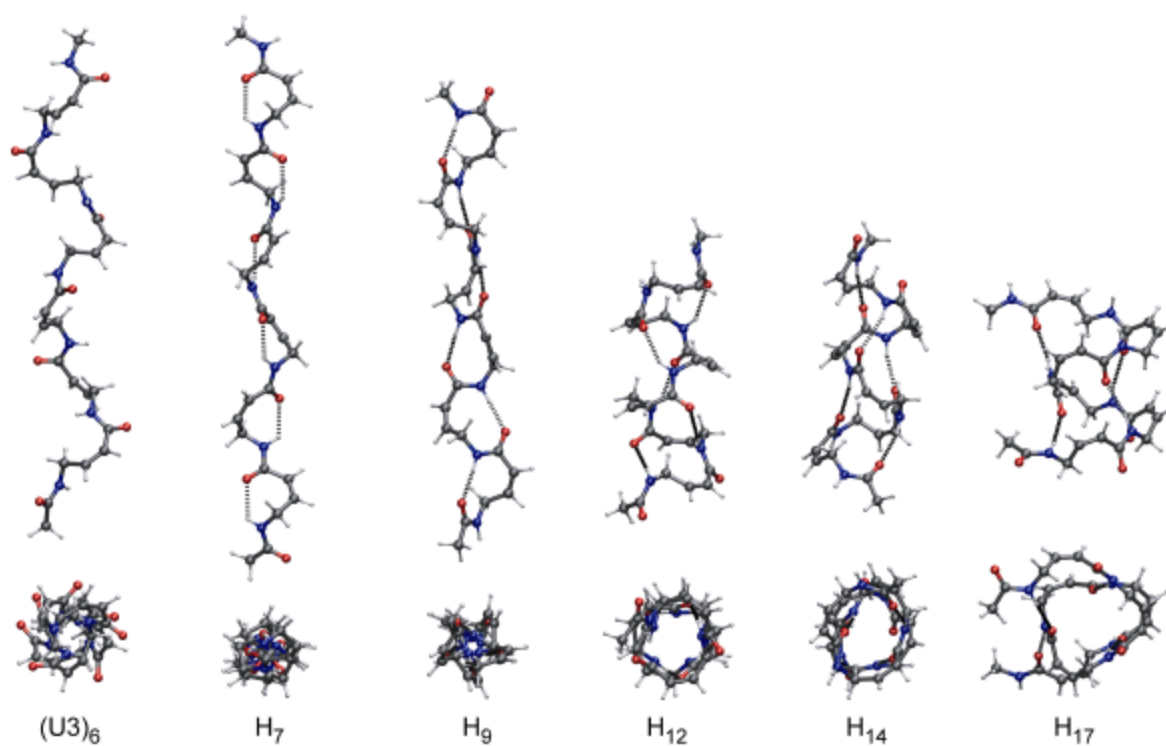


**FIGURE 6.** Most stable helices with and without hydrogen bonds of (Z)-vinylogous  $\gamma$ -peptide hexamers **2**.

**TABLE 8.** HF/6-31G\* Backbone Torsion Angles<sup>a</sup> of All Periodic Hexamer Structures either Derived from the Monomers U in Table 6 or Obtained in the Oligomer Approach on Hexamers of **2** (n=6)

Conf. <sup>b</sup>	$\varphi$	$\theta$	$\zeta$	$\psi$	Conf. <sup>b</sup>	$\varphi$	$\theta$	$\zeta$	$\psi$
H <sub>7</sub> (U1) <sub>6</sub>	83.7	73.6	-0.7	167.6	H <sub>14</sub>	105.0	-125.8	2.4	149.4
	86.7	72.7	-0.7	167.9		80.9	-104.4	-5.5	130.5
	87.7	72.4	-0.7	167.6		127.6	-116.8	1.8	65.5
	87.7	72.3	-0.7	167.8		174.0	-116.8	2.4	70.2
	87.7	72.5	-0.7	167.7		133.1	-99.2	-2.6	137.3
	85.7	73.3	-0.8	166.7		82.7	-107.3	-4.3	130.3
H <sub>9</sub> (U2) <sub>6</sub>	81.0	-122.6	0.5	47.7	H <sub>17</sub>	-96.8	-115.5	-2.5	132.9
	82.6	-122.2	0.5	46.4		174.9	-102.4	-2.1	126.3
	82.5	-122.2	0.6	46.4		173.8	-83.8	1.3	147.2
	82.5	-122.2	0.5	46.3		148.2	-83.5	0.3	162.7
	82.2	-122.6	0.4	47.0		138.8	-56.9	-2.7	127.9
	82.2	-123.0	0.1	44.2		-154.2	-154.5	0.3	172.5
H <sub>12</sub>	72.0	71.9	-3.5	41.3	(U3) <sub>6</sub>	83.3	127.0	0.0	52.7
	68.7	72.4	-2.2	62.3		82.6	127.8	-0.5	51.8
	66.3	63.9	-2.7	65.0		82.5	126.7	-0.5	52.8
	70.2	62.6	-2.4	67.3		82.4	126.1	-0.5	53.0
	71.0	59.4	-1.5	65.6		82.0	126.1	-0.6	53.5
	71.8	61.5	-1.7	68.1		83.4	125.0	-0.2	51.1

<sup>a</sup> Angles in degrees. <sup>b</sup> H<sub>x</sub> denotes a helix with x-membered hydrogen-bonded pseudocycles.

**TABLE 9.** Relative Energies<sup>a</sup> of Periodic Hexamers of **2** (n=6) at Various Approximation Levels of ab Initio MO Theory

Conf. <sup>b</sup>	$\Delta E$ (HF)	$\Delta E$ (B3LYP)	$\Delta E$ (PCM) <sup>c</sup>
H <sub>7</sub>	0.5	16.8	<b>0.0</b> <sup>d</sup>
H <sub>9</sub>	<b>0.0</b> <sup>e</sup>	<b>0.0</b> <sup>f</sup>	2.9
H <sub>12</sub>	95.1	111.1	133.1
H <sub>14</sub>	61.6	73.6	96.0
H <sub>17</sub>	79.8	90.3	98.9
(U3) <sub>6</sub>	143.9	168.6	85.8

<sup>a</sup> Energies in kJ/mol. <sup>b</sup> H<sub>x</sub> denotes a helix with x-membered hydrogen-bonded pseudocycles. <sup>c</sup>  $\epsilon=78.4$   
<sup>d</sup> E<sub>T</sub>=-1949.211699 a.u. <sup>e</sup> E<sub>T</sub>=-1949.205023 a.u.  
<sup>f</sup> E<sub>T</sub>=-1960.999645 a.u.

*(E)- vs. (Z)-double bonds – Nanotubes and channels*

Comparing the formation of hydrogen-bonded helices in (E)- and (Z)-vinylogous  $\gamma$ -peptides, it is most striking that the (E)-double bonds prevent the formation of helices with nearest-neighbor peptide bond interactions. Most stable are helices with 22- and 19-membered hydrogen-bonded rings, whereas the (Z)-double bonds favor peptidic nearest-neighbor interactions leading to helices with 7- and 9-membered pseudocycles. The other helix types are distinctly less stable in both cases. In the parent  $\gamma$ -peptides, the preferred helices span a much wider range of hydrogen-bonded ring sizes with the most stable  $H_{14}$  and  $H_9$  helices and the also relatively stable  $H_{12}$  and  $H_{17}$  helices. Obviously, the double bond configuration is able to direct the helix formation in a special direction. A detailed look at the helices of the (E)-vinylogous  $\gamma$ -peptides, as for instance the helices with 22-, 24-, and 27-membered rings, reveals that these structures have rather large inner diameters, which are comparable with the diameter of 3.5 Å of the well-known trans-membrane channel in gramicidin A.<sup>10</sup> Table 10 lists the relative energies and diameters for the three helix undecamers  $H_{19}$ ,  $H_{22}^I$  and  $H_{27}^I$ . The relatively stable periodic  $H_{19}$  structure (Table 10) cannot form channel-like structures and is only given for comparison. The diameters of  $H_{22}^I$  and  $H_{27}^I$  are large enough for ions and water molecules to pass. Therefore, (E)-vinylogous  $\gamma$ -peptides might become interesting for the design of ion channels or monomolecular nanotubes<sup>11</sup> as it is shown for the  $H_{22}^I$  and  $H_{27}^I$  undecamers of the (E)-vinylogous peptides in Figure 7. The high stability of the channel-like conformers of the (E)-vinylogous peptides in an apolar environment could support such a process. The formation of monomolecular nanotubes has some general advantages over that by self-assembly of cyclopeptides, because it is induced within the same molecule. Besides, it is possible to design channels and nanotubes with definite length and composition.

**TABLE 10.** Relative Energies<sup>a</sup> at the HF/6-31G\*, B3LYP/6-31G\* and PCM//HF/6-31G\*<sup>b</sup> Levels of ab Initio MO Theory and the Approximate Inner Diameters<sup>c</sup> for Selected Undecamers of **1** (n=11)

Conf. <sup>d</sup>	$\Delta E(\text{HF})$	$\Delta E(\text{B3LYP})$	$\Delta E(\text{PCM})$	Diameter
$H_{19}$	23.2	<b>0.0</b> <sup>e</sup>	59.4	-
$H_{22}^I$	<b>0.0</b> <sup>f</sup>	3.4	30.5	4.0
$H_{27}^I$	22.3	37.2	<b>0.0</b> <sup>g</sup>	5.5

<sup>a</sup> Energies in kJ/mol. <sup>b</sup>  $\epsilon=78.4$  <sup>c</sup> Averaged inner helix diameters in Å corrected by the respective van der Waals radii. <sup>d</sup>  $H_x$  denotes a helix with x-membered hydrogen-bonded pseudocycles. <sup>e</sup>  $E_T=-3388.079209$  a.u. <sup>f</sup>  $E_T=-3367.740976$  a.u. <sup>g</sup>  $E_T=-3367.798032$  a.u.

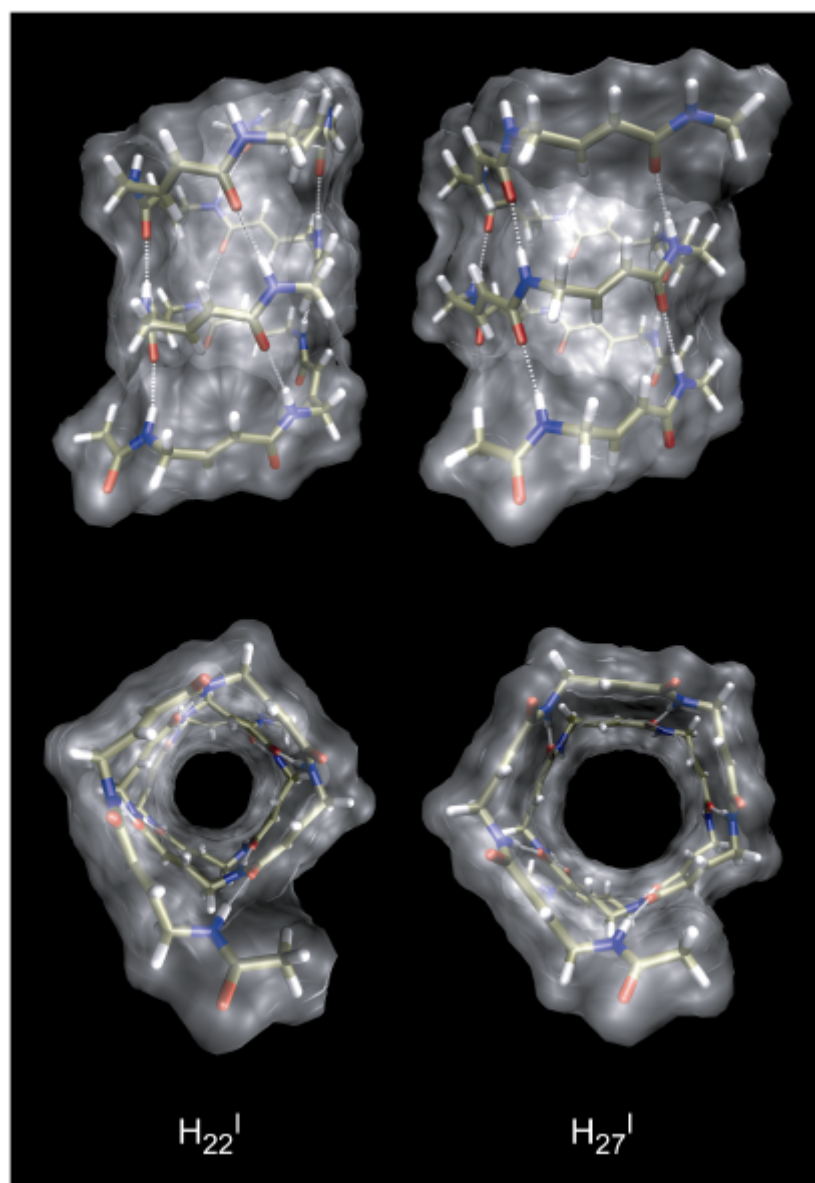


**FIGURE 7.** The helical undecamers  $H_{22}^I$  and  $H_{27}^I$  of the (E)-vinylogous  $\gamma$ -peptides as models for membrane channels and nanotubes.

#### *Monomer vs. oligomer approach*

For a better understanding of structure formation in oligomers and polymers, it is very tempting to refer the periodic secondary structure elements to special conformers of blocked monomer units. In fact, the  $\beta$ -strand conformations, the  $3_{10}$ -helices, and the  $\gamma$ -turns in  $\alpha$ -peptides and the  $H_{10}$ ,  $H_{12}$ , and  $H_{14}$  helices in  $\beta$ -peptides can be derived in this way. This is in some way surprising since the structural presuppositions for hydrogen bond linking in the aforementioned helices are not yet given in the blocked monomer units. However, this study on vinylogous  $\gamma$ -peptides and our preceding study on  $\gamma$ -peptides demonstrate that the monomer approach is only partially able to provide information on the characteristic periodic secondary structures in these classes of compounds. In particular, the helices with the larger hydrogen-bonded pseudocycles

between non-nearest-neighbor peptide bonds are missing now. This tendency is obviously increasing with lengthening of the monomer backbone. Within the monomer approach, it is always possible to predict those periodic structures of the oligomers which result from the oligomerization of the monomeric conformers without steric restrictions. This is independent of the possibility of additional hydrogen bonds or not. If there are hydrogen bonds between nearest-neighbor peptide bonds in the blocked monomer, such conformers are anyway favored. The hydrogen-bonded helices with the larger non-nearest neighbor pseudocycles can only be found by a systematic conformational analysis of oligomers. Thus, it is obvious that the oligomer approach, which principally allows the finding of all periodic structures, is superior over the monomer approach. However, the realization of a complete oligomer approach, as for instance for a hexamer, with relatively small grid intervals for the numerous torsion angles at a higher level of ab initio MO theory is rather tedious. Therefore, the combination of the monomer and a limited oligomer approach could be a good alternative to get a complete overview on all periodic secondary structures. Based on the monomer approach it is possible to find practically all periodic structures without hydrogen bonds and the structures with peptidic nearest-neighbor hydrogen bonds. A limited oligomer approach based on general criteria for hydrogen bonds predicts additionally the periodic structures with the non-nearest neighbor hydrogen bonds, which cannot be found within the monomer approach for larger backbones of the amino acid constituents.

## Conclusions

Our systematic theoretical investigation of helical structures in vinylogous  $\gamma$ -peptides provides a wide variety of alternative and competitive helices with and without hydrogen-bonded pseudocycles of different size. Contrary to the parent  $\gamma$ -peptides, there is a strict control of helix formation by the configuration of the double bond between the C( $\alpha$ ) and C( $\beta$ ) atoms of the monomer constituents. (E)-double bonds favor helices with larger pseudocycles beginning with 14- up to 27-membered rings. Contrary to this, the (Z)-configuration supports a distinct preference of helices with interactions between nearest neighbor peptide bonds. Therefore, helices with 22- and 19-membered rings are most stable in (E)-vinylogous  $\gamma$ -peptides, and those with 7- and 9-membered rings are the preferred ones in (Z)-vinylogous  $\gamma$ -peptides. In the case of the (E)-vinylogs, some helices without hydrogen bonds might become competitive to the hydrogen-bonded helices in polar environments. The rather stable helices  $H_{22}^I$ ,  $H_{24}$ , and  $H_{27}^I$  of the (E)-hexamers have inner diameters large enough to let molecules or ions pass. Thus, they could be interesting model compounds for the design of membrane channels and

monomolecular nanotubes. Our study shows that a combination of the monomer approach and a limited oligomer approach is able to provide a complete overview on all helical structures. Contrary to this, a complete oligomer approach search at a higher level of ab initio MO theory is too time-consuming and the monomer approach is not able find all possible helical structures.

**Acknowledgment.** We thank Deutsche Forschungsgemeinschaft (Project HO 2346/1 “Sekundärstrukturbildung in Peptiden mit nicht-proteinogenen Aminosäuren” and SFB 610 “Proteinzustände mit zellbiologischer und medizinischer Relevanz”) for support of this work.

**Supporting Information Available:** Tables with the backbone torsion angles of the monomers **1** and **2** at the B3LYP/6-31G\* and PCM/HF/6-31G\* levels, with the backbone torsion angles of the hexamers **1** and **2** at the B3LYP/6-31G level and with the backbone torsion angles of selected undecamers **1** at the HF/6-31G\* level of ab initio MO theory, with the enthalpies, free enthalpies, and entropies of all helix hexamers, coordinates of all helix hexamers and undecamers as pdb-files. This material is available on the compact disc attached at the end of this book.

## References

- (1) (a) Gellman, S. H. *Acc. Chem. Res.* **1998**, *31*, 173. (b) Hill, D. J.; Mio, M. J.; Prince, R. B.; Hughes, T. S.; Moore, J. S. *Chem. Rev.* **2001**, *101*, 3893. (c) Barron, A. E.; Zuckermann, R. N. *Curr. Opin. Chem. Biol.* **1999**, *3*, 681. (d) Cheng, R. P.; Gellman, S. H.; DeGrado, W. F. *Chem. Rev.* **2001**, *101*, 3219. (e) Seebach, D.; Beck, A. K.; Bierbaum, D. J. *Chem. & Biodiv.* **2004**, *1*, 1111.
- (2) (a) Fernández-Santín, J. M.; Aymamí, J.; Rodríguez-Galán, A.; Muñoz-Guerra, S.; Subirana, J. A. *Nature (London)* **1984**, *311*, 53. (b) Chandrakumar, N. S.; Stapelfeld, A.; Beardsley, P. M.; Lopez, O. T.; Drury, B.; Anthony, E.; Savage, M. A.; Williamson, L. N.; Reichman, M. *J. Med. Chem.* **1992**, *35*, 2928. (c) Appella, D. H.; Christianson, L. A.; Karle, I. L.; Powell, D. R.; Gellman, S. H. *J. Am. Chem. Soc.* **1996**, *118*, 13071. (d) Seebach, D.; Overhand, M.; Kühnle, F. N. M.; Martinoni, B.; Oberer, L.; Hommel, U.; Widmer, H. *Helv. Chim. Acta* **1996**, *79*, 913. (e) Krauthäuser, S.; Christianson, L. A.; Powell, D. R.; Gellman, S. H. *J. Am. Chem. Soc.* **1997**, *119*, 11719. (f) Seebach, D.; Matthews, J. L. *J. Chem. Soc., Chem. Commun.* **1997**, *21*, 2015. (g) Motorina, I. A.; Huel, C.; Quiniou, E.; Mispelter, J.; Adjadj, E.; Grierson, D. S. *J. Am. Chem. Soc.* **2001**, *123*, 8. (h) Martinek, T. A.; Fülöp, F. *Eur. J. Biochem.* **2003**, *270*, 3657.

- (3) (a) Rydon, H. N. *J. Chem. Soc.* **1964**, 1328. (b) Dado, G. P.; Gellman, S. H. *J. Am. Chem. Soc.* **1994**, *116*, 1054. (c) Hanessian, S.; Luo, X.; Schaum, R.; Michnick, S. *J. Am. Chem. Soc.* **1998**, *120*, 8569. (d) Brenner, M.; Seebach, D. *Helv. Chim. Acta* **2001**, *84*, 1181.
- (4) (a) Graf von Roedern, E.; Kessler, H. *Angew. Chem., Int. Ed. Engl.* **1994**, *33*, 687. (b) Graf von Roedern, E.; Lohof, E.; Hessler, G.; Hoffmann, M.; Kessler, H. *J. Am. Chem. Soc.* **1996**, *118*, 10156. (c) Smith, M. D.; Claridge, T. D. W.; Tranter, G. E.; Sansom, M. S. P.; Fleet, G. W. J. *Chem. Commun.* **1998**, 2041. (d) Szabo, L.; Smith, B. L.; McReynolds, K. D.; Parrill, A. L.; Morris, E. R.; Gervay, J. *J. Org. Chem.* **1998**, *63*, 1074. (e) Long, D. D.; Hungerford, N. L.; Smith, M. D.; Brittain, D. E. A.; Marquess, D. G.; Claridge, T. D. W.; Fleet, G. W. J. *Tetrahedron Lett.* **1999**, *40*, 2195. (f) Karig, G.; Fuchs, A.; Busing, A.; Brandstetter, T.; Scherer, S.; Bats, J. W.; Eschenmoser, A.; Quinkert, G. *Helv. Chim. Acta* **2000**, *83*, 1049. (g) Schwalbe, H.; Wermuth, J.; Richter, C.; Szalma, S.; Eschenmoser, A.; Quinkert, G. *Helv. Chim. Acta* **2000**, *83*, 1079. (h) Gregar, T. Q.; Gervay-Hague, J. *J. Org. Chem.* **2004**, *69*, 1001. (i) Ying, L. Q.; Gervay-Hague, J. *Carbohydr. Res.* **2004**, *339*, 367. (j) Banerjee, A.; Pramanik, A.; Bhattacharjya, S.; Balaram, P. *Biopolymers* **1996**, *39*, 769. (k) Shankaramma, S. C.; Singh, S. K.; Sathyamurthy, A.; Balaram, P. *J. Am. Chem. Soc.* **1999**, *121*, 5360. (l) Jiang, H.; Leger, J. M.; Huc, I. *J. Am. Chem. Soc.* **2003**, *125*, 3448. (m) Jiang, H.; Dolain, C.; Leger, J. M.; Gornitzka, H.; Huc, I. *J. Am. Chem. Soc.* **2004**, *126*, 1034.
- (5) (a) Daura, X.; Jaun, B.; Seebach, D.; van Gunsteren, W. F.; Mark, A. E. *J. Mol. Biol.* **1998**, *280*, 925. (b) Wu, Y.-D.; Wang, D.-P. *J. Am. Chem. Soc.* **1998**, *120*, 13485. (c) Wu, Y.; Wang, D.; Chan, K.; Yang, D. *J. Am. Chem. Soc.* **1999**, *121*, 11189. (d) Wu, Y.-D.; Wang, D.-P. *J. Am. Chem. Soc.* **1999**, *121*, 9352. (e) Möhle, K.; Günther, R.; Thormann, M.; Sewald, N.; Hofmann, H.-J. *Biopolymers* **1999**, *50*, 167. (f) Günther, R.; Hofmann, H.-J. *J. Am. Chem. Soc.* **2001**, *123*, 247. (g) Günther, R.; Hofmann, H.-J.; Kuczera, K. *J. Phys. Chem. B* **2001**, *105*, 5559. (h) Günther, R.; Hofmann, H.-J. *Helv. Chim. Acta* **2002**, *85*, 2149. (i) Baldauf, C.; Günther, R.; Hofmann, H.-J. *Helv. Chim. Acta* **2003**, *86*, 2573. (j) Baldauf, C.; Günther, R.; Hofmann, H.-J. *J. Mol. Struct. (Theochem)* **2004**, *675*, 19. (k) Baldauf, C.; Günther, R.; Hofmann, H.-J. *Angew. Chem., Int. Ed. Engl.* **2004**, *43*, 1594. (l) Baldauf, C.; Günther, R.; Hofmann, H.-J. *J. Org. Chem.* **2004**, *69*, 6214. (m) Beke, T.; Csizmadia, I. G.; Perczel, A. *J. Comput. Chem.* **2004**, *25*, 285.
- (6) (a) Appella, D. H.; Christianson, L. A.; Klein, D. A.; Powell, D. R.; Huang, X.; Barchi, J., Jr.; Gellman, S. H. *Nature (London)* **1997**, *387*, 381. (b) Appella, D. H.; Barchi, J., Jr.; Durell, S. R.; Gellman, S. H. *J. Am. Chem. Soc.* **1999**, *121*, 2309.



- (7) (a) Hagihara, M.; Anthony, N. J.; Stout, T. J.; Clardy, J.; Schreiber, S. L. *J. Am. Chem. Soc.* **1992**, *114*, 6568. (b) Henniges, H.; Gussetti, C.; Militzer, H. C.; Baird, M. S.; Demeijere, A. *Synthesis* **1994**, 1471. (c) Coutrot, P.; Grison, C.; Geneve, S.; Didierjean, C.; Aubry, A.; Vicherat, A.; Marraud, M. *Lett. Pept. Sci.* **1997**, *4*, 415. (d) Grison, C.; Geneve, S.; Halbin, E.; Coutrot, P. *Tetrahedron* **2001**, *57*, 4903.
- (8) (a) Wiberg, K. B.; Rosenberg, R. E.; Rablen, P. R. *J. Am. Chem. Soc.* **1991**, *113*, 2890. (b) Murcko, M. A.; Castejon, H.; Wiberg, K. B. *J. Phys. Chem.* **1996**, *100*, 16162. (c) Lee, P. S.; Du, W.; Boger, D. L.; Jorgensen, W. L. *J. Org. Chem.* **2004**, *69*, 5448.
- (9) (a) Frisch, M. J.; Trucks, G. W.; Schlegel, H. B.; Scuseria, G. E.; Robb, M. A.; Cheeseman, J. R.; J. A. Montgomery, J.; Vreven, T.; Kudin, K. N.; Burant, J. C.; Millam, J. M.; Iyengar, S. S.; Tomasi, J.; Barone, V.; Mennucci, B.; Cossi, M.; Scalmani, G.; Rega, N.; Petersson, G. A.; Nakatsuji, H.; Hada, M.; Ehara, M.; Toyota, K.; Fukuda, R.; Hasegawa, J.; Ishida, M.; Nakajima, T.; Honda, Y.; Kitao, O.; Nakai, H.; Klene, M.; Li, X.; Knox, J. E.; Hratchian, H. P.; Cross, J. B.; Adamo, C.; Jaramillo, J.; Gomperts, R.; Stratmann, R. E.; Yazyev, O.; Austin, A. J.; Cammi, R.; Pomelli, C.; Ochterski, J. W.; Ayala, P. Y.; Morokuma, K.; Voth, G. A.; Salvador, P.; Dannenberg, J. J.; Zakrzewski, V. G.; Dapprich, S.; Daniels, A. D.; Strain, M. C.; Farkas, O.; Malick, D. K.; Rabuck, A. D.; Raghavachari, K.; Foresman, J. B.; Ortiz, J. V.; Cui, Q.; Baboul, A. G.; Clifford, S.; Cioslowski, J.; Stefanov, B. B.; Liu, G.; Liashenko, A.; Piskorz, P.; Komaromi, I.; Martin, R. L.; Fox, D. J.; Keith, T.; Al-Laham, M. A.; Peng, C. Y.; Nanayakkara, A.; Challacombe, M.; Gill, P. M. W.; Johnson, B.; Chen, W.; Wong, M. W.; Gonzalez, C.; Pople, J. A.; Revision B.04 ed.; Gaussian Inc.: Pittsburgh PA, 2003. (b) Schmidt, M. W.; Baldrige, K. K.; Boatz, J. A.; Elbert, S. T.; Gordon, M. S.; Jensen, J. H.; Koseki, S.; Matsunaga, N.; Nguyen, K. A.; Su, S. J.; Windus, T. L.; Dupuis, M.; Montgomery, J. A. *J. Comput. Chem.* **1993**, *14*, 1347.
- (10) (a) Urry, D. W.; Goodall, M. C.; Glickson, J. D.; Mayers, D. F. *Proc. Natl. Acad. Sci. U. S. A.* **1971**, *68*, 1907. (b) Kovacs, F.; Quine, J.; Cross, T. A. *Proc. Natl. Acad. Sci. U. S. A.* **1999**, *96*, 7910.
- (11) (a) Bong, D. T.; Clark, T. D.; Granja, J. R.; Ghadiri, M. R. *Angew. Chem., Int. Ed. Engl.* **2001**, *40*, 988. (b) Koert, U.; Al-Momani, L.; Pfeifer, J. R. *Synthesis* **2004**, 1129.

## 4 *d*-Peptides and *d*-Amino Acids as Tools for Peptide Structure Design – A Theoretical Study

by Carsten Baldauf, Robert Günther, and Hans-Jörg Hofmann

published in JOURNAL OF ORGANIC CHEMISTRY

Vol. 69 (2004) pages 6214-6220



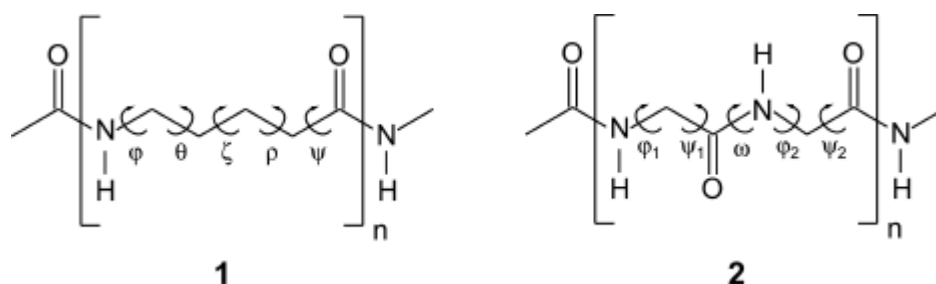
**Abstract.** An overview on all possible helix types in oligomers of *d*-amino acids (*d*-peptides) and their stabilities is given on the basis of a systematic conformational analysis employing various methods of ab initio MO theory (HF/6-31G\*, B3LYP/6-31G\*, PCM//HF/6-31G\*). A wide variety of novel helical structures with hydrogen-bonded pseudocycles of different size is predicted. Since a *d*-amino acid constituent may replace a dipeptide unit in *a*-peptides, there are close relationships between the secondary structures of peptides with *d*-amino acid residues and typical secondary structures of *a*-peptides. However, the preference of gauche conformations at the central C(*b*)-C(*g*) bonds of *d*-amino acids, which correspond to the peptide linkages in *a*-peptides, over staggered ones makes completely novel structure alternatives for helices and turns more probable. The peculiarities of *b*-turn formation by sugar amino acids derived from *d*-amino acids are compared with the turn formation in *d*-amino acid residues and in *a*-peptides. The considerable potential of secondary structure formation in *d*-peptides and single *d*-amino acid constituents predicted by ab initio MO theory may stimulate experimental work in the field of peptide and foldamer design.

## Introduction

In the last years, numerous examples of unnatural oligomeric sequences have been found that fold into well-defined conformations in solution.<sup>1</sup> It is popular to denote such oligomers as foldamers.<sup>1a</sup> In particular studies on oligomers of *b*- and  $\gamma$ -amino acids (*b*- and *g*-peptides) demonstrated their ability to adopt ordered secondary structures, e.g., helices, strands, and turns.<sup>2,3</sup> Thus, these homologues of *a*-peptides are candidates for mimicking the structure and function of their natural counterparts. In the meantime, experimental hints were also obtained for the formation of ordered structures in oligomers of *d*-amino acids (*d*-peptides),<sup>4</sup> although detailed structure information is still missing.

From the very beginning of peptide foldamer research the experimental investigations were accompanied by systematic investigations of the conformational space of *b*- and *g*-peptides employing theoretical methods.<sup>5</sup> The results of these studies contributed essentially to a better understanding of the origin and the features of the novel secondary structure types and predicted further possibilities of secondary structure formation. In the case of *b*-peptides, it was shown that all typical folding patterns can be derived from the conformers of the monomer constituents.<sup>5b,d,i</sup> On the contrary to this, the most favored helices of *g*-peptides do not correspond to conformers of blocked *g*-amino acids. They can only be localized by a detailed examination of longer oligomeric sequences.<sup>5k</sup>

Since experimental data on the secondary structure formation in oligomers of *d*-amino acids (*d*-peptides) **1** are still scarce, we extend our studies to this class of compounds following the same strategy as for the other homologues.<sup>5d,h,j,k</sup> Our aim is to get a complete overview on the possible folding alternatives and to compare them with those of *a*-peptides due to the close correspondence between *d*-amino acid residues and dipeptide elements in *a*-peptides **2**.



## Methodology

To examine the helix formation in *d*-peptides, a pool of 5,184 periodic conformations of the *d*-peptide hexamer **1** ( $n=6$ ) was generated by a systematic variation of the backbone torsion angles  $j$ ,  $y$ ,  $q$ ,  $z$ , and  $r$  in steps of  $60^\circ$ . All structures exhibiting the hydrogen bonding patterns of Figure 1 were selected as starting points for geometry optimizations at the HF/6-31G\* level of ab initio MO theory. The resulting minimum structures were reoptimized at the B3LYP/6-31G\* level of density functional theory to consider correlation energy effects. Finally, the influence of an aqueous environment (dielectric constant  $\epsilon = 78.4$ ) was estimated on the basis of the polarizable continuum model (PCM//HF/6-31G\*). The solvation energy includes the electrostatic, van der Waals and cavitation energy contributions. All turn conformers derived from *d*-amino acid constituents were examined at the same levels of ab initio MO theory.

The quantum chemical calculations were performed employing the Gaussian98, Gaussian03 and the Gamess-US program packages.<sup>7</sup>

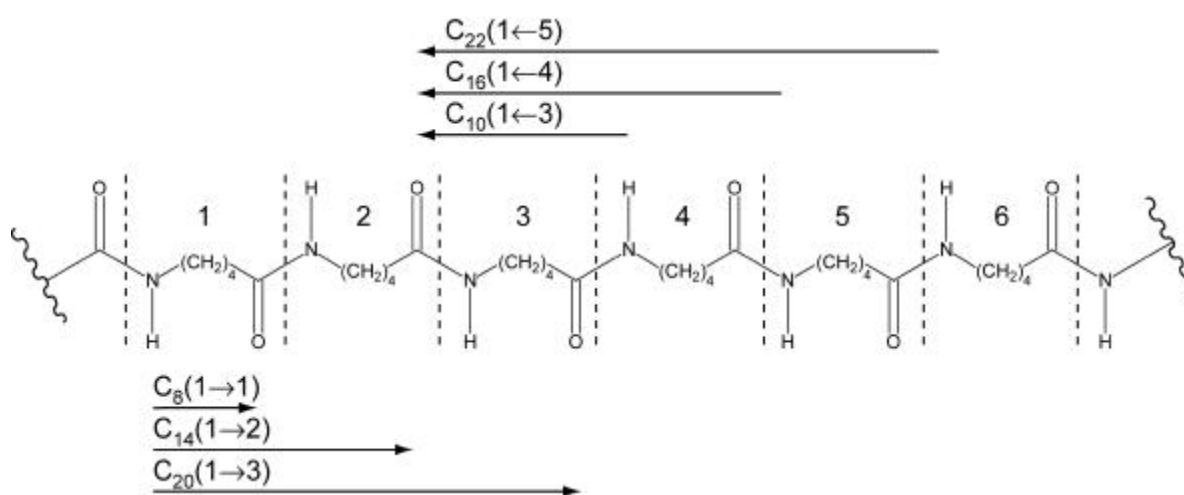


**FIGURE 1.** Possible hydrogen bonding patterns in *d*-peptides ( $C_x$  denotes the hydrogen-bonded pseudocycles with  $x$  atoms).

## Results and Discussion

### Helix Formation in *d*-Peptides

Our search for periodic structures in the *d*-peptide hexamer provided a large number of helices with different size of the hydrogen-bonded pseudocycles. As in the homologous *b*- and *g*-peptides, the hydrogen bonds can be formed in the forward or in backward direction along the sequence. Thus, hydrogen bonding patterns with 8-, 14- and 20-membered rings in the forward and with 10-, 16- and 22-membered rings in the backward direction occur according to the general scheme in Figure 1. The same hydrogen bonding pattern can be realized by various backbone conformations. Consequently, we find two helix alternatives with 8-membered, nine

**TABLE 1.** HF/6-31G\* Backbone Torsion Angles<sup>a</sup> for the Most Stable Helices of Each Ring Size in Hexamers of **1** (n=6)

conf. <sup>b</sup>	$\phi$	$\theta$	$\zeta$	$\rho$	$\psi$	conf. <sup>b</sup>	$\phi$	$\theta$	$\zeta$	$\rho$	$\psi$
H <sub>8</sub> <sup>I</sup>	-178.8	66.5	-143.5	69.1	-171.2	H <sub>10</sub> <sup>I</sup>	-97.3	62.8	68.2	-169.2	86.1
	-179.0	66.4	-142.5	69.2	-172.7		-97.9	62.6	68.3	-168.6	84.7
	-179.5	66.4	-142.2	69.1	-172.5		-98.1	62.4	68.4	-168.5	84.5
	-179.3	66.4	-142.2	69.2	-172.9		-98.2	62.4	68.4	-168.4	84.4
	-179.4	66.4	-142.5	69.3	-173.1		-98.3	62.4	68.4	-168.7	84.5
	-178.7	66.6	-143.9	69.7	-173.8		-99.0	62.6	68.8	-168.7	87.1
H <sub>14</sub> <sup>I</sup>	117.5	-73.5	169.9	-79.9	110.8	H <sub>16</sub> <sup>I</sup>	-77.8	179.8	-170.6	67.3	-113.1
	102.6	-71.9	172.1	-75.4	110.8		-75.3	-179.3	-170.6	70.1	-109.9
	105.9	-73.1	170.5	-77.1	111.5		-76.7	-178.8	-173.4	68.3	-108.0
	106.8	-73.0	170.0	-77.6	111.6		-75.6	-179.0	-173.6	68.5	-108.9
	106.0	-71.1	171.1	-75.0	108.8		-77.5	-177.0	-174.4	70.7	-107.1
	100.3	-74.1	175.8	-76.1	128.9		-78.7	-175.3	178.5	72.6	-105.8
H <sub>20</sub> <sup>I</sup>	158.6	-65.2	-176.6	178.0	129.4	H <sub>22</sub> <sup>I</sup>	-94.1	-175.4	177.0	70.7	-135.9
	130.4	-60.5	-177.5	-176.0	109.2		-91.3	-173.4	179.6	71.3	-136.3
	145.4	-59.5	-176.8	-174.5	132.7		-88.2	-173.7	178.1	72.8	-134.8
	115.7	-55.4	-172.8	-171.0	133.7		-88.5	-173.2	176.5	71.4	-128.4
	112.5	-56.8	-175.7	-174.3	140.2		-96.2	-172.5	175.6	72.2	-120.1
	111.7	-68.1	178.0	179.4	-151.4		-91.5	-179.8	173.2	64.2	-109.8

<sup>a</sup> Angles in degrees. <sup>b</sup> H<sub>x</sub> denotes a helix with hydrogen-bonded pseudocycles of x atoms. The superscript Roman number arranges helices of the same ring size according to their stability (cf. Table 2).

with 10-membered, six with 14-membered, four with 16-membered and three with 20- and 22-membered hydrogen-bonded pseudocycles. Helix alternatives with the same ring size are denoted by superscript Roman numbers at the helix symbol in the order of decreasing stability. Table 1 lists the backbone torsion angles of the most stable helices of each ring size obtained at the HF/6-31G\* level of ab initio MO theory. These helices are also visualized in Figure 2.

The corresponding backbone torsion angles at the B3LYP/6-31G\* level and those of the other helix alternatives at both approximation levels are given as Supporting Information. A

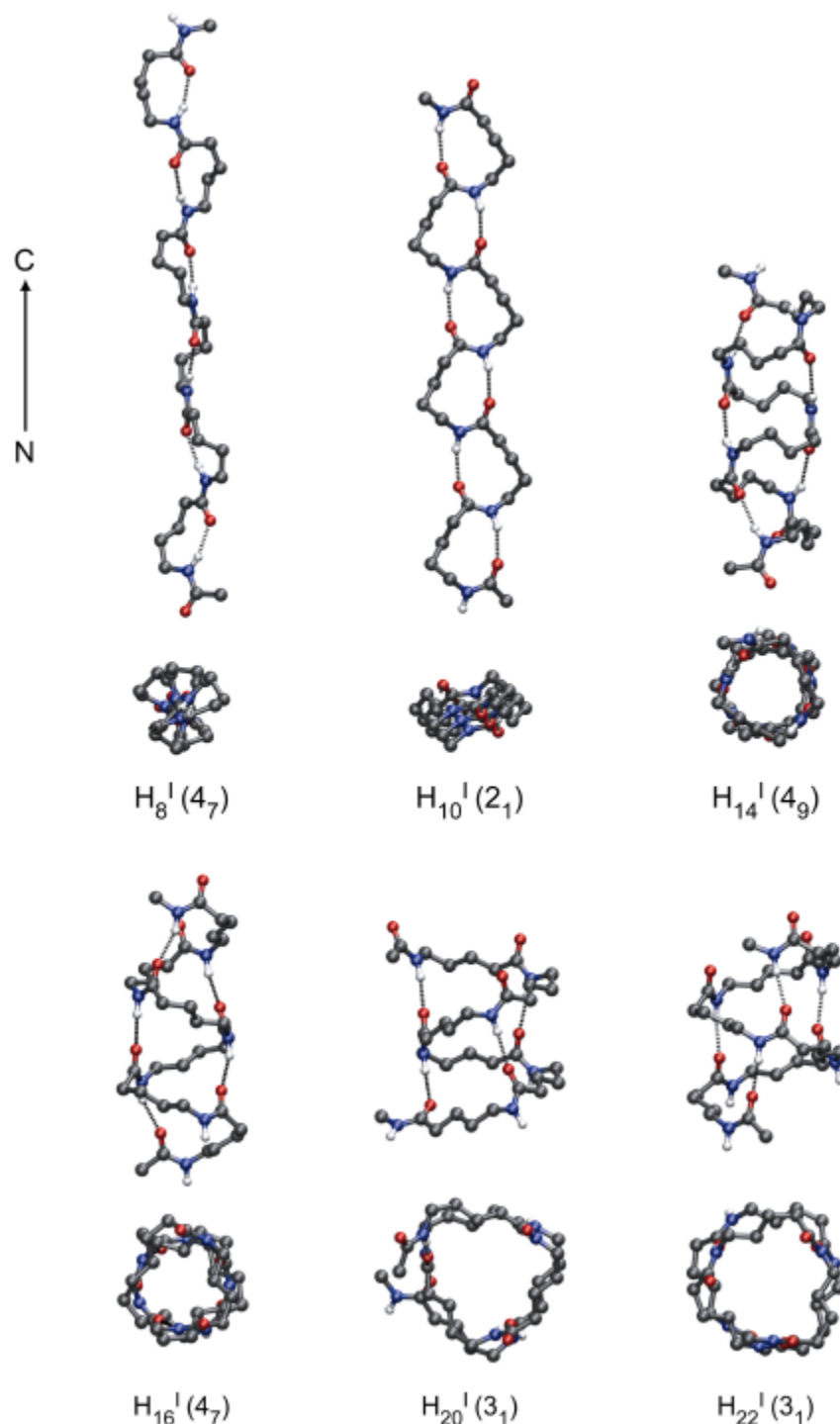


**FIGURE 2.** Most stable helices of **1** ( $n=6$ ) for each type of hydrogen-bonded pseudocycles obtained at the HF/6-31G\* level of ab initio MO theory (helix nomenclature in parentheses).

detailed look at the relative stabilization energies of all helical structures in Table 2 reveals that only a few of them have a chance to be found in experiments. Most stable is the conformer  $H_{10}^I$  according to the Hartree-Fock and density functional calculations followed by  $H_{14}^I$ ,  $H_{16}^I$  and  $H_8^I$ . In an aqueous environment, there is a stability increase in favor of helices with nearest-neighbor interactions.

Helices  $H_{10}$  and  $H_{16}$  deserve special attention with a value of about  $180^\circ$  for the torsion angle  $z$ , which describes the rotation around the central C(**b**)-C(**g**) bond of the **d**-amino acid

**TABLE 2.** Relative Energies<sup>a</sup> of the Helix Types in the Hexamer **1** at Various Approximation Levels of ab Initio MO Theory

Conf. <sup>b</sup>	$\Delta E(\text{HF})$	$\Delta E(\text{B3LYP})$	$\Delta E(\text{PCM})^c$
$H_8^I$	19.1	28.2	39.9
$H_8^{II}$	73.1	41.2	117.3
$H_{10}^I$	<b>0.0<sup>d</sup></b>	<b>0.0<sup>e</sup></b>	50.4
$H_{10}^{II}$	19.9	9.9	<b>0.0<sup>f</sup></b>
$H_{10}^{III}$	70.9	55.1	139.7
$H_{10}^{IV}$	71.9	64.1	130.9
$H_{10}^V$	82.8	66.9	153.8
$H_{10}^{VI}$	94.5	67.5	151.8
$H_{10}^{VII}$	100.2	90.3	133.6
$H_{10}^{VIII}$	105.4	92.7	145.2
$H_{10}^{IX}$	110.0	95.7	172.3
$H_{14}^I$	10.8	6.8	100.5
$H_{14}^{II}$	35.8	27.2	126.3
$H_{14}^{III}$	79.2	75.0	165.3
$H_{14}^{IV}$	84.1	78.2	176.1
$H_{14}^V$	113.9	108.8	203.1
$H_{14}^{VI}$	125.9	106.2	214.0
$H_{16}^I$	9.2	9.2	86.1
$H_{16}^{II}$	16.4	16.0	68.6
$H_{16}^{III}$	21.6	27.8	107.3
$H_{16}^{IV}$	95.3	84.2	192.8
$H_{20}^I$	30.1	38.0	81.6
$H_{20}^{II}$	49.7	64.1	114.2
$H_{20}^{III}$	60.4	66.7	121.5
$H_{22}^I$	18.7	22.0	76.2
$H_{22}^{II}$	33.2	37.1	81.7
$H_{22}^{III}$	61.8	52.8	123.0

<sup>a</sup> Relative energies in kJ/mol. <sup>b</sup> Cf. footnote b in Table 1. <sup>c</sup>  $\epsilon = 78.4$ .

<sup>d</sup>  $E_T = -2190.562661$  a.u. <sup>e</sup>  $E_T = -2204.282712$  a.u. <sup>f</sup>  $E_T = -2190.558820$  a.u.

constituents (cf. Supporting Information). The C(**b**)-C(**g**) bond in a **d**-amino acid constituent corresponds to the peptide bond in an **a**-dipeptide. Thus, it could be possible to find **d**-peptide helices that are formal analogues of the  $3_{10}$ - and **p**-helices of **a**-peptides with their 10- and 16-membered hydrogen-bonded rings. Among the  $H_{10}$  hexamers, only the rather unstable  $H_{10}^{VII}$  conformer is similar to the  $3_{10}$ -helix. For a close correspondence (cf. structures **1** and **2**), the torsion angles **j** and **r** in the **d**-peptide amino acid residues have to be about  $-60^\circ$  and the torsion angles **q** and **y** in between  $-20^\circ$  and  $-30^\circ$ , which are the typical values of **j** and **y** in a  $3_{10}$ -helix.

The actual values of about **j** =  $-51^\circ$ , **q** =  $-47^\circ$ , **r** =  $-72^\circ$ , and **y** =  $0^\circ$  in  $H_{10}^{VII}$  (cf. Supporting Information) show that the **d**-peptide helix  $H_{10}^{VII}$  is more similar to a periodic arrangement of **bI**-turns in **a**-peptides (cf. Table 3). The **d**-peptide counterpart for the postulated but not convincingly indicated **p**-helix in **a**-peptides is the conformer  $H_{16}^{III}$  with torsion angles of about **j** =  $-77^\circ$ , **q** =  $-59^\circ$ , **r** =  $-58^\circ$  and **y** =  $-65^\circ$  (cf. Supporting Information). These values agree with the torsion angles of **j** =  $-57^\circ$  and **y** =  $-70^\circ$  postulated for a **p**-helix in **a**-peptides.

The two examples illustrate the general capacity of **d**-peptide structures to fit approximately secondary structures of **a**-peptides. This was also demonstrated by the group of Balaram,<sup>6h</sup> who introduced a **d**-aminovaleric acid constituent into a sequence of **a**-amino acids and found that the **d**-amino acid adopts the  $3_{10}$ -helix conformation. However, this structure seems to be essentially enforced by the surrounding **a**-amino acids of the sequence. The stability relations in Table 2 show that helix alternatives with gauche conformations at the C(**b**)-C(**g**) bonds are distinctly favored over the staggered arrangements in oligomers of **d**-amino acids.

#### ***d**-Amino acid constituents as **b**-turn mimetics*

The typical **b**-turns of **a**-peptides consist of four consecutive **a**-amino acids. Most of them are characterized by a hydrogen bond between the peptidic CO bond of the first and the peptidic NH bond of the fourth amino acid, thus forming a 10-membered hydrogen-bonded pseudocycle (Figure 3). Since the first and the fourth amino acids of a **b**-turn are mostly part of periodic structures, the **b**-turn structure is determined by the conformation of the second and third amino acid. It is obvious that the replacement of the central **a**-dipeptide unit by a **d**-amino acid residue may be suited to mimic **b**-turns. In this case, the C(**b**)-C(**g**) bond of the **d**-amino acid replaces the peptide linkage between the second and third **a**-amino acids (cf. structures **1** and **2**). Turns in proteins are often exposed to the surrounding medium. Therefore, turns with **d**-amino acid



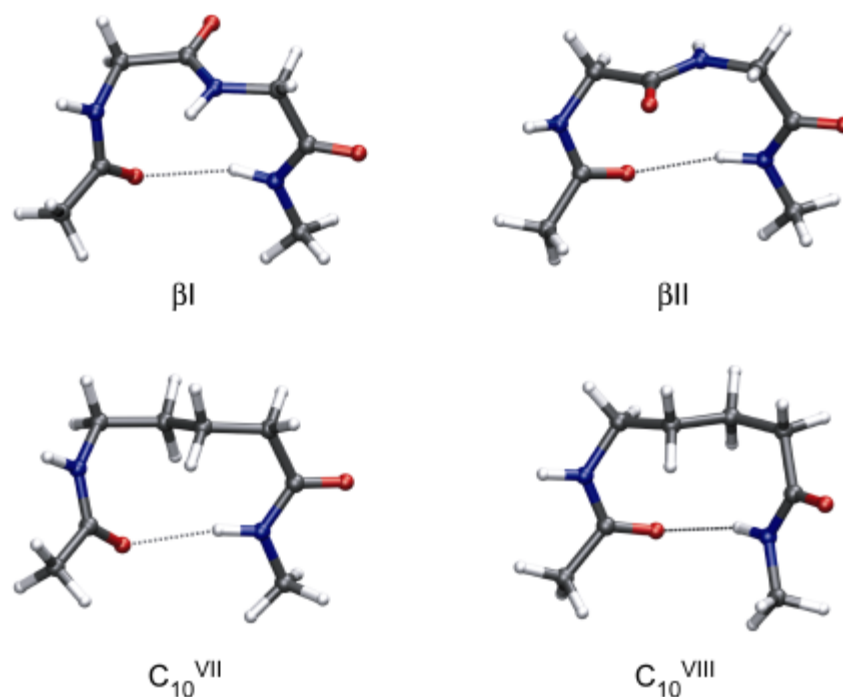


**FIGURE 3.** Comparison of the *bI*- and *bII*-turns of *a*-peptides with the two turn conformers  $C_{10}^{VII}$  and  $C_{10}^{VIII}$  of a blocked *d*-amino acid constituent.

residues may be attractive because of a higher resistance against proteases due to the missing central peptide bond. Besides, it is possible to design the interaction and recognition functions by special substitutions at the additional carbon atoms. The idealized backbone torsion angles<sup>8a</sup> for the predominating *bI*- and *bII*-turns of *a*-peptides and their approximate mirror images *bI'* and *II'* are given in Table 3 together with the calculated values.<sup>8b</sup>

Since the typical *b*-turns of *a*-peptides are characterized by a 10-membered hydrogen-bonded pseudocycle, one loop of the nine predicted  $H_{10}$  *d*-peptide conformers (Table 1 and Supporting Information) could potentially be a *b*-turn. A search for conformers with 10-membered hydrogen-bonded pseudocycles on a blocked *d*-amino acid monomer **1** with  $n=1$  in steps of  $30^\circ$  for the backbone torsion angles *j*, *y*, *q*, *z*, and *r*? confirms the loops of the helices  $H_{10}$  as conformers with about the same values of the backbone torsion angles and the same stability order (Tables 4 and 5). Further conformers of this type were not found. However, only conformers  $C_{10}^I$ ,  $C_{10}^{II}$ ,  $C_{10}^{VII}$  and  $C_{10}^{VIII}$  are suited to be *b*-turn mimetics. This was proved by an attachment of three *a*-amino acids at the N- and C- terminal ends of the 10-membered pseudocycles so that a *b*-sheet could be formed. Only the above-mentioned conformers were able to reverse the direction of the sequence of *a*-amino acids and to keep the *b*-sheet structure after geometry optimization (Figure 4). The conformational structure of the turn mimetics  $C_{10}^{VII}$  and  $C_{10}^{VIII}$  can immediately be related to that of the *bI/bI'*- and *bII/bII'*-turns in *a*-peptides

**TABLE 3.** Idealized and Calculated Backbone Torsion Angles<sup>a</sup> for the  $\beta$ I/I' and  $\beta$ II/II'-Turns in  $\alpha$ -Peptides

Turn	$\phi_1$	$\psi_1$	$\phi_2$	$\psi_2$
$\beta$ I	-60/-73	-30/-18	-90/-102	0/12
$\beta$ I'	60/73	30/18	90/102	0/-12
$\beta$ II	-60/-60	120/136	90/96	0/-12
$\beta$ II'	60/60	-120/-136	-90/-96	0/12

<sup>a</sup> Angles in degrees; first values idealized,<sup>8a</sup> second values calculated for a blocked glycine dipeptide.<sup>8b</sup>

**TABLE 4.** HF/6-31G\* Backbone Torsion Angles<sup>a</sup> for the C<sub>10</sub> Conformers of a Blocked  $\delta$ -Amino Acid Monomer **1**

Conf. <sup>b</sup>	$\phi$	$\theta$	$\zeta$	$\rho$	$\psi$
C <sub>10</sub> <sup>I</sup>	98.4	-62.5	-68.4	169.4	-90.4
C <sub>10</sub> <sup>II</sup>	83.0	-161.6	72.1	68.3	-104.9
C <sub>10</sub> <sup>III</sup>	121.3	-53.5	-46.7	-52.6	129.7
C <sub>10</sub> <sup>V</sup>	79.8	-161.8	76.8	-81.8	115.7
C <sub>10</sub> <sup>IV</sup>	96.4	-72.0	86.9	-168.3	82.9
C <sub>10</sub> <sup>VI</sup>	100.8	-67.9	-96.9	58.7	51.6
C <sub>10</sub> <sup>IX</sup>	68.3	52.0	-90.8	-67.7	106.4
C <sub>10</sub> <sup>VII</sup>	52.4	48.5	-177.8	69.9	9.8
C <sub>10</sub> <sup>VIII</sup>	66.4	-118.5	169.4	-67.5	-20.5

<sup>a</sup> Angles in degrees. <sup>b</sup> C<sub>10</sub> denotes a conformer with a hydrogen-bonded pseudocycle of ten atoms. The Roman numbers refer to the corresponding helices in Table 1.

(Tables 3 and 4, Figure 3). A comparison with the conformers C<sub>10</sub><sup>I</sup> and C<sub>10</sub><sup>II</sup> shows that gauche conformations at the C(**b**)-C(**g**) bond are more stable than staggered ones in turn-like conformers as it was already found for helical structures. Thus, **b**-turn alternatives that are impossible in **a**-peptides are preferred when inserting **d**-amino acid constituents into an **a**-peptide sequence. However, the less stable C<sub>10</sub><sup>VII</sup> and C<sub>10</sub><sup>VIII</sup> turns become predominant after introduction of a **b**, **g** double bond in the **d**-amino acid constituent mimicking the peptide bond of the **a**-peptide as it was tried several times.<sup>6a,c,d,f,g</sup>

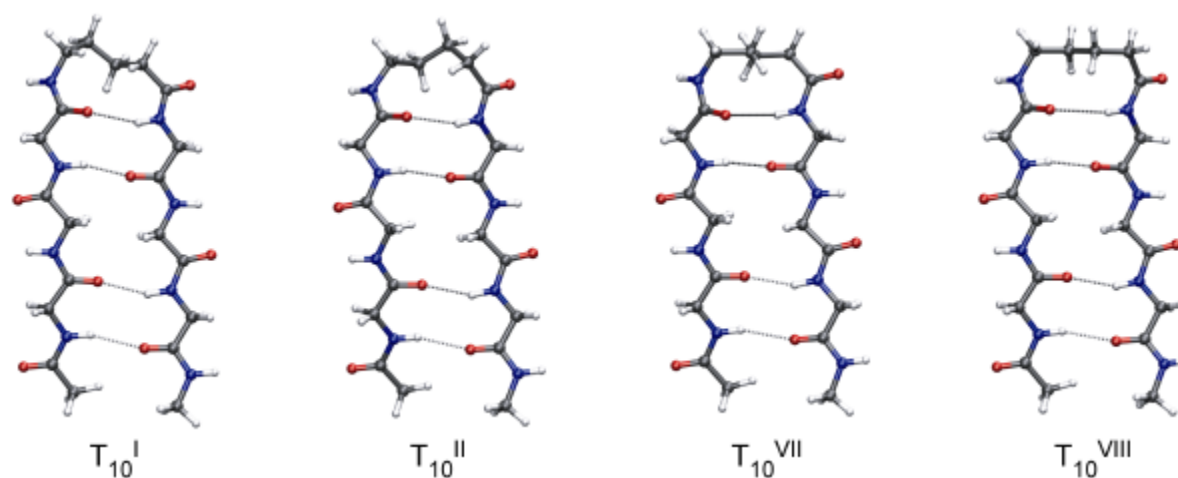
#### *Sugar amino acids as **b**-turn mimetics*

Some sugar amino acids can be considered as **d**-amino acid derivatives. Oligomers of such sugar amino acids represent pyranose- or furanose-based carbopeptoid foldamers. In several studies sugar amino acids have been inserted into **a**-peptide sequences to design reverse turns.<sup>6b,e</sup>

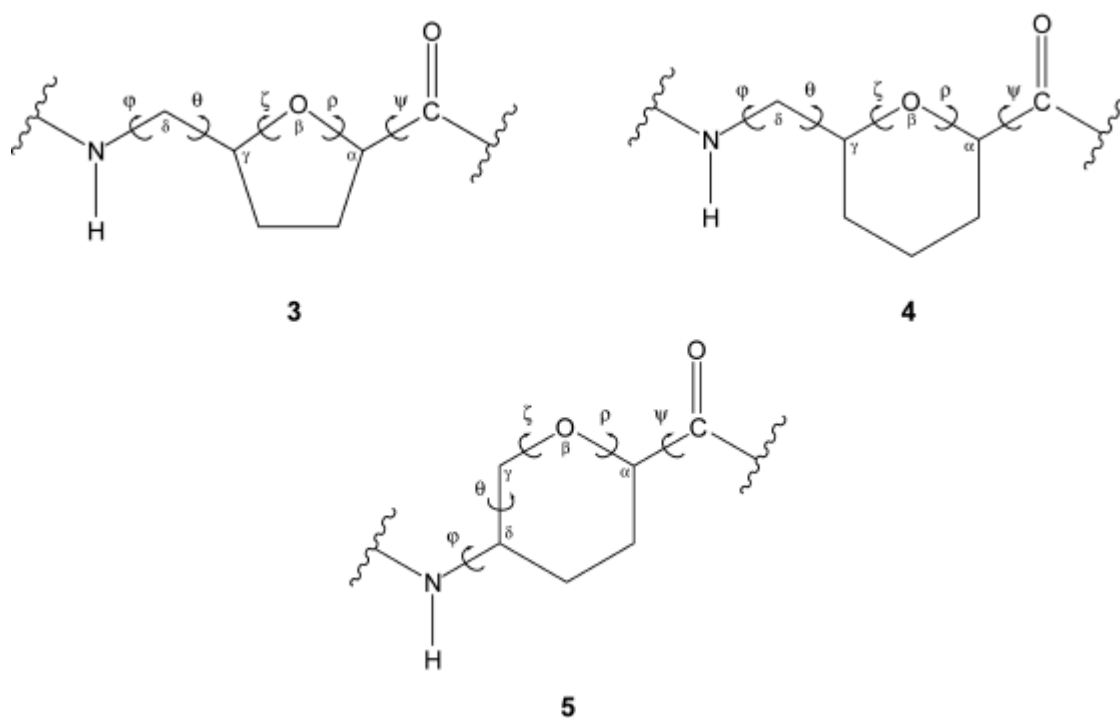
**TABLE 5.** Relative Energies<sup>a</sup> of the C<sub>10</sub> Conformers of a Blocked  $\delta$ -Amino Acid Monomer **1** (n=1) at Various Approximation Levels of ab Initio MO Theory

Conf. <sup>b</sup>	$\Delta E(\text{HF})$	$\Delta E(\text{B3LYP})$	$\Delta E(\text{PCM})^c$
C <sub>10</sub> <sup>I</sup>	<b>0.0</b> <sup>d</sup>	<b>0.0</b> <sup>e</sup>	<b>0.0</b> <sup>f</sup>
C <sub>10</sub> <sup>II</sup>	2.1	1.3	2.8
C <sub>10</sub> <sup>III</sup>	6.6	4.5	9.1
C <sub>10</sub> <sup>V</sup>	9.9	8.6	16.1
C <sub>10</sub> <sup>IV</sup>	10.9	10.0	9.8
C <sub>10</sub> <sup>VI</sup>	14.0	10.7	13.7
C <sub>10</sub> <sup>IX</sup>	14.3	13.1	13.8
C <sub>10</sub> <sup>VII</sup>	16.6	16.1	11.7
C <sub>10</sub> <sup>VIII</sup>	18.6	16.7	16.9

<sup>a</sup> Relative energies in kJ/mol. <sup>b</sup> C<sub>10</sub> denotes a conformer with a hydrogen-bonded pseudocycle of ten atoms. The Roman numbers refer to the corresponding helices in Table 1. <sup>c</sup>  $\epsilon = 78.4$ . <sup>d</sup> E<sub>T</sub> = -570.930590 a.u. <sup>e</sup> E<sub>T</sub> = -574.481381 a.u. <sup>f</sup> E<sub>T</sub> = -570.935718 a.u.

**FIGURE 4.** Conformers C<sub>10</sub><sup>I</sup>, C<sub>10</sub><sup>II</sup>, C<sub>10</sub><sup>VII</sup>, and C<sub>10</sub><sup>VIII</sup> as **b**-turn mimetics T<sub>10</sub><sup>I</sup>, T<sub>10</sub><sup>II</sup>, T<sub>10</sub><sup>VII</sup>, and T<sub>10</sub><sup>VIII</sup> embedded in a **b**-sheet structure after geometry optimization at the HF/6-31G\* level

These sugar amino acids can be derived from both furanose and pyranose residues. In particular, sugar amino acids of the types **3-5** might be able to form **b**-turns since they can be considered as **d**-amino acid derivatives representing dipeptide isosteres. It is interesting to compare the **b**-turns predicted for a blocked **d**-amino acid with those formed by these sugar amino acids. The secondary structure in sequences with sugar amino acid constituents depends strongly on the stereochemistry of the ring systems and the substitution type. Contrary to the ordinary **d**-amino acids, the torsion angles **z** and **r** in the furanose- and pyranose-based sugar amino acids **3** and **4** and the torsion angles **q**, **z** and **r** in the pyranose-based sugar amino acid **5** are determined by the



actual ring conformation. Therefore, the torsion angles in **b**-turn mimetics with sugar amino acids may differ from those predicted for the aliphatic **d**-amino acids. A detailed analysis of the possibilities of **b**-turn formation with the sugar amino acids **3** and **4** considering different substitution patterns provided four  $C_{10}$  ring conformers for **3** and two for **4** with (pseudo)axial/(pseudo)equatorial or (pseudo)equatorial/(pseudo)equatorial orientations of the ring substituents. These pseudocycles are shown in Figure 5. The torsion angles of the six  $C_{10}$  rings are given in Table 6. A perfect agreement between a  $C_{10}$  conformer of the sugar amino acids and a  $C_{10}$  ring of a **d**-amino acid constituent can only be seen for the pseudocycle  $C_{10}^{\text{IIP}}$  of the pyranose derivative **4** with the acetyl aminomethylene group in axial and the N-methyl amide group in equatorial positions of the chair. The  $C_{10}^{\text{IIP}}$  conformer corresponds immediately to the most stable pseudocycle  $C_{10}^{\text{I}}$  in Table 4. All other  $C_{10}$  ring conformations of the sugar amino acids are different from those in Table 4. The stability of the pyranose turn  $C_{10}^{\text{IIP}}$  is surpassed by that of the conformer  $C_{10}^{\text{IP}}$ , whose conformation is in good agreement with experimental structure data for cyclopeptides having this structure element inserted.<sup>6b,e</sup> The three furanose pseudocycles  $C_{10}^{\text{I-III}f}$  and the pyranose conformer  $C_{10}^{\text{IP}}$  of **4** and their mirror images can keep a **b**-sheet structure in an **a**-amino acid sequence without notable changes of the original turn conformation. This was again proved by complete geometry optimization of the corresponding **b**-sheet structures as described for the aliphatic **d**-amino acids inserted into an **a**-amino acid sequence as **b**-turn elements. The furanose and pyranose turns  $C_{10}^{\text{IV}f}$  and  $C_{10}^{\text{IIP}}$  maintain sheet structures only after changes of the torsion angles **j** and **y**. In the optimized conformation of the supersecondary structures, the hydrogen bonds in the  $C_{10}$  rings get lost. The possibility of **b**-turns

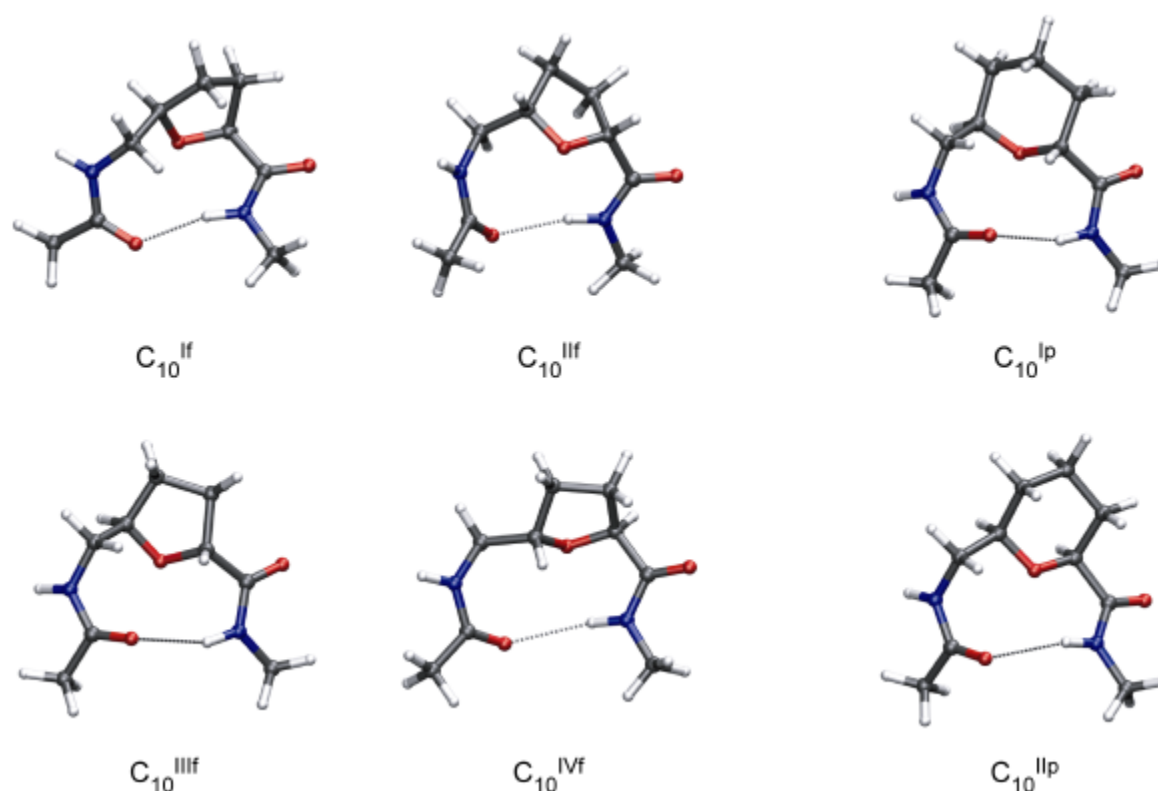


**FIGURE 5.** *b*-turns of furanose- and pyranose-based sugar amino acids.

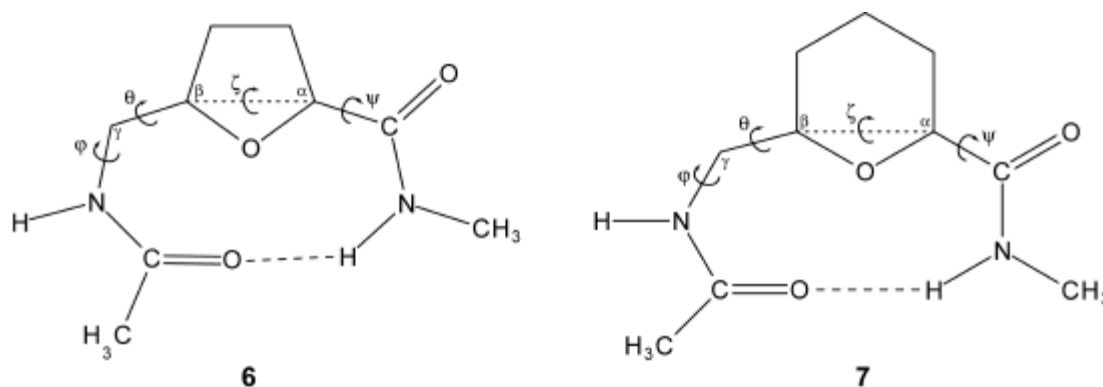
**TABLE 6.** HF/6-31G\* Backbone Torsion Angles and Stability Order of the  $C_{10}$  Conformers of the Sugar Amino Acid Derivatives **3** and **4**<sup>a</sup>

Conf. <sup>b</sup>	$\varphi$	$\theta$	$\zeta$	$\rho$	$\psi$	$\Delta E$
$C_{10}^{If}$ (eq,eq)	94.7	-57.5	-132.4	108.5	4.6	<b>0.0</b> <sup>c</sup>
$C_{10}^{IIIf}$ (eq,eq)	95.6	-59.6	-123.5	144.0	-20.6	4.8
$C_{10}^{IIIIf}$ (ax,eq)	86.6	-55.6	-96.1	-166.7	-61.4	24.0
$C_{10}^{IVf}$ (eq,ax)	63.3	-114.6	-166.9	-97.9	-4.9	26.1
$C_{10}^{Ip}$ (eq,eq)	91.4	-61.1	179.7	-179.1	-3.4	<b>0.0</b> <sup>d</sup>
$C_{10}^{IIp}$ (ax,eq)	92.0	-61.8	-76.1	179.6	-78.1	18.8

<sup>a</sup> Angles in degrees; Relative energies in kJ/mol. <sup>b</sup> Nomenclature: The  $C_{10}$  pseudocycles are differentiated by superscript Roman numerals in order of decreasing stability followed by “f” for the furanose-based and “p” for the pyranose-based derivatives. The axial or equatorial orientations of the substituents are given in parentheses in the order  $CH_3CONHCH_2$  group and  $CONH(CH_3)$  group. <sup>c</sup>  $E_T = -683.657605$  a.u. <sup>d</sup>  $E_T = -722.693949$  a.u.

with sugar amino acids of type **5** is more restricted. The only  $C_{10}$  pseudocycle obtained is not able to continue ordered secondary structures.

It is interesting to note that the furanose- and pyranose-based turns of **3** and **4** with the two substituents in equatorial orientations, but not the derivatives with the substituents in axial and equatorial orientations show a certain similarity to pseudocycles formed in oligomers of  $\delta$ -amino acids and their vinylogues. Thinking the oxygen bridge of the furanose ring of **3** and the pyranose



ring of **4** replaced by a fictive bond between the substituent-bearing ring atoms as indicated by a dotted line in the model structures **6** and **7**, the formal similarity becomes obvious. The turn torsion angles measured via the fictive bond correspond to those of the most stable  $C_9$  pseudocycles found in blocked  $g$ -amino acid derivatives (Table 7).<sup>5k</sup> Due to the equatorial orientation of the substituents, there is a change of the torsion angle  $z$  from a typical value for a gauche conformation to that of a *cis* orientation in the  $C_9$  ring of a blocked  $g$ -amino acid constituent, as it can be expected for blocked *cis*-vinylogous  $g$ -amino acids. Depending on the sugar ring stereochemistry, the secondary structure formation with sugar amino acids **3** and **4** can obviously be more related to the secondary structures of  $g$ -peptides and their *cis*- and *trans*-vinylogues than to those of  $d$ -peptides. A similar correspondence might also exist between the secondary structure elements of  $b$ -peptides and oligomers of sugar amino acids of type **5**. These aspects could be interesting for the structure interpretation of the experimentally found helices in oligomers of sugar amino acid derivatives **3-5**.<sup>4b,c,d,f,i</sup>

## Conclusions

The results of our systematic conformational analysis on  $d$ -amino acid monomers and oligomers demonstrate the considerable potential of secondary structure formation in this class of compounds. As in the homologous  $b$ - and  $g$ -peptides, a wide variety of helices with hydrogen-bonded pseudocycles of different size formed between the peptide bonds in the forward or backward direction along the sequence can be expected. This confirms the fact that elongation of the backbone of the amino acid constituents does not prevent the formation of ordered secondary structures due to a higher backbone flexibility, but increases the number of folding alternatives due to the well-defined conformational states arising from the additional single bonds. A peculiarity of a  $d$ -amino acid residue is its close correspondence to an  $a$ -di-peptide unit. Thus,  $d$ -amino acid monomers are able to adopt the secondary structures of  $a$ -peptide sequences.

**TABLE 7.** Comparison of the HF/6-31G\* Backbone Torsion Angles of the C<sub>10</sub> Conformers of **3** and **4** with Equatorial Substituent Orientations and those in the Most Stable C<sub>9</sub> Conformers of Blocked  $\mathbf{g}$ -Amino Acids and *cis*-Vinyllogous  $\mathbf{g}$ -Amino Acids<sup>a</sup>

Conf. <sup>b</sup>	<i>j</i>	<i>q</i>	<i>z</i>	<i>y</i>
C <sub>10</sub> <sup>If</sup>	94.7	-89.8	-24.2	41.9
C <sub>10</sub> <sup>IIf</sup>	95.6	-94.0	19.4	8.4
C <sub>10</sub> <sup>Ip</sup>	91.4	-60.8	0.8	-4.0
C <sub>9</sub> <sup>Ic</sup>	99.4	-70.7	-74.6	103.7
C <sub>9</sub> <sup>Id</sup>	80.5	-123.7	-0.1	45.7

<sup>a</sup>Angles in degrees. <sup>b</sup>For nomenclature cf. Table 6. <sup>c</sup>Blocked  $\gamma$ -amino acid monomer.<sup>5k</sup> <sup>d</sup>Blocked *cis*-vinyllogous  $\gamma$ -amino acid monomer.

However, this is considerably enforced by the  $\alpha$ -amino acids which the  $\mathbf{d}$ -amino acid residue is embedded in. The distinct preference of *gauche* orientations over staggered ones at the C(**b**)-C(**g**) bond makes novel helix types in oligomers of  $\mathbf{d}$ -amino acids more probable than the direct counterparts of  $\mathbf{a}$ -peptide helices. Even if a  $\mathbf{b}$ -sheet structure can be maintained in a sequence of  $\mathbf{a}$ -amino acids via a  $\mathbf{b}$ -turn with a  $\mathbf{d}$ -amino acid constituent instead of the central  $\mathbf{a}$ -di-peptide unit, novel turn conformations are preferred over those corresponding to the typical  $\mathbf{b}$ -turns of  $\mathbf{a}$ -peptides. Keeping in mind the additional possibilities of special backbone substitutions,  $\mathbf{d}$ -peptides and  $\mathbf{d}$ -amino acids enrich the field of secondary structures considerably and could be a useful tool in peptide and foldamer design.

**Acknowledgement.** We thank Deutsche Forschungsgemeinschaft (Project HO 2346/1 “Sekundärstrukturbildung in Peptiden mit nicht-proteinogenen Aminosäuren” and SFB 610 “Proteinzustände mit zellbiologischer und medizinischer Relevanz”) for support of this work.

**Supporting Information Available:** Tables with the backbone torsion angles of the most stable helices at the B3LYP/6-31G\* level, the backbone torsion angles of the lesser stable helix alternatives at the HF/6-31G\* and B3LYP/6-31G\* levels, and the backbone torsion angles of the C<sub>10</sub> conformers at the B3LYP/6-31G\* level of ab initio MO theory. This material is available on the compact disc attached at the end of this book.

## References

- (1) (a) Gellman, S. H. *Acc. Chem. Res.* **1998**, *31*, 173. (b) Barron, A. E.; Zuckermann, R. N. *Curr. Opin. Chem. Biol.* **1999**, *3*, 681. (c) Kirshenbaum, K.; Zuckermann, R. N.; Dill, K. A. *Curr. Opin. Struct. Biol.* **1999**, *9*, 530. (d) Stigers, K. D.; Soth, M. J.; Nowick, J. S. *Curr. Opin. Chem. Biol.* **1999**, *3*, 714. (e) Cheng, R. P.; Gellman, S. H.; DeGrado, W. F. *Chem. Rev.* **2001**, *101*, 3219. (f) Cubberley, M. S.; Iverson, B. L. *Curr. Opin. Chem. Biol.* **2001**, *5*, 650. (g) Hill, D. J.; Mio, M. J.; Prince, R. B.; Hughes, T. S.; Moore, J. S. *Chem. Rev.* **2001**, *101*, 3893. (h) Sanford, A. R.; Gong, B. *Curr. Org. Chem.* **2003**, *7*, 1649.
- (2) (a) Fernández-Santín, J. M.; Aymamí, J.; Rodríguez-Galán, A.; Muñoz-Guerra, S.; Subirana, J. A. *Nature (London)* **1984**, *311*, 53. (b) Chandrakumar, N. S.; Stapelfeld, A.; Beardsley, P. M.; Lopez, O. T.; Drury, B.; Anthony, E.; Savage, M. A.; Williamson, L. N.; Reichman, M. *J. Med. Chem.* **1992**, *35*, 2928. (c) Appella, D. H.; Christianson, L. A.; Karle, I. L.; Powell, D. R.; Gellman, S. H. *J. Am. Chem. Soc.* **1996**, *118*, 13071. (d) Seebach, D.; Overhand, M.; Kühnle, F. N. M.; Martinoni, B.; Oberer, L.; Hommel, U.; Widmer, H. *Helv. Chim. Acta* **1996**, *79*, 913. (e) Krauthäuser, S.; Christianson, L. A.; Powell, D. R.; Gellman, S. H. *J. Am. Chem. Soc.* **1997**, *119*, 11719. (f) Seebach, D.; Matthews, J. L. *J. Chem. Soc., Chem. Commun.* **1997**, 2015. (g) Seebach, D.; Abele, S.; Gademann, K.; Jaun, B. *Angew. Chem., Int. Ed. Engl.* **1999**, *38*, 1595. (h) Motorina, I. A.; Huel, C.; Quiniou, E.; Mispelter, J.; Adjadj, E.; Grierson, D. S. *J. Am. Chem. Soc.* **2001**, *123*, 8. (i) Martinek, T. A.; Fülöp, F. *Eur. J. Biochem.* **2003**, *270*, 3657.
- (3) (a) Rydon, H. N. *J. Chem. Soc.* **1964**, 1328. (b) Hanessian, S.; Luo, X.; Schaum, R.; Michnick, S. *J. Am. Chem. Soc.* **1998**, *120*, 8569. (c) Hintermann, T.; Gademann, K.; Jaun, B.; Seebach, D. *Helv. Chim. Acta* **1998**, *81*, 983. (d) Hanessian, S.; Luo, X. H.; Schaum, R. *Tetrahedron Lett.* **1999**, *40*, 4925. (e) Brenner, M.; Seebach, D. *Helv. Chim. Acta* **2001**, *84*, 1181. (f) Brenner, M.; Seebach, D. *Helv. Chim. Acta* **2001**, *84*, 2155. (g) Seebach, D.; Brenner, M.; Rueping, M.; Jaun, B. *Chem. Eur. J.* **2002**, *8*, 573.
- (4) (a) Smith, M. D.; Claridge, T. D. W.; Tranter, G. E.; Sansom, M. S. P.; Fleet, G. W. J. *J. Chem. Soc., Chem. Commun.* **1998**, 2041. (b) Szabo, L.; Smith, B. L.; McReynolds, K. D.; Parrill, A. L.; Morris, E. R.; Gervay, J. *J. Org. Chem.* **1998**, *63*, 1074. (c) Claridge, T. D. W.; Long, D. D.; Hungerford, N. L.; Aplin, R. T.; Smith, M. D.; Marquess, D. G.; Fleet, G. W. J. *Tetrahedron Lett.* **1999**, *40*, 2199. (d) Long, D. D.; Hungerford, N. L.; Smith, M. D.; Brittain, D. E. A.; Marquess, D. G.; Claridge, T. D. W.; Fleet, G. W. J. *Tetrahedron Lett.* **1999**, *40*, 2195. (e) Brittain, D. E. A.; Watterson, M. P.; Claridge, T. D. W.; Smith, M. D.; Fleet, G. W. J. *J. Chem. Soc., Perkin Trans. 1* **2000**, 3655. (f) Hungerford, N. L.; Claridge, T.



- D. W.; Watterson, M. P.; Aplin, R. T.; Moreno, A.; Fleet, G. W. J. *J. Chem. Soc., Perkin Trans. 1* **2000**, 3666. (g) Karig, G.; Fuchs, A.; Busing, A.; Brandstetter, T.; Scherer, S.; Bats, J. W.; Eschenmoser, A.; Quinkert, G. *Helv. Chim. Acta* **2000**, *83*, 1049. (h) Schwalbe, H.; Wermuth, J.; Richter, C.; Szalma, S.; Eschenmoser, A.; Quinkert, G. *Helv. Chim. Acta* **2000**, *83*, 1079. (i) McReynolds, K. D.; Gervay-Hague, J. *Tetrahedron: Asymmetry* **2000**, *11*, 337. (j) Jiang, H.; Léger, J. M.; Dolain, C.; Guionneau, P.; Huc, I. *Tetrahedron* **2003**, *59*, 8365. (k) Jiang, H.; Léger, J. M.; Huc, I. *J. Am. Chem. Soc.* **2003**, *125*, 3448. (l) Gregar, T. Q.; Gervay-Hague, J. *J. Org. Chem.* **2004**, *69*, 1001. (m) Ying, L.; Gervay-Hague, J. *Carbohydr. Res.* **2004**, *339*, 367. (n) Zhao, X.; Jia, M.-X.; Jiang, X.-K.; Wu, L.-Z.; Li, Z.-T.; Chen, G.-J. *J. Org. Chem.* **2004**, *69*, 270. (o) Jiang, H.; Dolain, C.; Leger, J.-M.; Gornitzka, H.; Huc, I. *J. Am. Chem. Soc.* **2004**, *126*, 1034.
- (5) (a) Daura, X.; Jaun, B.; Seebach, D.; van Gunsteren, W. F.; Mark, A. E. *J. Mol. Biol.* **1998**, *280*, 925. (b) Wu, Y.-D.; Wang, D.-P. *J. Am. Chem. Soc.* **1998**, *120*, 13485. (c) Daura, X.; van Gunsteren, W. F.; Mark, A. E. *Proteins: Struct. Funct. Genet.* **1999**, *34*, 269. (d) Möhle, K.; Günther, R.; Thormann, M.; Sewald, N.; Hofmann, H.-J. *Biopolymers* **1999**, *50*, 167. (e) Wu, Y.-D.; Wang, D.-P. *J. Am. Chem. Soc.* **1999**, *121*, 9352. (f) Aleman, C.; Leon, S. *J. Mol. Struct. (Theochem)* **2000**, *505*, 211. (g) Wu, Y.-D.; Wang, D.-P. *J. Chin. Chem. Soc.* **2000**, *47*, 129. (h) Günther, R.; Hofmann, H.-J. *J. Am. Chem. Soc.* **2001**, *123*, 247. (i) Günther, R.; Hofmann, H.-J.; Kuczera, K. *J. Phys. Chem. B* **2001**, *105*, 5559. (j) Günther, R.; Hofmann, H.-J. *Helv. Chim. Acta* **2002**, *85*, 2149. (k) Baldauf, C.; Günther, R.; Hofmann, H.-J. *Helv. Chim. Acta* **2003**, *86*, 2573. (l) Baldauf, C.; Günther, R.; Hofmann, H.-J. *Angew. Chem., Int. Ed. Engl.* **2004**, *43*, 1594. (m) Beke, T.; Csizmadia, I. G.; Perczel, A. *J. Comput. Chem.* **2004**, *25*, 285.
- (6) (a) Hann, M. M.; Sammes, P. G.; Kennewell, P. D.; Taylor, J. B. *J. Chem. Soc., Chem. Commun.* **1980**, 234. (b) Graf von Roedern, E.; Kessler, H. *Angew. Chem., Int. Ed. Engl.* **1994**, *33*, 687. (c) Wipf, P.; Fritch, P. C. *J. Org. Chem.* **1994**, *59*, 4875. (d) Gardner, R. R.; Liang, G. B.; Gellman, S. H. *J. Am. Chem. Soc.* **1995**, *117*, 3280. (e) Graf von Roedern, E.; Lohof, E.; Hessler, G.; Hoffmann, M.; Kessler, H. *J. Am. Chem. Soc.* **1996**, *118*, 10156. (f) Wipf, P.; Henninger, T. C.; Geib, S. J. *J. Org. Chem.* **1998**, *63*, 6088. (g) Gardner, R. R.; Liang, G. B.; Gellman, S. H. *J. Am. Chem. Soc.* **1999**, *121*, 1806. (h) Banerjee, A.; Pramanik, A.; Bhattacharjya, S.; Balaram, P. *Biopolymers* **1996**, *39*, 769. (i) Shankaramma, S. C.; Singh, S. K.; Sathyamurthy, A.; Balaram, P. *J. Am. Chem. Soc.* **1999**, *121*, 5360.
- (7) (a) Schmidt, M. W.; Baldridge, K. K.; Boatz, J. A.; Elbert, S. T.; Gordon, M. S.; Jensen, J. H.; Koseki, S.; Matsunaga, N.; Nguyen, K. A.; Su, S. J.; Windus, T. L.; Dupuis, M.;

- Montgomery, J. A. *J. Comput. Chem.* **1993**, *14*, 1347. (b) Frisch, M. J.; Trucks, G. W.; Schlegel, H. B.; Scuseria, G. E.; Robb, M. A.; Cheeseman, J. R.; J. A. Montgomery, J.; Vreven, T.; Kudin, K. N.; Burant, J. C.; Millam, J. M.; Iyengar, S. S.; Tomasi, J.; Barone, V.; Mennucci, B.; Cossi, M.; Scalmani, G.; Rega, N.; Petersson, G. A.; Nakatsuji, H.; Hada, M.; Ehara, M.; Toyota, K.; Fukuda, R.; Hasegawa, J.; Ishida, M.; Nakajima, T.; Honda, Y.; Kitao, O.; Nakai, H.; Klene, M.; Li, X.; Knox, J. E.; Hratchian, H. P.; Cross, J. B.; Adamo, C.; Jaramillo, J.; Gomperts, R.; Stratmann, R. E.; Yazyev, O.; Austin, A. J.; Cammi, R.; Pomelli, C.; Ochterski, J. W.; Ayala, P. Y.; Morokuma, K.; Voth, G. A.; Salvador, P.; Dannenberg, J. J.; Zakrzewski, V. G.; Dapprich, S.; Daniels, A. D.; Strain, M. C.; Farkas, O.; Malick, D. K.; Rabuck, A. D.; Raghavachari, K.; Foresman, J. B.; Ortiz, J. V.; Cui, Q.; Baboul, A. G.; Clifford, S.; Cioslowski, J.; Stefanov, B. B.; Liu, G.; Liashenko, A.; Piskorz, P.; Komaromi, I.; Martin, R. L.; Fox, D. J.; Keith, T.; Al-Laham, M. A.; Peng, C. Y.; Nanayakkara, A.; Challacombe, M.; Gill, P. M. W.; Johnson, B.; Chen, W.; Wong, M. W.; Gonzalez, C.; Pople, J. A.; Revision B.04 ed.; Gaussian Inc.: Pittsburgh PA, 2003.
- (8) (a) Venkatachalam, C. M. *Biopolymers* **1968**, *6*, 1425. (b) Möhle, K.; Gußmann, M.; Hofmann, H.-J. *J. Comput. Chem.* **1997**, *18*, 1415.

## 5 Mixed Helices - A General Folding Pattern in Homologous Peptides?

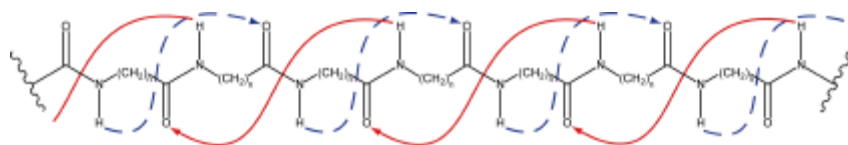
by Carsten Baldauf, Robert Günther, and Hans-Jörg Hofmann

published in ANGEWANDTE CHEMIE - INTERNATIONAL EDITION

Vol. 43 (2004) pages 1594-1597

and in ANGEWANDTE CHEMIE

Vol. 116 (2004) pages 1621-1624



**You may now exchange rings!** “Mixed helices” along a peptide sequence, in which rings of different sizes are held together by hydrogen bonds in alternating directions (see picture), prove to be a general folding principle in homologous  $\alpha$ -,  $\beta$ -,  $\gamma$ -, and  $\delta$ -peptides.

Oligomers composed entirely of unnatural monomers that form characteristic secondary structures have attracted considerable attention in the last years.<sup>[1]</sup> The motivation for work in this area ranges from gaining a better understanding of the structure and function of biomolecules and imitating them to developing polymers with novel properties. Considerable stimulation of research on these foldamers<sup>[2]</sup> came from the investigation of  $\beta$ -peptides.<sup>[3]</sup> Numerous secondary structures were found in these  $\beta$ -peptides as well as in homologous  $\gamma$ - and  $\delta$ -amino acids.<sup>[1,4]</sup>

In their studies on  $\beta$ -peptides, Seebach and co-workers found a unique type of secondary structure, which they referred to as a “mixed” helix.<sup>[5]</sup> Other authors have also described such mixed helices in the meantime.<sup>[6]</sup> In the familiar periodic helices all corresponding backbone torsion angles of the monomer constituents have the same values, and all peptide bonds form hydrogen bonds of the same type. In contrast, the periodicity of the mixed helices emerges at the level of dimer units. Here, the monomer constituents have alternating values for the backbone torsion angles, and the peptide bonds form hydrogen bonds of different type in an alternating way as well. The CO- und NH-groups of adjacent peptide linkages are involved in hydrogen

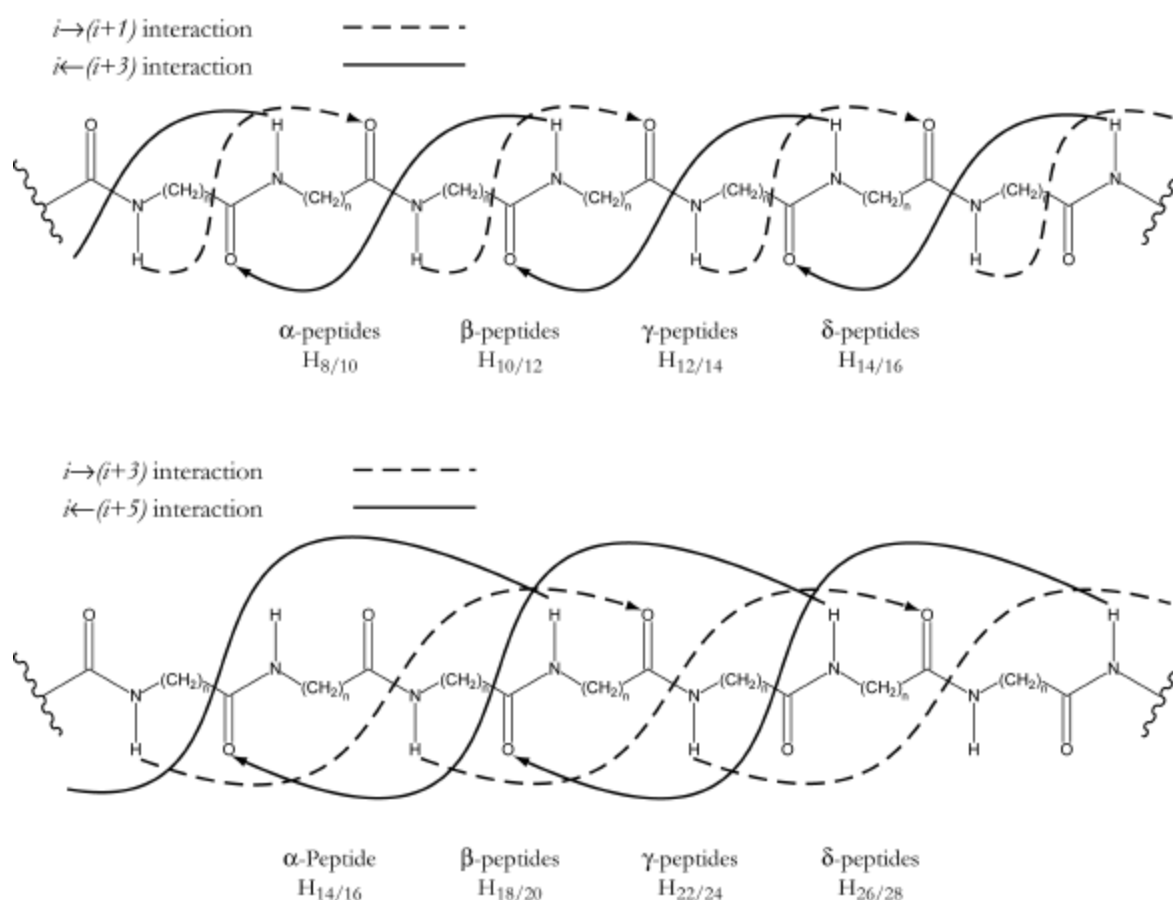


**Figure 1.** Alternative hydrogen bonding patterns in mixed helices  $H_{x/y}$  of homologous  $\alpha$ - ( $n = 1$ ),  $\beta$ - ( $n = 2$ ),  $\gamma$ - ( $n = 3$ ), and  $\delta$ -peptides ( $n = 4$ ). The index  $x/y$  denotes the number of atoms in the alternating hydrogen-bonded rings.

bonds that are formed alternately in the forward and backward direction. This leads to the formation of alternating hydrogen-bonded rings of different size along the sequence (Figure 1). In the mixed helices of the  $\beta$ -peptides 10-membered rings with an interaction between the amino acids  $i$  and  $(i+1)$  in forward direction are followed by 12-membered rings with an interaction between the amino acids  $i$  and  $(i+3)$  in backward direction of the sequence.

The existence of mixed helices in  $\beta$ -peptides raises the question whether this folding pattern might also exist in the homologous  $\gamma$ - and  $\delta$ -peptides and even in the native  $\alpha$ -peptides. The transfer of the folding principle to the homologous peptides leads to the hydrogen bonding patterns with  $i \rightarrow (i+1)/i \leftarrow (i+3)$ -interaction of the amino acids in Figure 1. Moreover, it is feasible that this principle can be extended to mixed helices with still larger alternating ring systems, as for instance with an  $i \rightarrow (i+3)/i \leftarrow (i+5)$ -interaction of the amino acids (Figure 1). Finally, it would be interesting to find further structure alternatives for a given hydrogen bonding pattern.

On the basis of theoretical methods it is possible to answer these questions. For this purpose the conformational space of hexamers of  $\alpha$ -,  $\beta$ -,  $\gamma$ - and  $\delta$ -Peptides was systematically searched for mixed helices having the hydrogen bonding patterns shown in Figure 1. In this search the backbone torsion angles  $\varphi$ ,  $\theta$ ,  $\zeta$ ,  $\rho$  and  $\psi$  of the oligomers (cf. structures in Table 1) were systematically varied.<sup>[7]</sup> Thus, about  $1.1 \times 10^5$ ,  $1.7 \times 10^6$ ,  $1.1 \times 10^6$  and  $6.3 \times 10^5$  conformations were generated for the  $\alpha$ -,  $\beta$ -,  $\gamma$ - and  $\delta$ -peptides, respectively. For the  $\delta$ -peptides only mixed helices with the combination of the smaller rings according to Figure 1 were sought. Since boundary effects cannot be excluded in oligomers of six amino acids, the two possible orders of the alternating rings were considered in the hexamers. In the corresponding conformation pools the candidates for mixed helices were selected on the basis of general geometry criteria for the formation of hydrogen bonds. Dependent on the peptide and helix types, these were in between 5 and 30 conformations that fulfilled the hydrogen bonding patterns in Figure 1. These structures were the starting points for geometry optimization<sup>[8a]</sup> at various levels of ab initio MO theory, which provide reliable results in the conformational analysis of peptides (HF/6-31G\*, B3LYP/6-31G\*<sup>[9]</sup>). The resulting stationary points on the potential energy surface were characterized by the eigenvalues of the matrix of force constants.

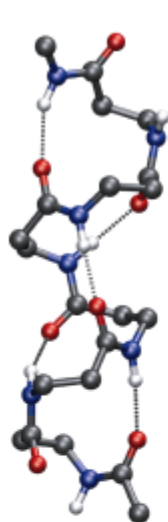
**Table 1:** Basic patterns of mixed helices in hexamers of  $\alpha$ -,  $\beta$ -,  $\gamma$ -, and  $\delta$ -hexamers characterized by the corresponding backbone torsion angles<sup>[a]</sup>  $\varphi$ ,  $\theta$ ,  $\zeta$ ,  $\rho$ , and  $\psi$ , and the relative energies<sup>[b]</sup> based on the most stable periodic helix.

Type <sup>[c]</sup>	<i>i</i>	<i>a</i>	<i>v</i>	$\Delta E$			Type <sup>[c]</sup>	<i>i</i>	<i>a</i>	<i>z</i>	<i>r</i>	<i>v</i>	$\Delta E$		
				HF	B3LYP	PCM							HF	B3LYP	PCM
$\alpha$ -peptides						$\gamma$ -peptides									
<b>H<sub>14/16</sub></b>	81		-67	<b>-36.2</b>	<b>-65.3</b>	46.4	<b>H<sub>14/12</sub><sup>I</sup></b>	-91	79	-80		162	19.9	13.7	49.1
	-81		85					94	84	-73		-29			
<b>H<sub>10</sub><sup>[d]</sup></b>	-63		-20	0.0	0.0	<b>0.0</b>	<b>H<sub>14/12</sub><sup>II</sup></b>	65	56	-126		-53	46.7	45.8	80.2
								-64	-37	-61		143			
$\beta$ -peptides						$\delta$ -peptides									
<b>H<sub>12/10</sub><sup>I</sup></b>	-102	61	89	<b>-82.6</b>	<b>-79.5</b>	<b>-10.7</b>	<b>H<sub>24/22</sub><sup>I</sup></b>	74	-177	-80		-168	12.3	9.9	40.9
	90	66	-111					-125	62	-77		154			
<b>H<sub>12/10</sub><sup>II</sup></b>	87	61	-96	-44.1	-54.6	31.0	<b>H<sub>24/22</sub><sup>II</sup></b>	117	-68	-174		128	44.5	45.8	68.1
	-27	-50	160					-89	-72	83		58			
<b>H<sub>10/12</sub><sup>III</sup></b>	179	-62	-21	-45.9	-56.0	26.6	<b>H<sub>24/22</sub><sup>III</sup></b>	94	79	-66		-102	72.0	67.1	87.0
	-93	51	87					123	64	66		16			
<b>H<sub>20/18</sub><sup>I</sup></b>	91	66	171	-69.5	-57.4	12.8	<b>H<sub>14</sub></b>	138	-60	-65		141	<b>0.0</b>	<b>0.0</b>	<b>0.0</b>
	-79	-57	149												
<b>H<sub>20/18</sub><sup>II</sup></b>	99	67	173	-35.3	-28.1	36.7	<b>H<sub>14/16</sub><sup>I</sup></b>	-172	159	-77	-68	131	<b>-1.9</b>	-10.0	89.5
	-150	57	47					76	69	-167	82	-126			
<b>H<sub>20/18</sub><sup>III</sup></b>	153	162	69	-27.9	-20.9	39.5	<b>H<sub>16/14</sub><sup>II</sup></b>	113	-54	-62	167	159	2.4	<b>-14.2</b>	90.0
	73	52	-144					-126	82	-66	-67	164			
<b>H<sub>18/20</sub><sup>IV</sup></b>	79	-171	100	-0.5	-1.4	67.7	<b>H<sub>10</sub></b>	98	-62	-68	169	-85	0.0	0.0	40.2
	110	-48	-43												
<b>H<sub>14</sub></b>	-148	61	-138	13.4	26.0	0.0	<b>H<sub>8</sub></b>	180	66	-142	69	-173	19.1	28.2	<b>0.0</b>
<b>H<sub>12</sub></b>	-87	92	-109	0.0	0.0	22.6									

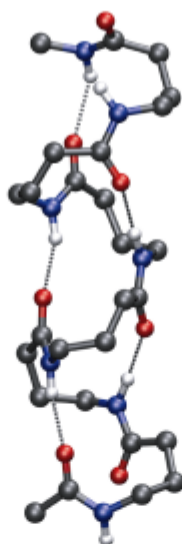
[a] Angles in degrees. For reasons of space, only the angles of the two central amino acids are given. The angles of all amino acids at all approximation levels are available as Supporting Information. [b] Relative energies at the HF/6-31G<sup>\*</sup>-, DFT/B3LYP/6-31G<sup>\*</sup>- and PCM//HF/6-31G<sup>\*</sup>-levels (Solvent water) in kJ/mol. Most stable structures are indicated. The total energies of the periodic reference helices are available as Supporting Information. [c] H<sub>*x/y*</sub> denotes a mixed helix with alternating hydrogen-bonded pseudo-cycles with *x* and *y* atoms, respectively. H<sub>*x*</sub> denotes periodic helices with hydrogen-bonded rings of *x* atoms. [d] <sub>3<sub>10</sub></sub>-helix.

Both ab initio models show mixed helices as energy minima for all homologous peptides. For the  $\beta$ -,  $\gamma$ - and  $\delta$ -peptides there are even several representatives for the hydrogen bonding patterns examined, which are denoted by superscript Roman numbers on the helix symbol in Table 1. The mixed helix of the  $\alpha$ -peptides shows a sequence of alternating 14- and 16-membered rings. Interestingly, the model structures of  $\alpha$ -peptides with the smaller 8- and 10-membered rings could not be localized as energy minima. The basic patterns of the mixed helices in the various homologous peptides are characterized by the backbone torsion angles listed in Table 1. Figure 2 shows the most stable helices for each peptide and hydrogen-bond type. Force field calculations

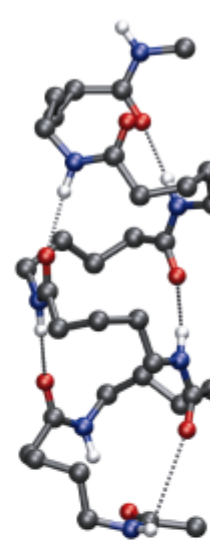
$i \rightarrow (i+1) / i \leftarrow (i+3)$  interaction



$H_{12/10}^I$  ( $\beta$ )

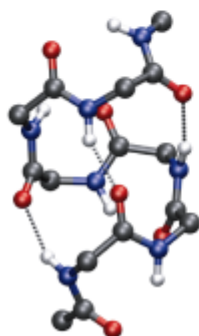


$H_{14/12}^I$  ( $\gamma$ )

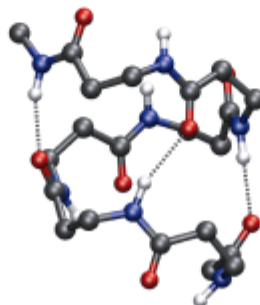


$H_{14/16}^I$  ( $\delta$ )

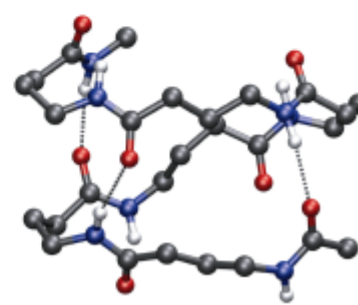
$i \rightarrow (i+3) / i \leftarrow (i+5)$  interaction



$H_{14/16}$  ( $\alpha$ )



$H_{20/18}^I$  ( $\beta$ )



$H_{24/22}^I$  ( $\gamma$ )

**Figure 2.** Most stable mixed helices in hexamers of homologous  $\alpha$ -,  $\beta$ -,  $\gamma$ -, and  $\delta$ -peptides for the investigated hydrogen-bonding patterns.

(CHARMm23.1)<sup>[10]</sup> proved that the hexamer structures are maintained in sequences up to 20 monomer constituents.

Even more impressive than the wide variety of mixed helices that are possible in the homologous peptides is the considerable stability of some structures in comparison to the periodic helices. This is most striking for the  $\beta$ -peptides (Table 1). In the case of the  $\alpha$ -peptides, we selected the  $3_{10}$ -helix characterized by 10-membered hydrogen-bonded rings for the energetic comparison. For the  $\beta$ -peptides, the experimentally determined helices with 14- and 12-membered rings,<sup>[11]</sup> which are confirmed by our calculations as particularly stable, served as references to estimate the stability of the mixed helix alternatives. The reference structure for the  $\gamma$ -peptides was an experimentally found and theoretically confirmed periodic structure with 14-membered rings.<sup>[4a,12]</sup> Finally, structures with 8- and 10-membered rings, respectively, which proved to be the most stable periodic structures according to our calculations, were the reference structures for the  $\delta$ -peptides. Both ab initio MO models agree fairly well in their stability predictions. Only for the  $\delta$ -peptides are the two mixed helices and the periodic reference helix energetically rather equivalent at the Hartree-Fock level, although the mixed helices are distinctly more stable according to the density functional theory.

It might be supposed that the influence of the medium could be the reason for the larger number of experimentally determined periodic helices in homologous peptides in comparison to the single representative of a mixed helix found until now. The hydrogen bonds in the mixed helix are formed alternately in forward and backward direction along the sequence. Thus, only a small helix dipole should result. This is confirmed by the dipole moments of  $m = 3.8$  D for the hexamers of the most stable mixed helix of the  $\beta$ -peptides and  $m = 31.5$  D for the periodic helix alternative with 14-membered rings. Since the formation of mixed helices is a disadvantage in polar media it is more likely to occur in less polar media. In order to estimate the influence of the environment, the solvation energies were calculated for the solvent water based on the polarizable continuum model (PCM//HF/6-31G\*<sup>[8b]</sup>). The results indicate that the mixed helices, in particular those of the  $\alpha$ -,  $\gamma$ - and  $\delta$ -peptides, indeed become more unstable than the periodic folding alternatives. Only the most stable mixed helices of the  $\beta$ -peptides remain competitive in strongly polar solvents (Table 1).

The formation of mixed helices can also be influenced by the introduction of substituents into the monomer units.<sup>[13]</sup> Our calculations on models of mixed helices of  $\beta$ -peptides for all possible substitution patterns, which we will report on elsewhere, reveal that a mixed helix with alternate substituents at the  $\alpha$ - and  $\beta$ -carbon atoms is especially stable. This substitution pattern is the



same as that in the mixed helix found by Seebach and co-workers. Thus, mixed helices prove to be a novel and interesting alternative of general importance for determining secondary structures in  $\alpha$ -peptides and their homologues.

## References

Supporting material is available on the compact disc attached at the end of this book.

- [1] D. J. Hill, M. J. Mio, R. B. Prince, T. S. Hughes, J. S. Moore, *Chem. Rev.* **2001**, *101*, 3893.
- [2] S. H. Gellman, *Acc. Chem. Res.* **1998**, *31*, 173.
- [3] a) R. P. Cheng, S. H. Gellman, W. F. DeGrado, *Chem. Rev.* **2001**, *101*, 3219; b) D. Seebach, J. L. Matthews, *J. Chem. Soc., Chem. Commun.* **1997**, 2015; c) W. F. DeGrado, J. P. Schneider, Y. Hamuro, *J. Peptide Res.* **1999**, *54*, 206.
- [4] a) T. Hintermann, K. Gademann, B. Jaun, D. Seebach, *Helv. Chim. Acta* **1998**, *81*, 983; b) S. Hanessian, X. Luo, R. Schaum, S. Michnick, *J. Am. Chem. Soc.* **1998**, *120*, 8569; c) D. D. Long, N. L. Hungerford, M. D. Smith, D. E. A. Brittain, D. G. Marquess, T. D. W. Claridge, G. W. J. Fleet, *Tetrahedron Lett.* **1999**, *40*, 2195.
- [5] a) D. Seebach, K. Gademann, J. V. Schreiber, J. L. Matthews, T. Hintermann, B. Jaun, *Helv. Chim. Acta* **1997**, *80*, 2033; b) M. Rueping, J. V. Schreiber, G. Lelais, B. Jaun, D. Seebach, *Helv. Chim. Acta* **2002**, *85*, 2577.
- [6] a) S. A. W. Gruner, B. Truffault, G. Voll, E. Locardi, M. Stöckle, H. Kessler, *Chem. Eur. J.* **2002**, *8*, 4366; b) G. V. M. Sharma, K. R. Reddy, P. R. Krishna, A. R. Sankar, K. Narsimulu, S. K. Kumar, P. Jayaprakash, B. Jagannadh, A. C. Kunwar, *J. Am. Chem. Soc.* **2003**, *125*, 13670.
- [7] Variation of the backbone torsion angles considering the alternation conditions for mixed helices:  $\alpha$ -peptides:  $\phi$ ,  $\psi$  in steps of  $30^\circ$ ;  $\beta$ -peptides:  $\phi$ ,  $\theta$ ,  $\psi$  in steps of  $30^\circ$ ;  $\gamma$ -peptides:  $\phi$ ,  $\theta$ ,  $\zeta$ ,  $\psi$  in steps of  $60^\circ$ ;  $\delta$ -peptides:  $\phi$  and  $\psi$  in steps of  $60^\circ$ ,  $\theta$ ,  $\zeta$  and  $\rho$  in steps of  $120^\circ$ ; changes of  $\pm 15^\circ$  were allowed for the torsion angle  $\omega = 180^\circ$  of the trans-peptide bonds.
- [8] a) Gaussian 98, Revision A.11.3, Gaussian, Inc., Pittsburgh PA, 2002; b) Gamess-US (Version: 20 JUN 2002 (R2)) M. W. Schmidt, K. K. Baldridge, J. A. Boatz, S. T. Elbert, M. S. Gordon, J. H. Jensen, S. Koseki, N. Matsunaga, K. A. Nguyen, S. J. Su, T. L. Windus, M. Dupuis, J. A. Montgomery, *J. Comput. Chem.* **1993**, *14*, 1347.
- [9] a) T. Head-Gordon, M. Head-Gordon, M. J. Frisch, C. L. Brooks III, J. A. Pople, *J. Am. Chem. Soc.* **1991**, *113*, 5989; b) G. Endredi, A. Perczel, O. Farkas, M. A. McAllister, G. I.

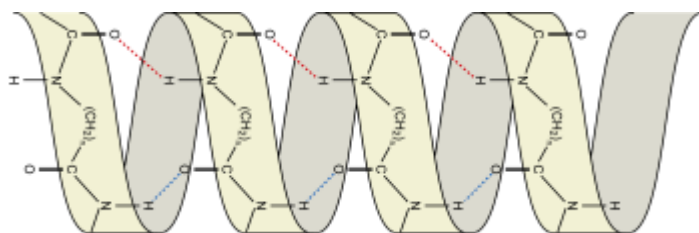
- Csonka, J. Ladik, I. G. Csizmadia, *J. Mol. Struct. (Theochem)* **1997**, 391, 15; c) K. Möhle, M. Gussmann, A. Rost, R. Cimiraglia, H.-J. Hofmann, *J. Phys. Chem. A* **1997**, 101, 8571.
- [10] a) F. A. Momany, R. Rone, *J. Comput. Chem.* **1992**, 13, 888; b) F. A. Momany, R. Rone, H. Kunz, R. F. Frey, S. Q. Newton, L. Schäfer, *J. Mol. Struct. (Theochem)* **1993**, 286, 1.
- [11] a) D. Seebach, M. Overhand, F. N. M. Kühnle, B. Martinoni, L. Oberer, U. Hommel, H. Widmer, *Helv. Chim. Acta* **1996**, 79, 913; b) D. H. Appella, L. A. Christianson, D. A. Klein, D. R. Powell, X. Huang, J. J. Barchi, Jr., S. H. Gellman, *Nature (London)* **1997**, 387, 381; c) K. Möhle, R. Günther, M. Thormann, N. Sewald, H.-J. Hofmann, *Biopolymers* **1999**, 50, 167; d) Y.-D. Wu, D.-P. Wang, *J. Am. Chem. Soc.* **1998**, 120, 13485; e) X. Daura, K. Gademann, B. Jaun, D. Seebach, W. F. van Gunsteren, A. E. Mark, *Angew. Chem.* **1999**, 111, 249; *Angew. Chem. Int. Ed.* **1999**, 38, 236. f) R. Günther, H.-J. Hofmann, K. Kuczera, *J. Phys. Chem. B* **2001**, 105, 5559.
- [12] C. Baldauf, R. Günther, H.-J. Hofmann, *Helv. Chim. Acta* **2003**, 86, 2573.
- [13] a) Y.-D. Wu, D. P. Wang, *J. Am. Chem. Soc.* **1999**, 121, 9352; b) T. A. Martinek, F. Fülöp, *Eur. J. Biochem.* **2003**, 270, 3657.

## 6 Side Chain Control of Folding of the Homologous $\alpha$ -, $\beta$ - and $\gamma$ -Peptides into “Mixed” Helices ( $\beta$ -Helices)

by Carsten Baldauf, Robert Günther, and Hans-Jörg Hofmann

to be published in BIOPOLYMERS (PEPTIDE SCIENCE)

Vol. 80 (2005) in press



**Abstract.** A systematic analysis of the substituent influence on the formation of the unique secondary structure type of “mixed” helices in the homologous  $\alpha$ -,  $\beta$ - and  $\gamma$ -peptides was performed on the basis of ab initio MO theory. Contrary to the common periodic peptide helices, mixed helices have an alternating periodicity and their hydrogen bonding pattern is similar to those of  $\beta$ -sheets. They belong, therefore, to the family of  $\beta$ -helices. It is shown that folding of peptide sequences into mixed helices is energetically preferred over folding into their periodic counterparts in numerous cases. The influence of entropy and solvents on the formation of the various competitive mixed and periodic helix types is discussed. Among the oligomers of the various homologous amino acids,  $\beta$ -peptides show the highest tendency to form  $\beta$ -helices. The rules of substituent influence derived from the analysis of a wide variety of backbone substitution patterns might be helpful for a rational design of mixed helix structures, which could be important for mimicking membrane channels.

## Introduction

Contrary to the periodic structure of common peptide and protein helices, e.g. the  $\alpha$ - and the  $3_{10}$ -helices, where the corresponding backbone torsion angles of all amino acids have the same values, mixed helices show the periodicity at the level of dimer units, i.e. the values of the corresponding backbone torsion angles of the monomers change alternately and adjacent peptide linkages are involved in hydrogen bonds that are formed alternately in the forward and backward directions of the sequence. Consequently, the resulting alternate hydrogen-bonded rings are of different size (Figure 1). Because of the similarity of the hydrogen bonding pattern of mixed helices to that of parallel  $\beta$ -sheet structures, these helices are classified as  $\beta$ -helices (Figure 2).<sup>1-4</sup> The most prominent representative of a  $\beta$ -helix in  $\alpha$ -peptides is the membrane channel-forming peptide gramicidin A<sup>5-7</sup> with alternating 20- and 22-membered hydrogen-bonded rings. Immediately after the discovery of gramicidin A, further types of  $\beta$ -helices were suggested for  $\alpha$ -peptides on the basis of general structure ideas, but only recently such secondary structures with

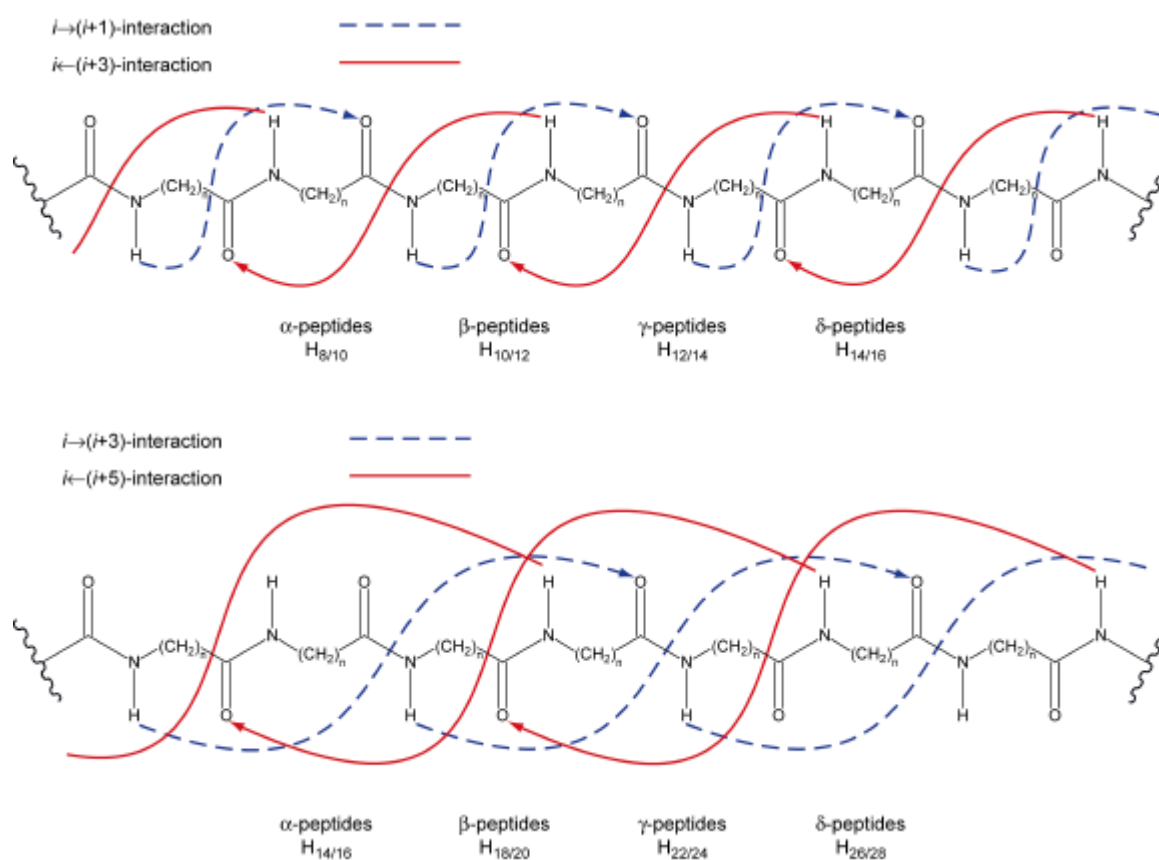


**FIGURE 1** Alternative hydrogen bonding patterns in mixed helices  $H_{x/y}$  of homologous  $\alpha$ - ( $n=1$ ),  $\beta$ - ( $n=2$ ), and  $\gamma$ -peptides ( $n=3$ ). The index  $x/y$  denotes the number of atoms in the alternating hydrogen-bonded rings.

alternating 14- and 16-membered hydrogen-bonded cycles were experimentally found.<sup>3,4</sup> In this context, it should be mentioned that anti-parallel double-strand  $\beta$ -helices are also possible.<sup>4,8</sup> Besides, the relationships between nanotube assemblies of cyclopeptides with alternately D,L-substituted monomers deserve attention.<sup>9,10</sup>

The concept of  $\beta$ -helices was originally confined to  $\alpha$ -peptides. This changed with the finding of a “mixed” helix in oligomers of  $\beta$ -amino acids ( $\beta$ -peptides) by Seebach and coworkers.<sup>11-13</sup> In this helix, 10-membered hydrogen-bonded rings with an interaction between the amino acids  $i$  and  $(i+1)$  in the forward direction are followed by 12-membered rings with an interaction between the amino acids  $i$  and  $(i+3)$  in the backward direction of the sequence ( $i \rightarrow (i+1) / i \leftarrow (i+3)$ ) interaction, Figure 1). This secondary structure type of  $\beta$ -peptides was confirmed in other experimental studies in the meantime.<sup>14-16</sup>

On the basis of ab initio MO theory, we could recently<sup>17</sup> extend the concept of mixed helices in several points:

- (i) Stable mixed helix conformers with  $i \rightarrow (i+1) / i \leftarrow (i+3)$  amino acid interactions are also possible in the homologous  $\gamma$ - and  $\delta$ -peptides (Figure 1).
- (ii) Mixed helices with still larger alternating ring systems, as for instance with  $i \rightarrow (i+3) / i \leftarrow (i+5)$  amino acid interactions (Figure 1) are thinkable in all homologous peptides.
- (iii) There are structure alternatives with differing backbone torsion angles for the same hydrogen bonding pattern in  $\beta$ -,  $\gamma$ - and  $\delta$ -peptides.

Remembering the outstanding role of gramicidin A as a membrane channel-forming compound, it may be useful to look for possibilities of a stabilization of this unusual and unique secondary structure type in all homologous peptides. In this way, novel types of membrane-channel forming peptides become accessible. It is well-known from  $\alpha$ -peptides, that the side chains of the amino acid residues have a significant influence on the secondary structure formation, which is for instance documented by the propensity scales for the proteinogenic amino acids to form helical, sheet and turn structures.<sup>18-20</sup> Gramicidin A itself is a good example for the substituent influence on the secondary structure formation, since an alternating sequence of D- and L-amino acids seems to be a basic requirement for the formation of the channel-like structure. Like in gramicidin A, experimental and theoretical data for  $\beta$ -peptides demonstrate the sensitivity of secondary structure formation to substituents.<sup>21-24</sup> Thus, folding into the two most important periodic folding patterns of  $\beta$ -peptides with 14- and 12-membered hydrogen-bonded

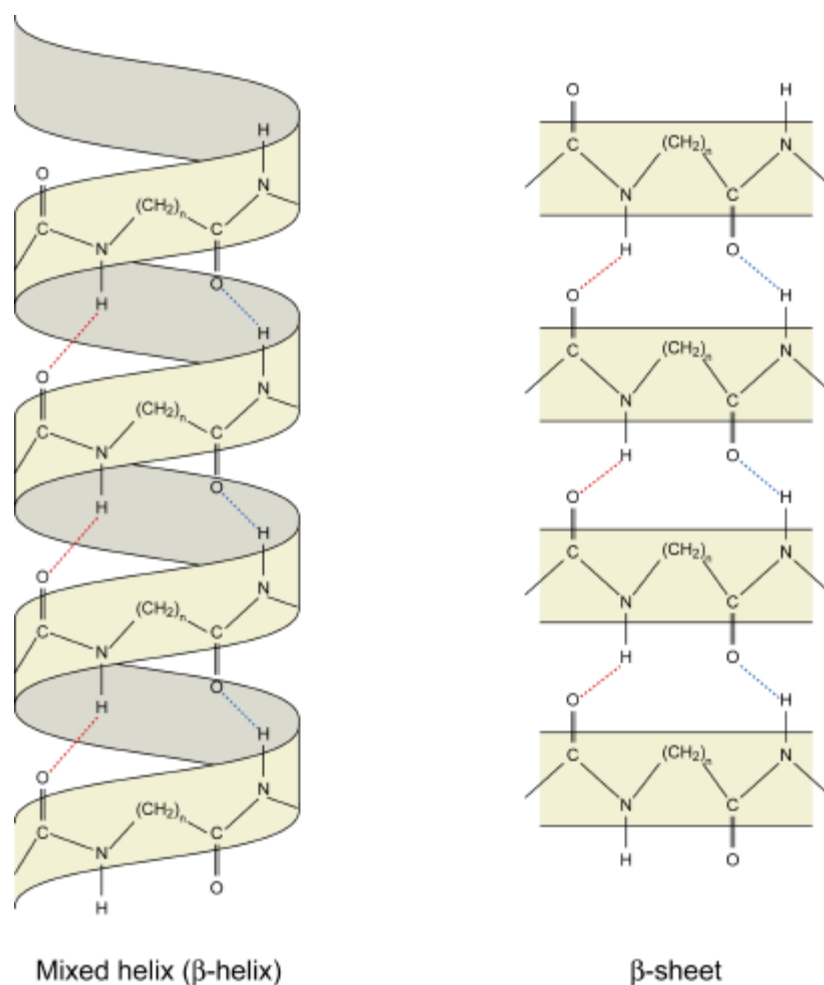


**FIGURE 2** Structural similarities of mixed helices ( $\beta$ -helices) of homologous peptides and parallel  $\beta$ -sheets. Red dotted lines indicate H-bonds in backward direction and blue dotted lines indicate H-bonds in forward direction along the sequence (cf. Fig. 1).

rings ( $H_{14}$ ,  $H_{12}$ ) is clearly influenced by the substitution type of the backbone.<sup>21,23,25</sup> There are also hints that the mixed helix found in  $\beta$ -peptide sequences is favored by alternating  $\beta^2$ - and  $\beta^3$ -substituted amino acids.<sup>11,22,24,26</sup>

In this paper, we present a systematic analysis on the substituent influence on folding into mixed helices for  $\alpha$ -,  $\beta$ -, and  $\gamma$ -peptides employing *ab initio* MO theory. The data are compared with those for the most important periodic structures that are competitive in folding. *Ab initio* MO theory has been rather successful in the actual field of peptide foldamers to describe secondary structure formation and provided hints for interesting novel secondary structure types.<sup>26-32</sup>

## Methods

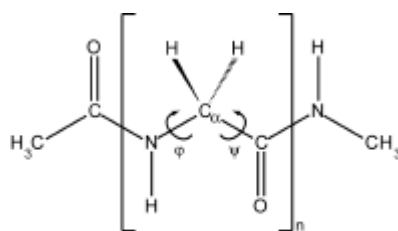
The starting point of our calculations were the various unsubstituted mixed helix conformers with  $i \rightarrow (i+1)/i \leftarrow (i+3)$  and  $i \rightarrow (i+3)/i \leftarrow (i+5)$  amino acid interactions, respectively, found for the homologous  $\alpha$ -,  $\beta$ -, and  $\gamma$ -peptides in our recent study.<sup>17</sup> After generation of the selected substitution patterns in blocked hexamers of  $\alpha$ -peptides, trimers and hexamers of  $\beta$ -peptides and tetramers of  $\gamma$ -peptides, respectively, the geometries of all structures were completely optimized at the HF/6-31G\* level of ab initio MO theory. In numerous studies, this approximation level has proved to be reliable for the description of peptide conformations.<sup>33-35</sup> The resulting optimized structures were checked for maintenance of the corresponding helix type and confirmed as minimum conformations by the determination of the eigenvalues of the matrix of force constants. The vibration frequencies arising from these calculations were used for the estimation of the free enthalpies and the entropies of the various helix types at the standard temperature of 300 K on the basis of statistical thermodynamics. Single-point calculations on the optimized HF/6-31G\* structures were performed to estimate the influence of the solvents methanol and water employing a polarizable continuum model (PCM//HF/6-31G\*). The solvation energy considers the electrostatic, van der Waals and cavitation energy contributions. The various substituted periodic structures of the homologous peptides, which were selected as reference structures for the stability comparisons, were treated in the same way.

The quantum chemical calculations were performed employing the Gaussian03<sup>36</sup> and the Gamess-US<sup>37</sup> program packages.

## Results and discussion

### *Mixed helices of $\alpha$ -peptides*

Our recent search for mixed helices with the hydrogen bonding patterns of Figure 1 on blocked glycine hexamers **1** (n=6) provided only one conformer with  $i \rightarrow (i+3)/i \leftarrow (i+5)$  amino acid interactions.<sup>17</sup> In this H<sub>14/16</sub> structure with torsion angles of  $\phi_1 = 80^\circ$ ,  $\psi_1 = -60^\circ$ ,  $\phi_2 = -60^\circ$ , and  $\psi_2 = 80^\circ$  in the periodic dimer unit, 14- and 16-membered hydrogen-bonded rings are alternating (Figures 1 and 3). The angle values predicted on the basis of simpler models for this helix type were  $\phi_1 = 125^\circ$ ,  $\psi_1 = -85^\circ$ ,  $\phi_2 = -80^\circ$  and  $\psi_2 = 100^\circ$ <sup>1</sup> and  $\phi_1 = 120^\circ$ ,  $\psi_1 = -82^\circ$ ,  $\phi_2 = -92^\circ$  and  $\psi_2 = 110^\circ$ ,<sup>2</sup> respectively. Mixed helices with an alternation of the smaller 8- and 10-membered pseudocycles arising from  $i \rightarrow (i+1)/i \leftarrow (i+3)$  amino acid interactions are impossible



1

for steric reasons. In Table I, the HF/6-31G\* stabilities of the right-handed mixed helix conformers of the blocked unsubstituted and  $\alpha$ -methylsubstituted hexamers **1** are given and compared with the data for the corresponding periodic  $3_{10}$ -helices. The total energies are available as a Supplemental file. It can be seen, that a very high folding tendency into the two energetically equivalent right- and left-handed mixed helices exists for the unsubstituted hexamer. The mixed helix conformer is by  $65.3 \text{ kJ}\cdot\text{mol}^{-1}$  more stable than the corresponding  $3_{10}$ -helix structure. The left- and right-handed helices of substituted hexamers are only approximate mirror images and are energetically different. However, it is always possible to derive the energies for the left-handed helices from the data for the right-handed ones in Table I, since the mirror image of a substituted right-handed helix corresponds exactly to the left-handed helix bearing the substituents with the opposite configuration. Obviously, the tendency to form mixed helices decreases after introduction of R- or, alternatively, S-configured substituents in all hexamer constituents. Although the energy difference between the most stable mixed helix and the  $3_{10}$ -helix is small, the latter is always more stable in these cases. Contrary to this, the formation of mixed helices in  $\alpha$ -peptides is supported by an alternating R- and S-substitution of the

**Table I** Relative Energies<sup>a</sup> of the Right-handed  $3_{10}$ -Helix and the Mixed  $H_{14/16}$  Helix of Unsubstituted and Methylsubstituted Hexamers of **1** at the HF/6-31G\* and at the PCM//HF/6-31G\* Levels of Ab Initio MO Theory.

Substitution <sup>c</sup>	$H_{14/16}$			$H_{10}$ <sup>b</sup>		
	HF	PCM (MeOH)	PCM (H <sub>2</sub> O)	HF	PCM (MeOH)	PCM (H <sub>2</sub> O)
U	<b>0.0</b>	32.4	46.4	65.3	<b>0.0</b>	<b>0.0</b>
R	0.8	73.1	74.6	35.9	32.2	30.6
S	7.6	83.6	84.7	<b>0.0</b>	<b>0.0</b>	<b>0.0</b>
RS	<b>0.0</b>	25.5	26.3	53.6	<b>0.0</b>	<b>0.0</b>
SR	79.6	98.5	99.4	59.2	3.0	2.8

<sup>a</sup> In  $\text{kJ}\cdot\text{mol}^{-1}$ , for total energies see Electronic supplementary information. <sup>b</sup>  $3_{10}$ -helix. <sup>c</sup> U: unsubstituted, R: R-configuration, S: S-configuration, RS and SR: alternating RS- or SR-configurations of the methyl-substituents.



monomers. Beginning the sequence with an R-amino acid, the right-handed mixed helix predominates and is by about  $50 \text{ kJ}\cdot\text{mol}^{-1}$  more stable than the  $3_{10}$ -helix conformer (Table I).

Helix formation is often discussed solely on the basis of energy data. It could be useful to estimate the free enthalpy differences between the competitive secondary structures and the influence of entropy contributions at standard temperature. Table II informs on the differences of the free enthalpies, the enthalpies including the zero-point vibration energies and thermal corrections and the entropies between the mixed helix conformers of  $\alpha$ -peptides and the corresponding  $3_{10}$ -helices. The values for the free enthalpy differences confirm the stability order, which was originally obtained on the basis of the total energies, also for a temperature of 300 K. However, the entropy influence is in favor of the periodic  $3_{10}$ -helices for all substitution patterns. Obviously,  $\beta$ -helices are states of higher order than the periodic secondary structures.

**Table II** Relative Enthalpies,<sup>a</sup> Free Enthalpies,<sup>a</sup> and Entropies<sup>a</sup> for the Right-Handed Mixed and  $3_{10}$ -Helices of Unsubstituted and Substituted Hexamers **1** of  $\alpha$ -Peptides

Substitution <sup>b</sup>		$H_{14/16}$	$H_{10}$ <sup>c</sup>
U	$\Delta H$	<b>0.0</b>	30.2
	$\Delta G$	<b>0.0</b>	19.6
	$\Delta S$	-35.5	<b>0.0</b>
R	$\Delta H$	6.2	35.8
	$\Delta G$	24.7	44.7
	$\Delta S$	-62.3	-29.8
S	$\Delta H$	13.9	<b>0.0</b>
	$\Delta G$	32.0	<b>0.0</b>
	$\Delta S$	-60.6	<b>0.0</b>
RS	$\Delta H$	<b>0.0</b>	49.2
	$\Delta G$	<b>0.0</b>	38.7
	$\Delta S$	-35.0	<b>0.0</b>
SR	$\Delta H$	82.6	54.6
	$\Delta G$	86.3	44.5
	$\Delta S$	-47.6	-1.3

<sup>a</sup> Relative enthalpies and free enthalpies in  $\text{kJ}\cdot\text{mol}^{-1}$ ; relative entropies in  $\text{J}\cdot\text{mol}^{-1}\cdot\text{K}^{-1}$ , for absolute values see Electronic supplementary information. <sup>b</sup> U: unsubstituted, R: R-configuration, S: S-configuration, RS and SR: alternating RS- or SR-configurations of the methyl substituents. <sup>c</sup>  $3_{10}$ -helix

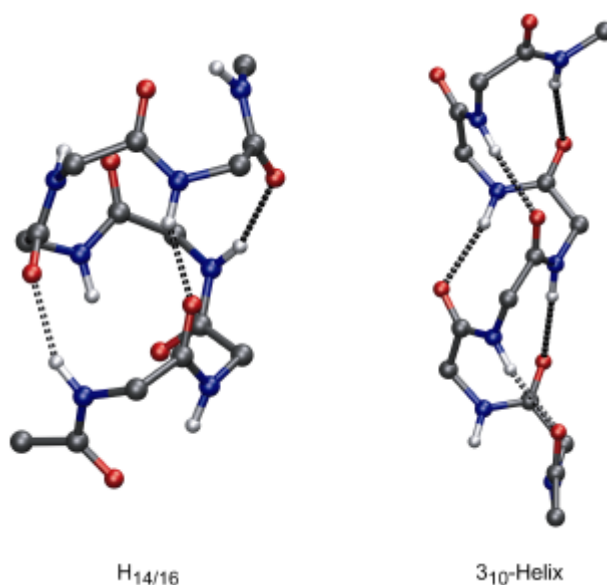
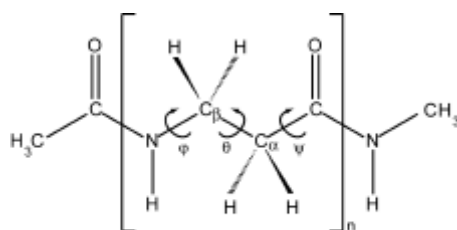


**FIGURE 3** Mixed  $H_{14/16}$  and  $3_{10}$  helices of  $\alpha$ -peptides.

Because of the alternating hydrogen bonding patterns, mixed helices have only rather small dipole moments in comparison to their periodic counterparts. Therefore, they are energetically disadvantaged in a polar environment. Estimation of the solvent influence for the solvents methanol and water at the PCM//HF/6-31G\* level of ab initio MO theory confirms the preference of the corresponding  $3_{10}$ -helix conformers (Table I). Nevertheless, the existence of the gramicidin A membrane channel as an  $H_{20/22}$  helix in an apolar membrane environment and a single-strand  $\beta^{4.4}$ -helix<sup>4,8</sup> found in NMR studies on oligonorleucine sequences in deuterated chloroform, which corresponds to the  $H_{14/16}$  conformer in our calculations, indicate the possibility of mixed helix formation in  $\alpha$ -peptides. It might be interesting to speculate on transitions between mixed and periodic helix alternatives dependent on changes of the environment.

#### *Mixed helices of $\beta$ -peptides*

Three types of mixed  $H_{12/10}$  helices (I, II, III) with alternating 12- and 10-membered hydrogen-bonded rings were found in our study<sup>17</sup> on unsubstituted  $\beta$ -peptide hexamers **2** ( $n=6$ ). Most stable was the conformer I with torsion angles of  $\varphi_1 = -100^\circ$ ,  $\theta_1 = 60^\circ$ ,  $\psi_1 = 90^\circ$ ,  $\varphi_2 = 90^\circ$ ,  $\theta_2 = 60^\circ$  and  $\psi_2 = -110^\circ$  in the periodic dimer unit that corresponds to the mixed helix found in the Seebach group with torsion angles of  $\varphi_1 = -100^\circ$ ,  $\theta_1 = 60^\circ$ ,  $\psi_1 = 90^\circ$ ,  $\varphi_2 = 90^\circ$ ,  $\theta_2 = 70^\circ$  and  $\psi_2 = -70^\circ$ .<sup>38</sup> Conformer I is much more stable than the periodic  $H_{14}$  helix of  $\beta$ -peptides (Table III). In Figure 4, the three  $H_{12/10}$  helices are visualized together with the three rather stable periodic secondary structure alternatives  $H_6$ ,  $H_{12}$  and  $H_{14}$ . In order to get an overview on the



2

substituent influence on mixed helix formation in  $\beta$ -peptides, all trimers **2** ( $n=3$ ) of the three basic mixed helix types with mono-methylsubstituted amino acid constituents were subject of examination. Since in short oligomers boundary effects cannot be excluded, both possible orders of the alternating hydrogen-bonded rings, 10/12 and 12/10, respectively, were considered.

To characterize the various substituted derivatives, substituents in 2-position ( $\alpha$ -position) of an amino acid monomer are denoted by an uppercase “A” for S-configuration and a lowercase “a” for R-configuration. The corresponding notations for substituents in 3-position ( $\beta$ -position) are an uppercase “B” for S- and a lowercase “b” for R-configuration. Confining our calculations to mono-substituted amino acid constituents and considering the dimer periodicity, a two-letter

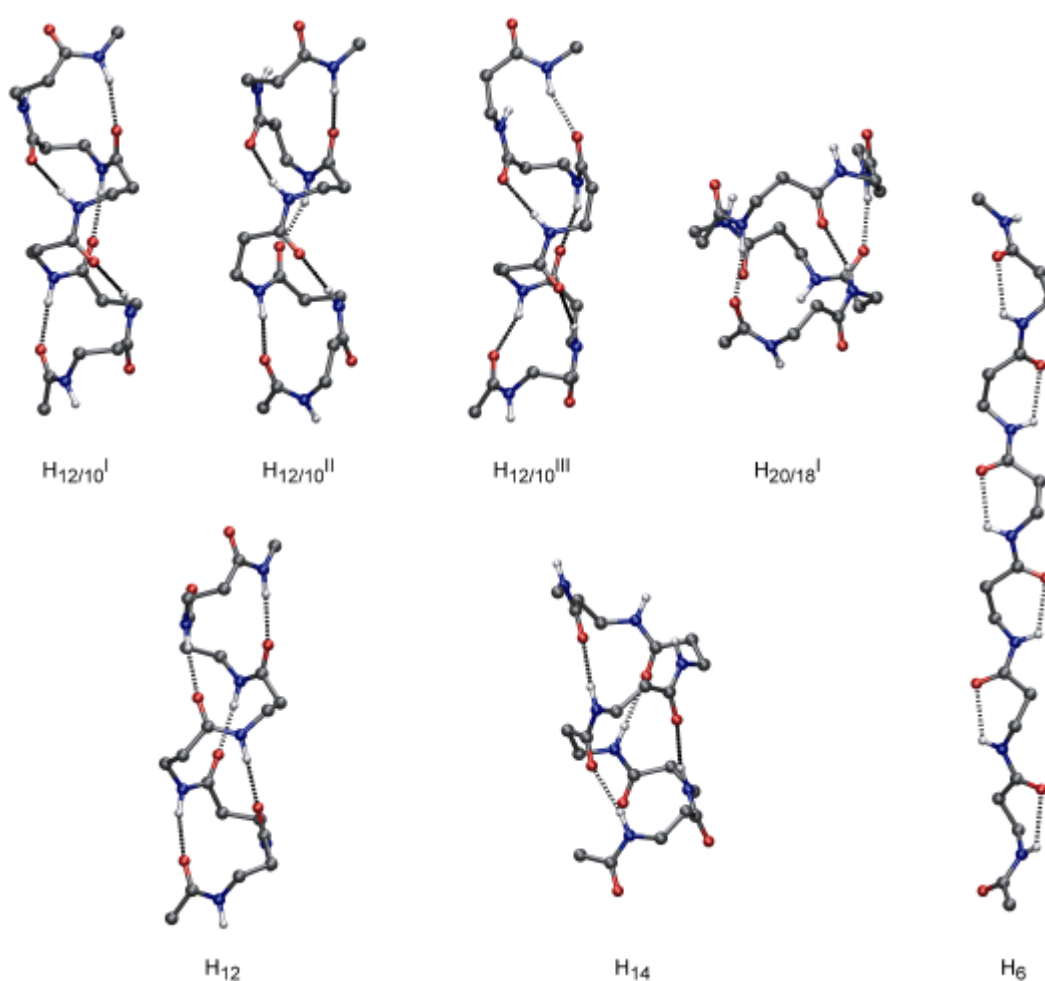


**FIGURE 4** Mixed helix types (first line) and selected periodic secondary structures (second line) of  $\beta$ -peptides.

code is sufficient to distinguish between the various substituted derivatives. Thus, the notation AB12/10 for a periodic dimer unit of **2** means an S-configured methyl group in the 2( $\alpha$ )-position of the first monomer and an S-configured methyl group in the 3( $\beta$ )-position of the second one. The hydrogen-bonded rings alternate in the order 12/10.

The spider plots of Figure 5 provide the complete information on the stabilities of all right-handed mixed helix trimers  $H_{10/12}$  and  $H_{12/10}$  of the types I, II and III with mono-substituted constituents together with the stabilities of the corresponding periodic  $\beta$ -peptide structures  $H_6$  with 6-membered hydrogen-bonded rings.<sup>26</sup> The periodic  $H_6$  secondary structure type was selected for comparison, since it tolerates all substituents, whereas most of the corresponding  $H_{14}$  helices could not be localized as minimum conformations at the trimer level. The stabilities are given as relative energies referred to the corresponding extended peptide conformations. Thus, it

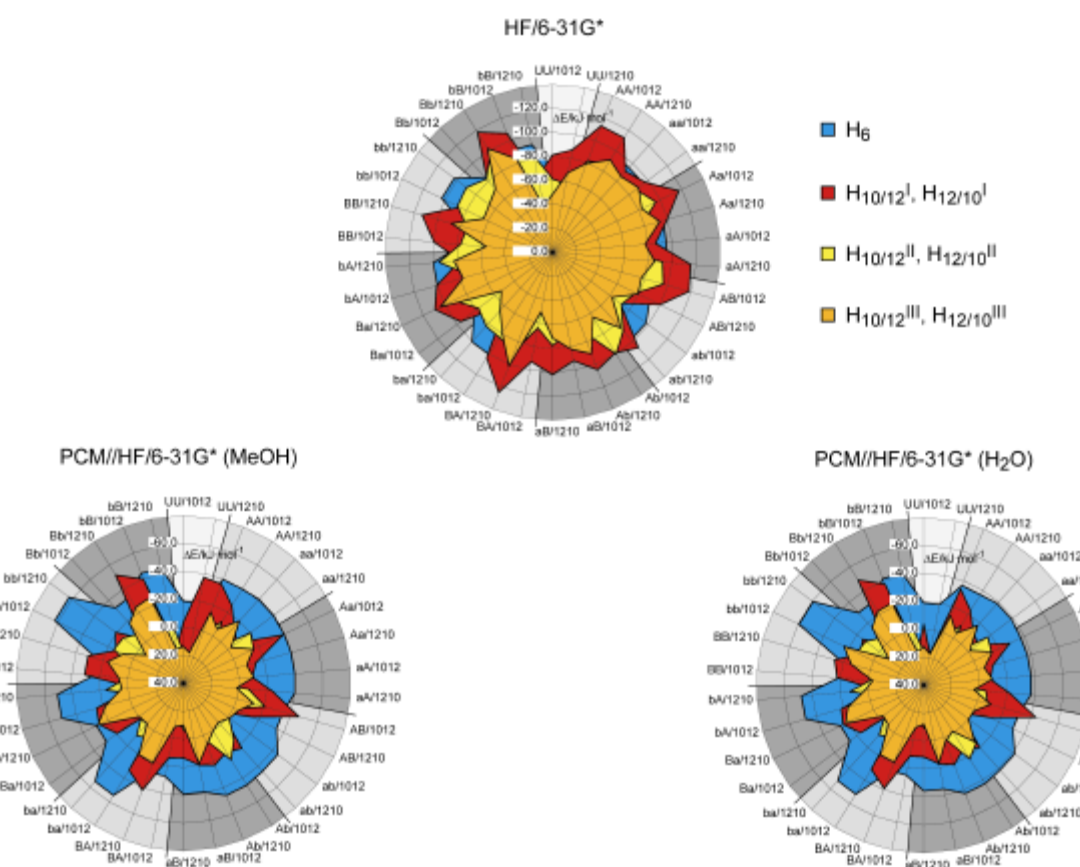


**FIGURE 5** Spider plots of the relative energies (in  $\text{kJ}\cdot\text{mol}^{-1}$ ) of the three different right-handed mixed helix types of  $\beta$ -peptides with alternating 10- and 12-membered hydrogen-bonded rings in trimer **2** for various substitution patterns in comparison to the corresponding periodic  $H_6$  secondary structures. The two alternative possibilities of the order of the hydrogen-bonded rings ( $H_{10/12}$  and  $H_{12/10}$ ) are considered. References for the energy comparison are the corresponding extended  $\beta$ -peptide sequences, i.e. structures with negative relative energies are more stable than the extended conformations. For the notation of the substituent patterns, see text.

is possible to compare the folding tendencies of all substituted peptide derivatives into the various helix alternatives starting from an extended peptide chain. All extended conformations were optimized keeping the backbone torsion angles fixed at  $180^\circ$ . The numerical data for the total energies and the backbone torsion angles for all trimers and the information on those trimer conformers that do not keep the mixed helix structure are available as a Supplemental file. It is possible to derive the information on all left-handed folding alternatives for a given substitution pattern from the spider plots of Figure 5, since a substituted left-handed conformer has the same energy as the right-handed conformer bearing the substituents with the opposite configuration. The HF/6-31G\* data of Figure 5 demonstrate a considerable folding potential into mixed helices for several substitution patterns of the mixed helix type I. Thus, it can be seen that right-handed mixed helices are favored in the derivatives AB10/12 and BA12/10, which correspond to the mixed helix found by the Seebach group, but also in derivatives with the substitution patterns AA12/10, AA10/12, BB10/12, BB12/10, Bb12/10, bB10/12, Aa10/12 and aA12/10, respectively. These conclusions may be transferred to the corresponding left-handed helices with the opposite configurations of the substituents. The mixed helix alternatives II and III are generally less stable than helix type I for most of the substitution patterns. Only, the derivatives Ab10/12 for type II and Ba12/10 for III have stabilities which are comparable with those of the other competitive structures. As expected, the stability of all mixed helices, in particular for the types II and III, decreases in polar environments. Nevertheless, the spider plots for the solvents methanol and water in Figure 5 show that some of the substituted mixed helices of type I like Bb12/10 and AB10/12 are still rather stable in these media.

The calculations on the trimers indicate important general trends of substituent effects in mixed helix formation. For an estimation of the influence of the sequence length on the helix formation, it could be interesting to extend the study to the hexamers **2** ( $n=6$ ). Now, there is also the opportunity to compare the stabilities of the mixed helices with those of the periodic  $H_{14}$  and  $H_{12}$  helices which were experimentally found in  $\beta$ -peptides.<sup>21,25</sup> Besides, it becomes possible to examine the formation of mixed helices with the still larger alternating 20- and 18-membered hydrogen-bonded rings (Figures 1 and 4), which are only possible in longer sequences. Table III provides the energy data for substituted mixed helix hexamers and the corresponding periodic structures, which indicate the considerable stability of mixed helices at the HF/6-31G\* level of ab initio MO theory.

With respect to the influence of various substitution patterns on mixed helix formation, the conclusions drawn from the trimer data can be maintained. Moreover, the general rules of substituent influence on the formation of the periodic  $H_{12}$  and  $H_{14}$  helices, which were derived

from the conformational properties of blocked  $\beta$ -peptide monomers in one of our former studies,<sup>23</sup> are confirmed by the direct study of these helices at the hexamer level and extended by consideration of further substituent patterns. It is rather impressive, that several substituted mixed helices of the  $H_{12/10}$  type keep their stability advantages over their periodic counterparts also in polar solvents. Thus, for the substitution types AA, Ab, Ba, Bb, and, last but not least, for BA, the substitution type of the experimentally found mixed helix,  $\beta$ -helix formation is still preferred. Obviously, the tendency to form mixed helices is much greater in  $\beta$ - than in  $\alpha$ -peptides.

**Table III** Relative Energies<sup>a</sup> of the Right-handed Mixed  $H_{12/10}$ <sup>I</sup> and  $H_{20/18}$ <sup>I</sup> Helices of Substituted Hexamers of **2** in Comparison to the Right-handed Periodic  $H_{12}$  and  $H_{14}$   $\beta$ -Peptide Helices at the HF/6-31G\* and PCM//HF/6-31G\* Levels of Ab Initio MO

Subst. <sup>b,c</sup>	$H_{12/10}$ <sup>I</sup>			$H_{20/18}$ <sup>I</sup>			$H_{12}$			$H_{14}$		
	HF	PCM MeOH	PCM H <sub>2</sub> O	HF	PCM MeOH	PCM H <sub>2</sub> O	HF	PCM MeOH	PCM H <sub>2</sub> O	HF	PCM MeOH	PCM H <sub>2</sub> O
U	<b>0.0</b>	<b>0.0</b>	<b>0.0</b>	13.1	19.1	23.5	82.6	30.3	33.5	96.0	8.0	10.7
AA	<b>0.0</b>	<b>0.0</b>	<b>0.0</b>	-	-	-	72.2	31.8	25.6	-	-	-
aa	57.6	53.3	51.7	-	-	-	126.0	76.7	75.8	81.0	14.7	8.3
BB	<b>0.0</b>	25.7	25.6	22.2	56.0	55.9	53.0	24.8	23.3	-	-	-
bb	62.8	70.6	76.6	36.6	67.8	67.8	139.2	124.5	124.0	47.8	<b>0.0</b>	<b>0.0</b>
Aa	47.7	54.4	52.9	-	-	-	97.7	49.8	47.4	124.3	69.7	69.3
aA	<b>0.0</b>	<b>0.0</b>	<b>0.0</b>	13.9	21.5	22.7	95.2	44.8	40.5	-	-	-
Ab	<b>0.0</b>	<b>0.0</b>	<b>0.0</b>	-	-	-	90.4	50.6	51.1	90.5	47.9	47.4
aB	22.0	25.3	29.4	26.3	36.5	38.7	73.3	26.4	26.1	-	-	-
BA	<b>0.0</b>	<b>0.0</b>	<b>0.0</b>	33.8	42.6	42.7	92.8	37.9	37.6	-	-	-
ba	134.4	123.2	121.0	-	-	-	161.6	117.0	115.0	94.6	20.7	18.1
Ba	0.1	<b>0.0</b>	<b>0.0</b>	-	-	-	66.6	20.5	19.1	-	-	-
bA	30.3	30.0	29.9	<b>0.0</b>	10.9	13.6	87.5	45.6	44.5	-	-	-
Bb	<b>0.0</b>	<b>0.0</b>	<b>0.0</b>	30.8	33.7	35.8	111.1	65.8	63.8	-	-	-
bB	96.6	94.1	94.3	55.2	66.0	68.5	115.0	72.9	72.7	-	-	-

<sup>a</sup> In  $\text{kJ}\cdot\text{mol}^{-1}$ ; for total energies see Electronic supplementary information. <sup>b</sup> For substitution pattern notation see text. <sup>c</sup> Hyphens denote structures where the helix type is not kept after geometry optimization.

**Table IV** Relative Enthalpies<sup>a</sup>, Free Enthalpies<sup>a</sup> and Entropies<sup>a</sup> for the Right-handed Mixed and Periodic Helix Alternatives of Unsubstituted and Substituted Hexamers **2** of  $\beta$ -Peptides

Substitution <sup>b,c</sup>		H <sub>12/10</sub>	H <sub>20/18</sub>	H <sub>12</sub>	H <sub>14</sub>
U	$\Delta H$	<b>0.0</b>	8.6	80.9	88.6
	$\Delta G$	<b>0.0</b>	7.5	70.2	77.1
	$\Delta S$	-38.6	-34.9	-2.8	<b>0.0</b>
AA	$\Delta H$	<b>0.0</b>	-	70.8	-
	$\Delta G$	<b>0.0</b>	-	62.0	-
	$\Delta S$	-37.6	-	-8.1	-
aa	$\Delta H$	58.2	-	126.0	74.5
	$\Delta G$	60.4	-	128.6	63.3
	$\Delta S$	-45.0	-	-46.4	<b>0.0</b>
BB	$\Delta H$	<b>0.0</b>	18.6	50.1	-
	$\Delta G$	<b>0.0</b>	20.7	37.9	-
	$\Delta S$	-41.8	-48.9	-1.1	-
bb	$\Delta H$	64.5	31.7	140.0	38.9
	$\Delta G$	68.3	24.0	141.3	26.5
	$\Delta S$	-54.5	-16.3	-46.2	<b>0.0</b>
Aa	$\Delta H$	47.8	-	96.6	118.7
	$\Delta G$	48.8	-	87.4	104.2
	$\Delta S$	-52.1	-	-17.8	<b>0.0</b>
aA	$\Delta H$	<b>0.0</b>	11.6	93.6	-
	$\Delta G$	<b>0.0</b>	12.0	85.0	-
	$\Delta S$	-48.7	-50.0	-19.8	-
Ab	$\Delta H$	<b>0.0</b>	-	89.8	84.7
	$\Delta G$	<b>0.0</b>	-	87.0	73.2
	$\Delta S$	-38.5	-	-29.0	<b>0.0</b>
aB	$\Delta H$	22.7	23.7	71.5	-
	$\Delta G$	25.5	27.2	64.7	-
	$\Delta S$	-47.6	-50.1	-15.7	-
BA	$\Delta H$	<b>0.0</b>	31.4	91.1	-
	$\Delta G$	<b>0.0</b>	32.4	81.5	-
	$\Delta S$	-36.5	-39.8	-4.3	-
ba	$\Delta H$	136.6	-	162.3	87.5
	$\Delta G$	143.0	-	161.9	76.6
	$\Delta S$	-58.2	-	-35.4	<b>0.0</b>
Ba	$\Delta H$	3.2	-	68.4	-
	$\Delta G$	4.3	-	61.6	-
	$\Delta S$	-26.4	-	<b>0.0</b>	-
bA	$\Delta H$	34.8	<b>0.0</b>	90.4	-
	$\Delta G$	38.0	<b>0.0</b>	86.0	-
	$\Delta S$	-33.5	-22.6	-7.6	-
Bb	$\Delta H$	<b>0.0</b>	25.9	110.2	-
	$\Delta G$	<b>0.0</b>	22.0	109.4	-
	$\Delta S$	-13.0	<b>0.0</b>	-10.3	-
bB	$\Delta H$	98.2	51.5	114.2	-
	$\Delta G$	105.1	56.9	112.5	-
	$\Delta S$	-35.9	-31.0	-7.1	-

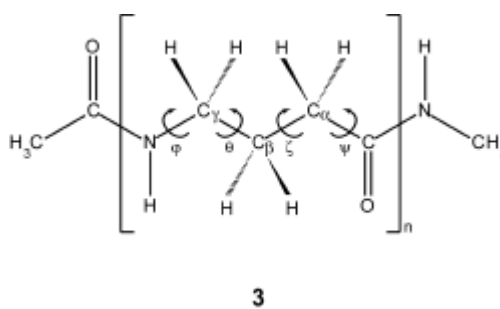
<sup>a</sup> In kJ·mol<sup>-1</sup>; for total energies see supplementary information. <sup>b</sup> For substitution pattern notation see text.<sup>c</sup> Hyphens denote structures where the helix type is not kept after geometry optimization.

The energy data in Table III demonstrate that mixed helices with the larger alternating 20- and 18-membered hydrogen-bonded rings (Figures 1 and 4) are also more stable than the competitive periodic secondary structures in vacuo or in an apolar environment. However, in most cases the mixed  $H_{12/10}$  helices with the smaller ring sizes are preferred. Only the right-handed  $H_{20/18}$  helix with the bA substitution pattern is superior over the corresponding right-handed  $H_{12/10}$  helix and has approximately the same energy as the left-handed bA12/10 conformer.

As in the case of  $\alpha$ -peptides, the free enthalpies and entropies were estimated for the various helix types of  $\beta$ -peptides. Table IV provides the differences of the free enthalpies, the enthalpies with inclusion of the zero-point vibration energies and the thermal corrections and the entropies for the main types of mixed and periodic  $\beta$ -peptide helices. Although the preference of mixed helices for the above-mentioned substitution patterns is also kept at the free enthalpy level, it is striking that the periodic helices  $H_{14}$  and  $H_{12}$  have greater entropy values than the corresponding mixed helices. In particular, the formation of periodic  $H_{14}$  helices is favored by entropy effects. As already discussed for the mixed helices of  $\alpha$ -peptides, the mixed helices of  $\beta$ -peptides represent higher-ordered states than their periodic counterparts.

#### Mixed helices of $\gamma$ -peptides

Several mixed helix conformers were localized in our recent ab initio study<sup>17</sup> for unsubstituted  $\gamma$ -peptide hexamers **3** ( $n=6$ ). Thus, two folding alternatives (I, II) with alternating 14- and 12-membered hydrogen-bonded rings ( $i \rightarrow (i+1)/i \leftarrow (i+3)$  amino acid interactions, Figure 1) and even



three (I, II, III) with alternating 24- and 22-membered rings ( $i \rightarrow (i+3)/i \leftarrow (i+5)$  amino acid interactions, Figures 1 and 6) were found. Contrary to the situation in  $\beta$ -peptides, all mixed  $\gamma$ -peptide helices are less stable than the periodic folding alternatives at the HF/6-31G\* level of ab initio MO theory. Thus, it seems to be relatively improbable to get mixed helices in  $\gamma$ -peptide sequences.



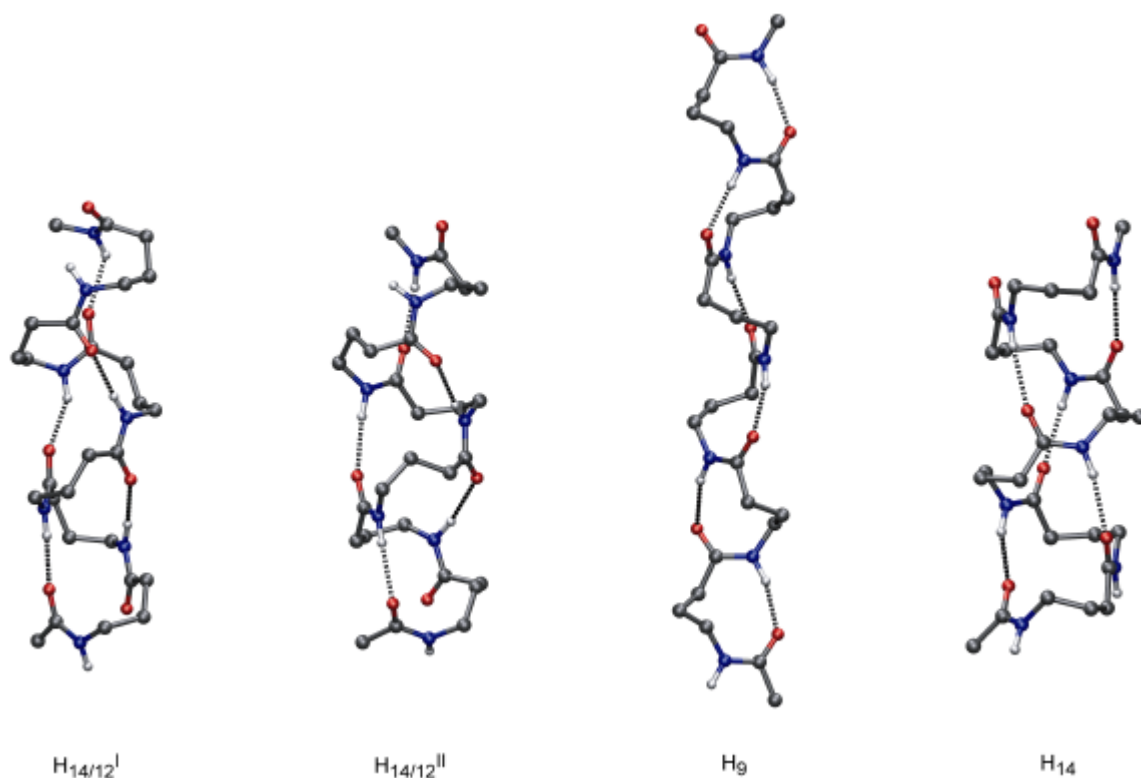


**FIGURE 6** Mixed  $H_{14/12}$  helices and selected periodic secondary structures of  $\gamma$ -peptides.

In our estimation of substituent effects, we considered tetramer structures **3** ( $n=4$ ) of the two  $H_{14/12}$  helices and selected the corresponding derivatives of the periodic  $H_{14}$  helix, which was experimentally found in  $\gamma$ -peptide sequences,<sup>39</sup> and the periodic  $H_9$  helix, which is rather stable according to our former calculations,<sup>29,40</sup> as folding alternatives for the energy comparison (Figure 6). Our nomenclature for the substituted  $\gamma$ -peptide derivatives has to be supplemented by an uppercase “C” for an S-configured substituent in 4-position ( $\gamma$ -position) of a  $\gamma$ -amino acid constituent and by a lowercase “c” for an R-configured substituent in this position. Considering only mono-methylsubstituted amino acid constituents and the dimer periodicity, the two-letter code can be maintained.

Figure 7 shows the spider plots of the stabilities for the various right-handed methyl-substituted  $\gamma$ -peptide tetramers. In Table V, the relative energies for the mixed and periodic helix alternatives of the most important substituted  $\gamma$ -peptide tetramers are explicitly given. A complete overview on the numerical geometry and energy data for all derivatives is again available in the Supplemental file. The spider plots at all approximation levels demonstrate that mixed helices in  $\gamma$ -peptide sequences, if they could be formed at all, need an apolar environment for their formation. Most promising are the substituent patterns aA and Ab for the formation of right-handed  $H_{14/12}^I$  helices, whereas right-handed  $H_{14/12}^{II}$  helices are favored by the substitution patterns Ac, Bc, cA and Cc. The  $H_{14/12}^I$  helix tolerates the various substitution patterns, but the

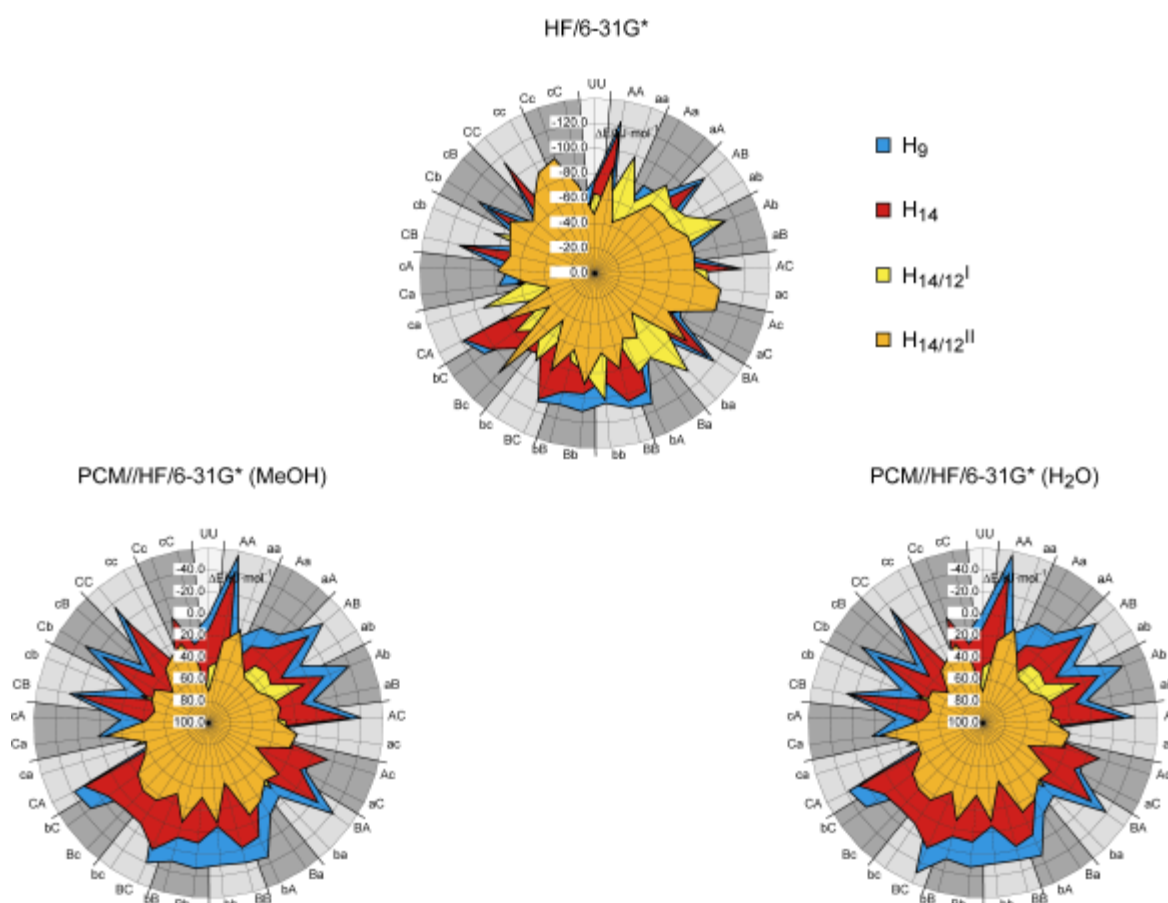


**FIGURE 7** Spider plots of the relative energies (in  $\text{kJ}\cdot\text{mol}^{-1}$ ) of the two different right-handed mixed  $\gamma$ -peptide helices  $H_{14/12}^I$  and  $H_{14/12}^{II}$  for various substitution patterns of tetramer **3** in comparison to the periodic right-handed  $H_9$  and  $H_{14}$  helices. References for the energy comparison are the corresponding extended  $\gamma$ -peptide sequences, i.e. structures with negative relative energies are more stable than the extended conformations. For the notation of the substituent patterns, see text.

$H_{14/12}^{II}$  helix is rather sensitive to substituent effects. In particular, R-substituents in  $\beta$ -position of the first  $\gamma$ -amino acid constituent of the dimer units and R-substituents in  $\alpha$ -position of the second  $\gamma$ -amino acid constituent of the dimer units destroy the right-handed mixed helix conformation.

It may be useful to give also some hints on the substituent influence on the formation of the two rather stable periodic  $\gamma$ -peptide structures  $H_9$  and  $H_{14}$  from our comparative study because the secondary structures of  $\gamma$ -peptides have not yet been so intensively investigated as those of  $\beta$ -peptides until now. Since there are only minor differences between the backbone torsion angles of the two helices, which are in a similar relation as the  $3_{10}$ - and  $\alpha$ -helices of  $\alpha$ -peptides, the substituent influence on both helices is rather similar. Independent of the actual stability, the  $H_9$  structure is kept for all substitution patterns, whereas the experimentally found  $H_{14}$   $\gamma$ -peptide helix<sup>39</sup> is more influenced by substituents (Figure 7). The right-handed  $\gamma$ -peptide helices  $H_9$  and

$H_{14}$  are clearly disadvantaged by R- and favored by S-substituents in the  $\alpha$ -position of the amino acid constituents. R-substituents in the  $\gamma$ -positions are only accepted in a few cases. Substituents in  $\beta$ -position show an indifferent behavior. Generally, it seems to be difficult to support the formation of  $H_9$  and  $H_{14}$  helices in  $\gamma$ -peptides selectively by special substitution patterns.

**Table V** Relative Energies<sup>a</sup> of the Right-handed Mixed  $H_{14/12}^I$  and  $H_{14/12}^{II}$  Helices of Substituted Tetramers of **3** in Comparison to the Right-handed Periodic  $H_9$  and  $H_{14}$   $\gamma$ -Peptide Helices at the HF/6-31G\* and PCM//HF/6-31G\* Levels of Ab Initio MO Theory

Subst. <sup>b,c</sup>	$H_{14/12}^I$			$H_{14/12}^{II}$			$H_9$			$H_{14}$		
	HF	PCM MeOH	PCM H <sub>2</sub> O	HF	PCM MeOH	PCM H <sub>2</sub> O	HF	PCM MeOH	PCM H <sub>2</sub> O	HF	PCM MeOH	PCM H <sub>2</sub> O
UUU	10.6	46.6	50.9	27.3	69.2	73.2	3.1	12.9	14.9	<b>0.0</b>	<b>0.0</b>	<b>0.0</b>
AA	62.8	97.7	97.3	37.9	79.4	79.8	8.4	14.6	17.6	<b>0.0</b>	<b>0.0</b>	<b>0.0</b>
aa	24.6	64.9	65.3	-	-	-	100.7	101.8	102.2	-	-	-
Aa	25.2	59.7	59.8	-	-	-	31.3	23.6	24.0	-	-	-
aA	<b>0.0</b>	36.2	36.0	19.9	51.0	53.1	23.2	15.8	16.1	9.2	<b>0.0</b>	<b>0.0</b>
Ab	0.7	44.0	42.3	32.9	75.4	75.8	15.6	24.2	23.3	<b>0.0</b>	<b>0.0</b>	<b>0.0</b>
aB	58.4	93.9	91.6	31.7	71.0	71.6	52.2	51.2	50.4	-	-	-
Ac	5.0	34.1	33.3	<b>0.0</b>	36.3	35.4	13.3	<b>0.0</b>	<b>0.0</b>	-	-	-
aC	40.8	70.5	68.4	34.9	65.3	64.9	32.2	19.7	17.7	-	-	-
BB	67.1	102.5	100.1	32.6	75.5	74.6	5.3	14.3	13.1	<b>0.0</b>	<b>0.0</b>	<b>0.0</b>
bb	9.3	48.9	48.6	-	-	-	25.3	37.4	35.1	6.9	1.8	0.7
Bc	47.6	88.7	88.2	<b>0.0</b>	46.9	47.1	27.6	23.3	22.5	-	-	-
bC	32.1	70.9	68.8	-	-	-	7.8	19.3	20.2	1.7	<b>0.0</b>	<b>0.0</b>
Ca	22.8	62.4	60.8	-	-	-	15.4	36.7	26.6	0.8	<b>0.0</b>	<b>0.0</b>
cA	5.1	52.3	53.6	<b>0.0</b>	44.4	46.1	30.2	40.8	40.7	8.4	20.9	22.1
CC	43.9	81.4	79.7	37.7	73.3	73.1	<b>0.0</b>	14.9	8.4	3.3	<b>0.0</b>	<b>0.0</b>
cc	54.9	96.7	94.5	21.9	66.5	67.4	86.1	74.7	81.4	-	-	-
Cc	9.1	33.0	33.0	<b>0.0</b>	25.3	25.4	17.8	<b>0.0</b>	<b>0.0</b>	-	-	-
cC	55.6	81.5	79.7	25.9	47.2	47.4	55.9	28.8	28.0	-	-	-

<sup>a</sup> In  $\text{kJ}\cdot\text{mol}^{-1}$ ; for total energies see Electronic supplementary information. <sup>b</sup> For substitution pattern notation see text. <sup>c</sup> Hyphens denote structures where the helix type is not kept after geometry optimization.

## Conclusions

Our quantum chemical analysis of the substituent influence on the folding of sequences of homologous  $\alpha$ -,  $\beta$ -, and  $\gamma$ -peptides demonstrates considerable possibilities to enforce the formation of the unique secondary structure type of “mixed” or  $\beta$ -helices by special backbone substitution patterns. In numerous cases, folding of homologous peptide sequences into mixed helices is superior over that into periodic structures, with the greatest probability to get mixed helices in  $\beta$ -peptides. The predominance of periodic peptide helices in peptides and proteins seems to be essentially caused by the influence of polar environments.

Our study provides both, information on the substituent influence on the mixed helix formation in the various classes of homologous peptides and on the formation of mixed helix alternatives within the same class of homologous peptides. Table VI summarizes the substitution patterns which should be preferred to get mixed helix types in the various classes of homologous peptides. This information might be helpful for chemists in the rational design of peptide structures with membrane channel-forming properties.

**Table VI** Favorable Substitution Patterns for the Formation of Right-Handed Mixed Helices in  $\alpha$ -,  $\beta$ -,  $\gamma$ -, and  $\delta$ -Peptides.

Peptide	Helix type <sup>a</sup>	Substitution Pattern <sup>b</sup>
$\alpha$	H <sub>14/16</sub>	U, RS
$\beta$	H <sub>12/10</sub> <sup>I</sup>	U, BA, BB, Bb, AA, Aa
	H <sub>12/10</sub> <sup>II</sup>	ba,
	H <sub>12/10</sub> <sup>III</sup>	Ba
	H <sub>20/18</sub> <sup>I</sup>	bA
$\gamma$	H <sub>14/12</sub> <sup>I</sup>	aA, Ab
	H <sub>14/12</sub> <sup>II</sup>	Ac, Bc, Cc, cA

<sup>a</sup> See Fig. 1. <sup>b</sup> See text for nomenclature.

We thank Deutsche Forschungsgemeinschaft (Project HO 2346/1 "Sekundärstrukturbildung in Peptiden mit nicht-proteinogenen Aminosäuren" and SFB 610 "Proteinzustände mit zellbiologischer und medizinischer Relevanz") for support of this work.

*Supplemental file:* Comprehensive material of tables with the total energies and geometry data of all  $\alpha$ -,  $\beta$ - and  $\gamma$ -peptide conformers, with the absolute values for the free enthalpies, enthalpies and entropies, and with the relative energies, which the spider plots of the  $\beta$ - and  $\gamma$ -peptides are based on. This material is available on the compact disc attached at the end of this book.

## References

1. Ramachandran, G. N.; Chandrasekaran, R. *Indian J Biochem Biophys* 1972, 9, 1.
2. De Santis, P.; Morosetti, S.; Rizzo, R. *Macromolecules* 1974, 7, 52.
3. Navarro, E.; Tejero, R.; Fenude, E.; Celda, B. *Biopolymers* 2001, 59, 110.
4. Navarro, E.; Fenude, E.; Celda, B. *Biopolymers* 2004, 73, 229.
5. Urry, D. W.; Goodall, M. C.; Glickson, J. D.; Mayers, D. F. *Proc Natl Acad Sci USA* 1971, 68, 1907.
6. Kovacs, F.; Quine, J.; Cross, T. A. *Proc Natl Acad Sci USA* 1999, 96, 7910.
7. Arndt, H. D.; Bockelmann, D.; Knoll, A.; Lamberth, S.; Griesinger, C.; Koert, U. *Angew Chem Int Ed* 2002, 41, 4062.
8. Navarro, E.; Fenude, E.; Celda, B. *Biopolymers* 2002, 64, 198.
9. Bong, D. T.; Clark, T. D.; Granja, J. R.; Ghadiri, M. R. *Angew Chem Int Ed* 2001, 40, 988.
10. Okamoto, H.; Nakanishi, T.; Nagai, Y.; Kasahara, M.; Takeda, K. *J Am Chem Soc* 2003, 125, 2756.
11. Seebach, D.; Gademann, K.; Schreiber, J. V.; Matthews, J. L.; Hintermann, T.; Jaun, B. *Helv Chim Acta* 1997, 80, 2033.
12. Rueping, M.; Schreiber, J. V.; Lelais, G.; Jaun, B.; Seebach, D. *Helv Chim Acta* 2002, 85, 2577.
13. Seebach, D.; Beck, A. K.; Bierbaum, D. *J Chem & Biodiv* 2004, 1, 1111.
14. Gruner, S. A. W.; Truffault, V.; Voll, G.; Locardi, E.; Stockle, M.; Kessler, H. *Chem Eur J* 2002, 8, 4366.

15. Sharma, G. V. M.; Reddy, K. R.; Krishna, P. R.; Sankar, A. R.; Narsimulu, K.; Kumar, S. K.; Jayaprakash, P.; Jagannadh, B.; Kunwar, A. C. *J Am Chem Soc* 2003, 125, 13670.
16. Sharma, G. V. M.; Reddy, K. R.; Krishna, P. R.; Sankar, A. R.; Jayaprakash, P.; Jagannadh, B.; Kunwar, A. C. *Angew Chem Int Ed* 2004, 43, 3961.
17. Baldauf, C.; Günther, R.; Hofmann, H.-J. *Angew Chem Int Ed* 2004, 43, 1594.
18. Chou, P. Y.; Fasman, G. D. *Biochemistry* 1974, 13, 211.
19. Chou, P. Y.; Fasman, G. D. *Annu Rev Biochem* 1978, 47, 251.
20. Chou, P. Y.; Fasman, G. D. *Adv Enzymol* 1978, 47, 45.
21. Seebach, D.; Overhand, M.; Kühnle, F. N. M.; Martinoni, B.; Oberer, L.; Hommel, U.; Widmer, H. *Helv Chim Acta* 1996, 79, 913.
22. Wu, Y.-D.; Wang, D.-P. *J Am Chem Soc* 1999, 121, 9352.
23. Günther, R.; Hofmann, H.-J. *Helv Chim Acta* 2002, 85, 2149.
24. Martinek, T. A.; Fülöp, F. *Eur J Biochem* 2003, 270, 3657.
25. Applequist, J.; Bode, K. A.; Appella, D. H.; Christianson, L. A.; Gellman, S. H. *J Am Chem Soc* 1998, 120, 4891.
26. Möhle, K.; Günther, R.; Thormann, M.; Sewald, N.; Hofmann, H.-J. *Biopolymers* 1999, 50, 167.
27. Wu, Y.; Wang, D.; Chan, K.; Yang, D. *J Am Chem Soc* 1999, 121, 11189.
28. Günther, R.; Hofmann, H.-J. *J Am Chem Soc* 2001, 123, 247.
29. Baldauf, C.; Günther, R.; Hofmann, H.-J. *Helv Chim Acta* 2003, 86, 2573.
30. Baldauf, C.; Günther, R.; Hofmann, H.-J. *J Mol Struct (Theochem)* 2004, 675, 19.
31. Baldauf, C.; Günther, R.; Hofmann, H.-J. *J Org Chem* 2004, 69, 6214.
32. Beke, T.; Csizmadia, I. G.; Perczel, A. *J Comput Chem* 2004, 25, 285.
33. Head-Gordon, T.; Head-Gordon, M.; Frisch, M. J.; Brooks III., C. L.; Pople, J. A. *J Am Chem Soc* 1991, 113, 5989.
34. Endredi, G.; Perczel, A.; Farkas, O.; McAllister, M. A.; Csonka, G. I.; Ladik, J.; Csizmadia, I. G. *J Mol Struct (Theochem)* 1997, 391, 15.
35. Möhle, K.; Gussmann, M.; Rost, A.; Cimiraglia, R.; Hofmann, H.-J. *J Phys Chem A* 1997, 101, 8571.

36. Frisch, M. J.; Trucks, G. W.; Schlegel, H. B.; Scuseria, G. E.; Robb, M. A.; Cheeseman, J. R.; J. A. Montgomery, J.; Vreven, T.; Kudin, K. N.; Burant, J. C.; Millam, J. M.; Iyengar, S. S.; Tomasi, J.; Barone, V.; Mennucci, B.; Cossi, M.; Scalmani, G.; Rega, N.; Petersson, G. A.; Nakatsuji, H.; Hada, M.; Ehara, M.; Toyota, K.; Fukuda, R.; Hasegawa, J.; Ishida, M.; Nakajima, T.; Honda, Y.; Kitao, O.; Nakai, H.; Klene, M.; Li, X.; Knox, J. E.; Hratchian, H. P.; Cross, J. B.; Adamo, C.; Jaramillo, J.; Gomperts, R.; Stratmann, R. E.; Yazyev, O.; Austin, A. J.; Cammi, R.; Pomelli, C.; Ochterski, J. W.; Ayala, P. Y.; Morokuma, K.; Voth, G. A.; Salvador, P.; Dannenberg, J. J.; Zakrzewski, V. G.; Dapprich, S.; Daniels, A. D.; Strain, M. C.; Farkas, O.; Malick, D. K.; Rabuck, A. D.; Raghavachari, K.; Foresman, J. B.; Ortiz, J. V.; Cui, Q.; Baboul, A. G.; Clifford, S.; Cioslowski, J.; Stefanov, B. B.; Liu, G.; Liashenko, A.; Piskorz, P.; Komaromi, I.; Martin, R. L.; Fox, D. J.; Keith, T.; Al-Laham, M. A.; Peng, C. Y.; Nanayakkara, A.; Challacombe, M.; Gill, P. M. W.; Johnson, B.; Chen, W.; Wong, M. W.; Gonzalez, C.; Pople, J. A. Gaussian 03; Revision B.04 ed.; Gaussian Inc.: Pittsburgh PA, 2003.
37. Schmidt, M. W.; Baldrige, K. K.; Boatz, J. A.; Elbert, S. T.; Gordon, M. S.; Jensen, J. H.; Koseki, S.; Matsunaga, N.; Nguyen, K. A.; Su, S. J.; Windus, T. L.; Dupuis, M.; Montgomery, J. A. *J Comput Chem* 1993, 14, 1347.
38. Seebach, D.; Abele, S.; Gademann, K.; Guichard, G.; Hintermann, T.; Jaun, B.; Matthews, J. L.; Schreiber, J. V.; Oberer, L.; Hommel, U.; Widmer, H. *Helv Chim Acta* 1998, 81, 932.
39. Hintermann, T.; Gademann, K.; Jaun, B.; Seebach, D. *Helv Chim Acta* 1998, 81, 983.
40. Dado, G. P.; Gellman, S. H. *J Am Chem Soc* 1994, 116, 1054.

## Appendix 1: Contents of the Compact Disc

To access the contents of the compact disc open the file index.htm with a browser.

(Tested with Mozilla Firefox, MS Internet Explorer and KDE Konqueror)

---

Item	Description
index.htm	Html-file
pdbs_ch4	Folder with pdb-files of the structures of ( <i>E</i> )- and ( <i>Z</i> )-vinylogous $\gamma$ -Peptides (hexamers and undecamers) described in chapter 4
pdfs	Folder with Supporting Information to the chapters 2, 3, 4, 5, and 6 with additional tables with torsion angles and energies in Adobe's Portable Document Format (PDF)

---



## Appendix 2: Publications

Baldauf, C.; Günther, R.; Hofmann, H.-J.; **Helix Formation and Folding in  $\gamma$ -Peptides and Their Vinylogues** *Helv. Chim. Acta* **2003** (86), 2573-2588.

Baldauf, C.; Günther, R.; Hofmann, H.-J.; **Mixed Helices - A General Folding Pattern in Homologous Peptides?**, *Angew. Chem. Int. Ed.* **2004** (43), 1594-1597. *Angew. Chem.* **2004** (116), 1621-1624.

Baldauf, C.; Günther, R.; Hofmann, H.-J.; **Conformational properties of sulfonamido peptides**, *J. Mol. Struct. (Theochem)* **2004** (675), 19-28.

Baldauf, C.; Günther, R.; Hofmann, H.-J.; **d-Peptides and d-Amino Acids as Tools for Peptide Structure Design - A Theoretical Study** *J. Org. Chem.* **2004** (69), 6214-6220.

Baldauf, C.; Günther, R.; Hofmann, H.-J.; **Vinylogous  $\gamma$ -Amino Acids as Building Blocks for Foldamers**, In: *Peptides - Peptide Revolution: Genomics, Proteomics & Therapeutics. Proc. of the 18th American Peptide Symposium*; Eds. Chorev, M.; Sawyer, T. K.; American Peptide Society: San Diego, **2004**; 441-442.

Baldauf, C.; Günther, R.; Hofmann, H.-J.; **Helix Formation in Oligomers of  $\gamma$ -Amino Acids**, In: *Peptides - Peptide Revolution: Genomics, Proteomics & Therapeutics. Proc. of the 18th American Peptide Symposium*; Eds. Chorev, M.; Sawyer, T. K.; American Peptide Society: San Diego, **2004**; 439-440.

Baldauf, C.; Günther, R.; Hofmann, H.-J.; **Control of Helix Formation in Vinylogous  $\gamma$ -Peptides by (E)- and (Z)-Double Bonds – A Way to Ion Channels and Monomolecular Nanotubes** *J. Org. Chem.* **2005** (70), in press.

Baldauf, C.; Günther, R.; Hofmann, H.-J.; **Side Chain Control of Folding of the Homologous  $\alpha$ -,  $\beta$ - and  $\gamma$ -Peptides into “Mixed” Helices ( $\beta$ -Helices)** *Biopolymers (Pept. Sci.)* **2005** (80), in press.

## Curriculum vitae

**Name:** Carsten

**Surname:** Baldauf

**Date of birth:** December 23<sup>rd</sup> 1977

**Place of birth:** Karl-Marx-Stadt

**1996** Abitur, Dr.-Wilhelm-André-Gymnasium, Chemnitz

**1996-1997** Alternative service, psychiatric clinic in Chemnitz

**1997-1998** Studies in Biochemistry at the Ruhr-Universität Bochum

**1998-2002** Studies in Biochemistry at the Universität Leipzig

**2002** Diploma thesis 'Sulfonamidopeptide und Vinyloge Peptide als Foldamere'

**since 2002** Ph.D. student in the group of Prof. Hofmann, Institute of Biochemistry, University of Leipzig;  
Funded by DFG (Project HO 2346/1 "Sekundärstrukturbildung in Peptiden mit nicht-proteinogenen Aminosäuren")

### **Erklärung**

Ich erkläre hiermit, dass ich die vorliegende Arbeit selbständig und ohne fremde Hilfe verfasst, andere als die von mir angegebenen Quellen und Hilfsmittel nicht verwendet und die den benutzten Werken wörtlich oder inhaltlich entnommenen Stellen als solche kenntlich gemacht habe. Ebenfalls sind alle von anderen Personen bereitgestellten Materialien oder erbrachten Dienstleistungen als solche gekennzeichnet.

Diese Arbeit wurde bisher an keiner anderen Hochschule oder Universität zur Promotion eingereicht.

Leipzig, den 25. Februar 2005

Carsten Baldauf